



Universidade do Estado do Rio de Janeiro

Centro Biomédico

Faculdade de Odontologia

Manuel Gustavo Chávez Sevillano

**Avaliação tridimensional das alterações no côndilo e na cavidade glenóide
decorrentes do uso dos aparelhos funcionais Twin Block e de Herbst no
tratamento das maloclusões de Classe II**

Rio de Janeiro

2023

Manuel Gustavo Chávez Sevillano

Avaliação tridimensional das alterações no côndilo e na cavidade glenóide decorrentes do uso dos aparelhos funcionais Twin Block e de Herbst no tratamento das maloclusões de Classe II

Tese apresentada, como requisito parcial para obtenção do título de Doutor, ao Programa de Pós-Graduação em Odontologia, da Universidade do Estado do Rio de Janeiro. Área de concentração: Ortodontia

Orientadores: Prof.^a Dra. Cátia Cardoso Abdo Quintão
Prof. Dr. Felipe de Assis Ribeiro Carvalho

Rio de Janeiro

2023

CATALOGAÇÃO NA FONTE
UERJ/REDE SIRIUS/CB/B

B238 Chávez-Sevillano, Manuel Gustavo.
Avaliação tridimensional das alterações no côndilo e na cavidade glenóide decorrentes do uso dos aparelhos funcionais Twin Block e de Herbst no tratamento das maloclusões de Classe II / Manuel Gustavo Chávez - Sevillano. – 2023.
86 f.
Orientadores: Cátia Cardoso Abdo Quintão, Felipe de Assis Ribeiro Carvalho.

Tese (doutorado) – Universidade do Estado do Rio de Janeiro, Faculdade de Odontologia.

1. Má oclusão de Classe II. 2. Aparelho Funcional. 3. Ortodontia. 4. Crescimento craniofacial. 5. Tomografia computadorizada de feixe cônico. I. Quintão, Cátia Cardoso Abdo. II. Carvalho, Felipe de Assis Ribeiro. III. Universidade do Estado do Rio de Janeiro. Faculdade de Odontologia. IV. Título.
CDU 616.314

Bibliotecária: Adriana Caamaño CRB7/5235

Autorizo, apenas para fins acadêmicos e científicos, a reprodução total ou parcial desta tese, desde que citada a fonte.

Assinatura

Data

Manuel Gustavo Chávez Sevillano

Avaliação tridimensional das alterações no côndilo e na cavidade glenóide decorrentes do uso dos aparelhos funcionais Twin Block e de Herbst no tratamento das maloclusões de Classe II

Tese apresentada, como requisito parcial para obtenção do título de Doutor, ao Programa de Pós- Graduação em Odontologia, da Universidade do Estado do Rio de Janeiro.
Área de concentração: Ortodontia.

Aprovada em 07 de novembro de 2023.

Orientadores:

Prof.^a Dra. Cátia Cardoso Abdo Quintão

Faculdade de Odontologia – UERJ

Prof. Dr. Felipe de Assis Ribeiro Carvalho

Faculdade de Odontologia – UERJ

Banca Examinadora:

Prof. Dr. Jose Augusto Mendes Miguel

Faculdade de Odontologia - UERJ

Prof.^a Dra. Flavia Raposo Gebara Artese

Faculdade de Odontologia - UERJ

Prof.^a Dra. Rhita Cristina Cunha Almeida

Faculdade de Odontologia - UERJ

Prof.^a Dra. Luciane Macedo de Menezes

Pontifícia Universidade Católica do Rio Grande do Sul

Prof.^a Dra. Tatiana Araújo de Lima

Universidade Veiga de Almeida

Rio de Janeiro

2023

DEDICATÓRIA

Dedico este trabalho aos meus avós, Lucha e Melquiades, in memoriam, pelo amor incondicional, e ensinar-me valores que facilitam meu caminho nesta vida.

A meus pais, Victor e Mary, que nunca mediram esforços para que eu realizasse meus sonhos, abrindo mão por vezes de seus próprios.

Aos meus irmãos Yéssica e Eraldo, por quem tenho grande admiração e amor imensurável.

AGRADECIMENTOS

A Deus por conduzir e orientar todos os meus passos até aqui.

Aos meus pais Victor e Mary por me darem todo o suporte necessário.

Aos meus irmãos Yéssica e Eraldo que são os melhores do mundo.

Ao meu amigo e pai acadêmico, Prof. Miguel Pardo Bancalari, pela constante motivação, apoio incondicional e exemplo de vida pessoal e profissional.

À Profa. Dra. Cátia Cardoso Abdo Quintão pela orientação dedicada à elaboração deste e de outros trabalhos, com muita compreensão e amizade que me fez crescer como ser humano e ortodontista. Muito obrigado pelos ensinamentos acadêmicos, profissionais e pessoais.

Ao Prof. Dr. Felipe de Assis Ribeiro Carvalho, pela orientação constante, incentivo e muita paciência em me ensinar a metodologia desenvolvida neste trabalho. Você me ensinou uma nova linha de pesquisa que jamais esquecerei.

Ao Prof. Jonas Capelli Junior pela confiança em mim depositada, pela amizade oferecida e pelos ensinamentos transmitidos.

À Profa. Dra. Flavia Raposo Gebara Artese, por mostrar ao mundo a excelência do Curso de Ortodontia da Universidade do Estado de Rio de Janeiro (UERJ). Pela senhora sinto orgulho e admiração.

Ao coordenador do curso de Doutorado em Ortodontia da UERJ, Prof. Dr. José Augusto Mendes Miguel, pela colaboração essencial no desenvolvimento deste trabalho, pela constante motivação em continuar pesquisando e pela confiança em mim depositada.

Ao Prof. Dr. Klaus Barreto Lopes, pela colaboração neste trabalho, pelos ensinamentos e pela amizade proporcionada.

À colega de linha de pesquisa, Profa. Dra. Tatiana Araújo de Lima, pela grande ajuda no desenvolvimento desta pesquisa. Muito obrigado pelo envio dos dados coletados previamente ao meu ingresso no doutorado.

À colega de linha de pesquisa e minha amiga do doutorado, Dra. Nathália Barbosa Palomares, pela entrega de informações como vídeos e monografias que me fizeram entender melhor a metodologia a ser desenvolvida na tese.

Aos demais professores do curso de Pós-graduação em Ortodontia da faculdade de Odontologia da UERJ: Dra Cristiane Canavarro Martins, Dr. Marco Antônio de Oliveira Almeida, Dra. Rhita Cristina Cunha Almeida, Dra Vera Lucia Cosendy Corte-Real, Dr.

Alvaro Francisco Carrielo Fernandes, pelos quais tenho grande respeito e admiração.

À minha amiga e parceira do doutorado Luciana Quintanilha Pires Fernandes, pelos ensinamentos e ajuda nas publicações que fizemos juntos.

Às amigas de turma de Doutorado, Caroline Pelagio Maués Casagrande e Isabella Simoes Holz, que foram um presente de valor inestimável.

Ao meu amigo e parceiro do doutorado David Silveira Alencar pelos ensinamentos e muita ajuda nas diversas metodologias 3D.

Aos meus amigos da ORTOUERJ Bruno Moreira Das Neves e Miguel Côco, pelo recepção e grande ajuda que me deram quando cheguei no Rio de Janeiro. Muito obrigado.

Aos demais amigos do Doutorado, Livia Kelly Ferraz Nunes, Sergio Roberto de Oliveira Caetano, Arthur Cunha da Silva, Mariana Caires Sobral de Aguiar e Luísa Schubach da Costa Barreto, pela alegria do convívio.

Aos demais amigos da Especialização e Mestrado, Larissa Barbosa Moda, Veronica Santos Conde, Maria Fernanda Ramos Mattos, Luana Karine Amaro Silva, Emerson Carvalho da Silva Anapurús, Kenia Lorena Monteiro de Moura, Amanda Marques Gonçalves e Anderson Carlos de Oliveira, por momentos tão felizes e por toda a ajuda.

Aos novos integrantes da Especialização e Mestrado em Ortodontia da UERJ.

À UERJ por me dar a oportunidade de ter esta inesquecível formação acadêmica em ortodontia.

À FAPERJ pelo apoio financeiro e intelectual que tornou o curso possível.

O presente trabalho foi realizado com apoio da Coordenação da Fundação de Amparo à Pesquisa do Estado do Rio de Janeiro – Brasil (FAPERJ) – No do Processo E-26/201.088/2019.

Aos funcionários da odontologia da Policlínica Piquet Carneiro pela ajuda e carinho.

Aos demais professores da Banca pelo aceite: Dr. Jose Augusto Mendes Miguel, Dra. Flavia Raposo Gebara Artese, Dra. Rhita Cristina Cunha Almeida, Dra. Luciane Macedo de Menezes, Dra. Tatiana Araújo de Lima, Dr. Klaus Barreto Lopes, Dra. Cristiane Canavarro Rodrigues Martins e Dr. Marco Abdo Gravina que prontamente aceitaram participar da banca de defesa desta tese. A trajetória acadêmica de vocês inspira a todos nós, ortodontistas e pesquisadores.

À maravilhosa equipe de professores do Departamento de Odontologia Preventiva e Comunitária da FO-UERJ.

Por fim, agradeço a todos os amigos e familiares que sempre estiveram ao meu lado nessa jornada.

RESUMO

CHAVEZ-SEVILLANO, Manuel Gustavo. **Avaliação tridimensional das alterações no côndilo e na cavidade glenóide decorrentes do uso dos aparelhos funcionais Twin Block e de Herbst no tratamento das maloclusões de Classe II.** 2023. 86 f. Tese (Doutorado em Odontologia) – Faculdade de Odontologia, Universidade do Estado do Rio de Janeiro, Rio de Janeiro, 2023.

Um estudo observacional retrospectivo 3D e um estudo piloto retrospectivo longitudinal 3D compor esta tese. **O protocolo foi aprovado pelo Comitê de Ética (UERJ).** O primeiro estudo teve como objetivo avaliar as alterações ocorridas no côndilo (CO) e na cavidade glenóide (CG) decorrentes do uso dos aparelhos funcionais Twin Block (TB) e de Herbst (HB) no tratamento das maloclusões de classe II. Os grupos TB e HB tiveram 12 pacientes cada (TB, $11,92 \pm 1,08$ anos; HB, $12,5 \pm 1,87$ anos). Tomografias computadorizadas de feixe cônico (TCFC) foram registradas antes (T0) e depois (T1) do tratamento (12 meses). Modelos tridimensionais (3D) completos de T0 e T1 foram sobrepostos no programa Dolphin Imaging. Modelos 3D parciais do CO e CG foram segmentados no programa ITK-SNAP. No programa Geomagic Qualify um sistema de coordenadas (eixos X, Y e Z) foi criado em cada modelo 3D T0 e, em seguida, os modelos CO e CG foram alinhados nos modelos 3D T0 e T1. Em cada CO e CG foi gerado um ponto centróide 3D que foi avaliado entre T0 e T1. Os testes de Wilcoxon, Mann-Whitney e Spearman foram usados com 95% de confiança. No grupo com TB, houve crescimento do CO direito (1,33mm), CO esquerdo (1,34mm), CG direita (0,80mm) e CG esquerda (0,48mm) em direção posterior. O grupo HB mostrou crescimento do CO direito (1,43mm), CO esquerdo (1,77mm), CG direita (0,12mm) e CG esquerda (0,17) em direção posterior. Não houve diferença nos efeitos sobre CO e CG quando TB e HB foram usados. O estudo piloto teve como objetivo avaliar as alterações no CO e na CG decorrentes do uso do TB no tratamento das má oclusões de Classe II após um ano da remoção do TB. Neste estudo 12 pacientes ($11,92 \pm 1,08$ anos) foram avaliados por meio da CBCT e foram registrados antes (T0), durante (T1: 12 meses) e após (T2: 12 meses) tratamento. Modelos 3D completos de T0, T1 e T2 foram sobrepostos no Dolphin Imagin. Modelos 3D parciais do CO e CG foram segmentados no ITK-SNAP. No Geomagic Qualify um sistema de coordenadas (eixos X, Y e Z) foi criado em cada modelo 3D T0 e T1 completo e, em seguida, os modelos parciais do CO e CG foram alinhados. Em cada CO e CG foi gerado um ponto centróide 3D que foi avaliado em T0 - T1, T0 - T2 e T1 - T2. Os testes multivariados de Wilcoxon e Friedman foram usados com 95% de confiança. Nos períodos T0 - T1 e T0 - T2, foi encontrado crescimento significativo do CO e da CG direita e esquerda, respectivamente, em sentido posterior. O CO também cresceu significativamente na direção superior e a CG na direção inferior, embora não significativamente. Os pacientes que usaram TB tiveram crescimento do CO em direção posterior e superior e da CG em direção posterior e inferior. A quantidade de crescimento de CO foi maior do que a quantidade de crescimento da CG.

Palavras-chave: maloclusão de classe II; aparelho funcional; crescimento craniofacial; tomografia computadorizada de feixe cônico.

ABSTRACT

CHAVEZ-SEVILLANO, Manuel Gustavo. **Three-dimensional evaluation of changes in the condyle and glenoid cavity resulting from the use of functional Twin Block and Herbst appliances in the treatment of Class II malocclusions.** 2023. 86 f. Tese (Doutorado em Odontologia) – Faculdade de Odontologia, Universidade do Estado do Rio de Janeiro, Rio de Janeiro, 2023.

A 3D retrospective observational study and a 3D longitudinal retrospective pilot study constitute this thesis. **The protocol was approved by the Ethics Committee (UERJ).** The first study aimed to evaluate the alterations that occurred in the condyle (CO) and in the glenoid cavity (GC) resulting from the use of functional Twin Block (TB) and Herbst (HB) appliances in the treatment of class II malocclusions. The TB and HB groups had 12 patients (TB, 11.92 ± 1.08 years; HB, 12.5 ± 1.87 years). Cone-beam computed tomography (CBCT) scans were recorded before (T0) and after (T1) treatment (12 months). Complete three-dimensional (3D) models of T0 and T1 were superimposed in the Dolphin Imaging program. Partial 3D models of the CO and GC were segmented in the ITK-SNAP program. In the Geomagic Qualify program a coordinate system (axes X, Y and Z) was created in each 3D model T0 and then the CO and GC models were aligned in the 3D models T0 and T1. In each CO and GC a 3D centroid point was generated and evaluated between T0 and T1. Wilcoxon, Mann-Whitney and Spearman tests were used with 95% confidence. In the TB group, there was growth of the right CO (1.33mm) and, left CO (1.34mm), and of the right GC (0.80mm) and left GC (0.48mm) in a posterior direction. In the HB group there was growth of the right CO (1.43mm), and left CO (1.77mm), and of the right GC (0.12mm) and left GC (0.17) in a posterior direction. There was no difference in effects on CO and GC when TB and HB were used. The pilot study aimed to evaluate the changes in CO and GC resulting from the use of TB in the treatment of Class II malocclusions after one year of TB removal. In this study, 12 patients (11.92 ± 1.08 years) were evaluated using CBCT and were registered before (T0), during (T1: 12 months) and after (T2: 12 months) treatment. Full 3D models of T0, T1 and T2 were superimposed on Dolphin Imaging. Partial 3D models of the CO and GC were segmented in ITK-SNAP. In Geomagic Qualify a coordinate system (X, Y and Z axes) was created on each complete T0 and T1 3D models and then the CO and GC partial models were aligned. In each CO and CG, a 3D centroid point was generated and evaluated at T0 - T1, T0 - T2 and T1 - T2. Wilcoxon and Friedman multivariate tests were used with 95% confidence. In the periods T0 - T1 and T0 - T2, significant growth of right and left CO and GC, respectively, was found in the posterior direction. CO also grew significantly in the upward direction and GC in the downward direction, although not significantly. Patients who used TB had growth of the CO in a posterior and superior direction and of the GC in a posterior and inferior direction. The amount of CO growth was greater than the amount of GC growth

Keywords: class II malocclusion; functional appliance; craniofacial growth; cone beam computed tomography.

SUMÁRIO

	INTRODUÇÃO.....	9
1	PROPOSIÇÃO.....	12
2	DESENVOLVIMENTO.....	13
2.1	Analysis of three-dimensional condyle and glenoid fossa alterations following treatment with Twin Block and Herbst functional appliances for the treatment of Class II malocclusions (Artigo científico).....	13
2.2	An analysis of condyle and glenoid fossa alterations after utilization of the Twin Block appliance in patients Class II malocclusion: A longitudinal retrospective 3D study (Artigo científico).....	39
	CONCLUSÃO.....	67
	REFERÊNCIAS.....	68
	ANEXO A – Metodologia do Estudo.....	72
	ANEXO B – Aprovação do Comitê de Ética em Pesquisa 1 e Pesquisa 2.....	81
	ANEXO C – Política de compartimentos do Artigo.....	82
	ANEXO D – Autorização dos Coautores artigo 1.....	83
	ANEXO E – Autorização dos Coautores artigo 2.....	84
	ANEXO F – Constância de submissão do Artigo 1.....	85
	ANEXO G – Constância de submissão do Artigo 2.....	86

INTRODUÇÃO

A maloclusão dentária e esquelética de Classe II é frequentemente encontrada e tratada na prática ortodôntica. Essa maloclusão pode ser causada por protrusão maxilar, retrusão mandibular ou uma combinação de ambas as alterações. No entanto, a retrusão mandibular esquelética é sua característica mais comum (Mcnamara, 1981).

As maloclusões de Classe II não tendem a autocorrigir-se com o crescimento e requerem tratamento para corrigi-las, principalmente a anormalidade esquelética. Em pacientes em fase de crescimento, a modificação do crescimento de certas estruturas esqueléticas, como a mandíbula, pode ser alcançada por aparelhos funcionais, interceptando assim, a maloclusão (Hagg; Pancherz, 1988). O momento ideal relatado para modificar o crescimento ósseo é durante o pico de crescimento puberal (Ruf; Pancherz, 2006).

Os aparelhos funcionais para estimular o crescimento mandibular durante o tratamento da maloclusão de Classe II são basicamente de dois tipos: fixos e removíveis. Esses dispositivos buscam reposicionar e avançar a mandíbula, aguardando um estímulo de crescimento no nível condilar e na cavidade glenóide. Os aparelhos removíveis funcionais dependem totalmente da cooperação do paciente para obter resultados favoráveis, enquanto os aparelhos fixos funcionais eliminam esse fator de colaboração e fornecem forças contínuas na base óssea afetada (McNamara *et al.*, 1987).

Buscando identificar os efeitos esqueléticos e dentários dos aparelhos funcionais, estudos têm sido relatados usando ferramentas de avaliação bidimensionais (2D) como as radiografias cefalométricas (Pancherz, 1982) e tridimensionais (3D), como a ressonância magnética (Aidar *et al.*, 2013), a Tomografia axial Computadorizada (TC) (Arici *et al.*, 2008; Croft *et al.*, 1999) e a Tomografia Computadorizada de Feixe Cônico (TCFC) (Cevidanes *et al.*, 2006; Cevidanes *et al.*, 2009; Lecornu *et al.*, 2013; Yildirim *et al.*, 2014).

A TC e especialmente a TCFC são atualmente consideradas o "padrão ouro" como ferramenta para identificar e avaliar estruturas ósseas no diagnóstico 3D em Odontologia. Assim, várias análises que incluem a articulação temporomandibular (ATM) usando TC (Croft *et al.*, 1999; Arici *et al.*, 2008) e TCFC (Lecornu *et al.*, 2013; Yildirim *et al.*, 2014) foram realizadas em pacientes com mal oclusão esquelética de Classe II, que usavam dispositivos de propulsão da mandíbula. Dentre os estudos encontrados, destaca-se a utilização do aparelho de Herbits (HB) (Atresh *et al.*, 2018; Batista *et al.*, 2017; Cheib *et al.*, 2019; Croft *et al.*, 1999; Fan *et al.*, 2020; Nindra *et al.*, 2021; Lecornu *et al.*, 2013; Pancherz,

1982; Souki *et al.*, 2017; Taylor *et al.*, 2020;) e do aparelho Twin Block (TB) (Bowen *et al.*, 2013; Clark, 2002; Elfeky *et al.*, 2018; Jiang *et al.*, 2020; Lima, 2016; Yildirim *et al.*, 2014; MOHAMED *et al.*, 2020; Shetty *et al.*, 2021). A seleção dos aparelhos está relacionada à eficácia encontrada em estudos anteriores dos respectivos dispositivos (COzza *et al.*, 2006; Santamaria – Villegas *et al.*, 2017).

Quando o aparelho de HB foi utilizado como protocolo de tratamento, Souki *et al.*, (2017) encontraram 3,5mm de crescimento do côndilo na direção posterior, enquanto Croft *et al.*; (1999) encontraram 2,1 mm na mesma direção. É importante destacar, que ambos os trabalhos tiveram um grupo-controle. Souki *et al.*, (2017) utilizaram um grupo de tratamento ortodôntico sem forças ortopédicas e Croft *et al.*, (1999) utilizaram um grupo sem tratamento ortodôntico. Um fator a considerar na diferença de resultados, é que Souki *et al.*, (2017) usaram a TCFC e o método de identificação e superposição de volume, enquanto Croft *et al.*, (1999) usaram a TC e um método de superposição bidimensional baseado na cefalometria.

Souki *et al.*, (2017) também encontraram um crescimento do côndilo em direção superior, o que concorda com os resultados de Batista *et al.*, (2017), que encontrou no côndilo um crescimento de 8,4mm. Porém, Nindra *et al.*, (2021) relataram um aumento na altura do côndilo no lado direito de 1,35mm e no lado esquerdo de 1,21mm.

Lecornu *et al.*, (2013) num estudo prospectivo utilizando o aparelho de HB, observaram valores de deslocamento na direção anterior de 1,20mm para o côndilo direito e de 1,29mm para o côndilo esquerdo. O grupo-controle incluiu pacientes com elásticos classe II. No mesmo estudo, foram registrados deslocamentos na direção anterior da cavidade glenóide, sendo estes de 1,69mm. para a cavidade glenóide direita e de 1,43mm. para a cavidade glenóide esquerda. No entanto, Croft *et al.* (1999), observaram deslocamentos de 0,7mm na direção posterior e inferior da cavidade glenóide.

Lima (2016) analisou as alterações morfológicas do côndilo em uma amostra de 22 pacientes. Na amostra, 7 pacientes usaram o aparelho de HB e 15 usaram o aparelho TB. No grupo TB, o crescimento do côndilo direito foi de 6,12mm e do côndilo esquerdo foi de 6,34mm. No grupo com HB, o crescimento do côndilo direito foi de 7,01mm. e do côndilo esquerdo foi de 6,84mm. Não foi encontrada diferença significativa no crescimento do côndilo entre os grupos que usaram HB e TB.

Yildirim *et al.* (2014) realizaram um estudo retrospectivo de pacientes que faziam uso do aparelho TB. Foi encontrado crescimento na direção superior e posterior do côndilo. A amostra foi composta por trinta pacientes e não houve grupo-controle. A metodologia foi desenvolvida para calcular o volume do côndilo para identificar a quantidade de crescimento

ou remodelação óssea.

Bowen *et al.* (2013) avaliaram vinte pacientes que usaram o aparelho TB por 12 meses. Foi encontrado um aumento na altura do côndilo de $6,2 \pm 0,61$ mm. e um aumento anteroposterior de $7,22 \pm 0,84$ mm. Lima (2016), Yildirim *et al.* (2014) e Bowen *et al.* (2013) usaram o aparelho TB e as TCFC como ferramentas de avaliação em suas pesquisas.

O aumento do uso de imagens tridimensionais (3D) em Ortodontia permitiu o desenvolvimento de novas técnicas de sobreposição (Dot *et al.*, 2020) . Esses procedimentos usam estruturas anatômicas estáveis como referência para comparar as TCFC do mesmo paciente em momentos diferentes. Três métodos de sobreposições são descritos na literatura: sobreposições baseadas em marcas, sobreposições baseadas em superfícies e sobreposições baseadas em voxel.

Cevidanes *et al.* (2006) e Cevidanes *et al.* (2009) validaram um determinado método de sobreposição de imagens 3D de estruturas anatômicas. Os pacientes tinham média de idade de 11,4 anos. Foi realizada a sobreposição das tomografias registradas antes e depois do tratamento, encontrando um excelente grau de reprodução do método ao identificar deslocamentos e remodelações ósseas na maxila e mandíbula.

Ruellas *et al.* (2016) identificaram um método de sobreposição para avaliar o crescimento do côndilo. As estruturas estáveis da mandíbula foram selecionadas por registro e por região mandibular onde dentes, osso alveolar, ramo e côndilos não foram incluídos.

A TC e a TCFC permitem conhecer quantitativa e qualitativamente os efeitos sobre o côndilo e cavidade glenóide ao utilizar aparelhos com forças ortopédicas. No entanto, os efeitos causados pelos aparelhos funcionais durante o tratamento da Classe II ainda não estão bem esclarecidos (Al-Saleh *et al.*, 2015; Ding *et al.*, 2022; Kinzinger *et al.*, 2018; Koretsi *et al.*, 2015; Kyburz *et al.*, 2019; Zymperdikas *et al.*, 2016; Rzuchowski *et al.*, 2020; Santana *et al.*, 2020).

Portanto, um melhor entendimento das alterações ósseas que ocorrem nos componentes da ATM é de extrema relevância para que o ortodontista possa atuar com maior segurança e previsibilidade

1 PROPOSIÇÃO

A presente tese apresentou como objetivos:

Objetivo Geral

Avaliar as alterações ocorridas no côndilo e na cavidade glenóide decorrentes do uso dos aparelhos funcionais Twin Block e de Herbst no tratamento das maloclusões de classe II, através de observações tridimensionais após 1 ano de tratamento.

Objetivos específicos

- a) Comparar as modificações esqueléticas ocorridas no côndilo e na cavidade glenóide decorrentes do uso dos aparelhos funcionais Twin Block e de Herbst;
- b) Correlacionar as modificações esqueléticas ocorridas no côndilo e na cavidade glenóide decorrentes do uso dos aparelhos funcionais Twin Block e de Herbst.

2 DESENVOLVIMENTO

Nessa seção serão apresentados os artigos provenientes da tese de doutorado.

2.1 Analysis of three-dimensional condyle and glenoid fossa alterations following treatment with Twin Block and Herbst functional appliances for the treatment of Class II malocclusions (Artigo Científico)

Artigo Submetido no periódico American Journal of Orthodontics and Dentofacial Orthopedic classificado no Qualis da CAPES (Coordenação de Aperfeiçoamento de Pessoal de Nível Superior), na Área de Avaliação de Odontologia, como A1.

Chávez-Sevillano Manuel Gustavo¹, Felipe de Assis Ribeiro Carvalho², Tatiana Araújo de Lima³, Jose Augusto Mendes Miguel⁴, Klaus Barreto dos Santos Lopes Batista⁵, Daniel José Blanco-Victorio⁶, Luciana Quintanilha Pires Fernandes⁷, Cátia Cardoso Abdo Quintão⁸

¹ PhD student, Department of Orthodontics, Rio de Janeiro State University, Rio de Janeiro, RJ, Brazil. Address: Boulevard 28 de Setembro, 157; Vila Isabel – Rio de Janeiro, RJ, Brazil. E-mail: mchavezs@unmsm.edu.pe.

² Professor, Department of Orthodontics, Rio de Janeiro State University, Rio de Janeiro, RJ, Brazil. Address: Boulevard 28 de Setembro, 157; Vila Isabel – Rio de Janeiro, RJ, Brazil. E-mail: carvalhofar@gmail.com.

³ Professor, Department of Orthodontics, Veiga de Almeida University, Rio de Janeiro, RJ, Brazil. Address: R. Ibituruna, 108; Maracanã – Rio de Janeiro, RJ, Brazil. E-mail: tatiorto@gmail.com

⁴ Professor (chairman), Department of Orthodontics, Rio de Janeiro State University, Rio de Janeiro, RJ, Brazil. Address: Boulevard 28 de Setembro, 157; Vila Isabel – Rio de Janeiro, RJ, Brazil. E-mail: jamiguel66@gmail.com.

⁵ Professor, Department of Orthodontics, Rio de Janeiro State University, Rio de Janeiro, RJ, Brazil. Address: Boulevard 28 de Setembro, 157; Vila Isabel – Rio de Janeiro, RJ, Brazil. E-mail: : Klausbarreto@uol.com.br

⁶ Professor, Department of Medicine, Faculty of Health Sciences, University of Señor de Sipán, Lambayeque , Perú. E-mail: danielblanco92@outlook.com

⁷ PhD student, Department of Orthodontics, Rio de Janeiro State University, Rio de Janeiro, RJ, Brazil. Address: Boulevard 28 de Setembro, 157; Vila Isabel – Rio de Janeiro, RJ, Brazil. E-mail: lqpfernandes@hotmail.com

⁸ Professor, Department of Orthodontics, Rio de Janeiro State University, Rio de Janeiro, RJ, Brazil. Address: Boulevard 28 de Setembro, 157; Vila Isabel – Rio de Janeiro, RJ, Brazil. E-mail: catiacaq@gmail.com

Abstract

Introduction: The objective of the study was to evaluate the alterations in the condyle (CO) and glenoid fossa (GF) after treatment using Twin Block (TB) and Herbst (HB) functional appliances for skeletal Class II malocclusions. **Methods:** In this retrospective study, both the TB and HB groups consisted of 12 patients (TB, 11.92 ± 1.08 years; HB, 12.5 ± 1.87 years). Cone beam computed tomography (CBCT) scans were recorded before (T0) and after (T1) treatment (12 months). Full 3-dimensional (3D) models of T0 and T1 were superimposed on the Dolphin Imaging software. Partial 3D models of the CO and GF were segmented in ITK-SNAP (version 3.6; Cognitica, Philadelphia, Pa). In Geomagic Qualify (3D Systems, Rock Hill, SC), a coordinate system (X, Y and Z axes) was created in each 3D T0 model, and the CO and GF models were aligned in the 3D T0 and T1 models. In each CO and GF, a 3D centroid point was generated between T0 and T1. We analyzed data using the Wilcoxon, Mann-Whitney and Spearman tests at 95% confidence. **Results:** In the TB group, we observed a posterior growth in the right CO (1.33 mm, $p = 0.0186$), left CO (1.34 mm, $p = 0.023$), right GF (0.80 mm, $p = 0.0413$), and left GF (0.48, $p = 0.0414$). In the HB group, we observed a posterior growth in the right CO (1.43 mm, $p = 0.0060$), left CO (1.77 mm, $p = 0.0022$), right GF (0.12 mm, $p = 0.7240$), and left GF (0.17, $p = 0.5047$). **Conclusions:** In both groups, CO and GF grew posteriorly; CO grew vertically in the superior direction, and GF in the inferior direction. The effects on CO and GF were similar when using TB or HB

Keywords: Cone beam computed tomography, Class II Malocclusion, Functional Appliance.

Introduction

Class II dental and skeletal malocclusions are frequently encountered in orthodontic practice. They are caused by superior dentoalveolar and/or skeletal protrusion, mandibular retrusion, or their combination. However, mandibular retrusion is the most common feature¹. In children and adolescent patients, the growth stimulus of the mandible can be attained using functional orthopedic appliances, thus intercepting mandibular retrusion². The ideal period to modify bone growth coincides with the pubertal growth spurt³. Functional orthopedic appliances that stimulate mandibular growth are fixed and removable. They relocate and advance the mandible while waiting for growth at the level of the condyle (CO) and the glenoid fossa (GF)⁴.

Identifying the skeletal and dental effects of functional orthopedic appliances has prompted the use of different methods: lateral telerradiographs with cephalometric analysis⁵, magnetic resonance imaging (MRI)⁶, computed tomography (CT)^{7,8} and cone beam computed tomography (CBCT)⁹⁻¹². CBCTs are currently considered the "gold standard" in three-dimensional (3D) evaluations of bone structures in dentistry. CT and CBCT have been used to evaluate the effects of treating Class II skeletal malocclusion, considering the efficacy of some orthopedic devices^{13,14}, thereby prompting the use of Twin Blocks (TB)^{11,12,15-17} and Herbst appliances (HB)^{7,9,10,18-22}.

When TBs were used as treatment protocol, Yidirim *et al.*¹⁵ retrospectively evaluated 30 patients who used TB for 7.4 months. CO grew posterior-superiorly. Bowen *et al.*¹⁶ evaluated 20 patients who used TB for 12 months. An increase in CO height of 6.2 ± 0.61 mm and an anteroposterior increase of 7.22 ± 0.84 mm were detected. Elfeky *et al.*¹⁷ evaluated the condylar growth of 22 patients who used TB for 9.4 months, finding an anteroposterior dimensional increase in CO of 0.88 mm and 0.53 mm right and left respectively. They also found an increase in CO height by 1.59 mm and 1.10 mm in the right and left respectively. Finally, they described an anterior displacement of the CO of 1.5 mm and 1.3mm to the right and left, respectively. Jiang *et al.*¹¹ evaluated the CO in 17 patients who used TB for 8 months, and found that the CO grew posteriorly and superiorly. They also reported an anterior displacement of the CO. Shetty *et al.*¹² analyzed the CO of 15 patients who used TB for 12 months. They found that the CO grew superiorly and posteriorly.

Croft *et al.*⁷ analyzed 40 patients who used HB for 11 months using CT only. They found a significant posterior growth of 2.1 mm in the CO. They also reported a GF displacement of 0.7 mm in the postero-inferior direction. LeCornu *et al.*¹⁸ evaluating 7

patients who used HB for 11.42 ± 1.4 months, found an anterior displacement of CO and GF: CO was displaced by 1.2 mm and 1.29 mm on the right and left side respectively; GF was displaced 1.69 mm and 1.43 mm on the right and left side respectively. Souki *et al.*¹⁹ retrospectively evaluated 25 patients who used HB for 8 months. The CO grew by 3.5 mm in the superior and posterior direction. Batista *et al.*²⁰ evaluated 20 patients using the HB combined with skeletal anchorage for 12 months, and found that CO grew superiorly by 8.4 mm. Atresh *et al.*²¹ evaluated the CO and GF of 16 patients who used HB for 7.6 months. A posterior displacement of the CO and GF was found. Vilefort *et al.*²² evaluated 41 patients who used HB for 8–12 months. The displacement of CO was less than 0.75 mm. Fan *et al.*¹⁰ evaluated 20 patients who used HB for 8 months. Their CO grew by 1.5–2 mm in the superior direction. Nindra *et al.*⁹ evaluated CO and GF in 15 patients who used HB for 8–10 months. CO grew superiorly by 1.35 mm and 1.21 mm on the right and left sides respectively. They also found an anterior remodeling of the GF

The increased use of 3D imaging in orthodontics has facilitated the development of new tomographic superimposition methods to assess craniofacial bone changes. Three main techniques have been described in the literature based on landmarks, surfaces and voxels²³. Cevdanes *et al.*^{24,25} validated a method of superimposing 3D images of anatomical structures such as the maxilla and mandible in growing patients. Teixeira *et al.*²⁶ used the geometric center of each bone structure to be superimposed called the centroid. The changes in the position of the centroid made it possible to assess bone modifications presented in the anatomical structure in the X, Y and Z axes. Ruellas *et al.*²⁷ devised a superposition method to evaluate the growth of the CO based on stable structures of the mandible.

CT and CBCT provide quantitative and qualitative knowledge of bone effects of using functional orthopedic devices. However, these effects are still understudied and unclear; thereby **prompting** our study aimed at evaluating the changes in CO and GF caused by using TB and HB in the treatment of skeletal Class II malocclusions.

Material and Methods

This retrospective study was reviewed and approved by the Ethics Committee of the Pedro Ernesto University Hospital of the State University of Rio de Janeiro (Protocol number: CEP/HUPE: 2918). Considering an effect size of 0.95 with a significance level of 5% and a power of 80% to detect changes of 1.4 mm, a sample size of 12 patients was obtained for each group.

The sample was randomly divided into two groups according to the type of mandibular propulsion device used. The group that used the TB was made up of seven men (11.86 ± 1.07 years) and five women (12 ± 1.22 years). The group that used the HB was made up of six men (13.17 ± 0.98 years) and six women (11.83 ± 0.75 years). All patients had an ANB angle within 4.5° to 11.5° and an FMA angle within 16.7° to 36.2° . The sample was selected for convenience using the following inclusion criteria: Class II skeletal relationship, Class II division 1 malocclusion, ANB angle greater than 4° , minimum overjet of 6 mm and vertebral stages CS3-CS4²⁸. We excluded those with: previous orthodontic treatment, presence of cleft lip and palate, presence of dental agenesis or supernumerary teeth, and signs of temporomandibular dysfunction.

All patients were initially evaluated using CBCT (T0) and were placed on treatment for 12 months (T1) immediately after the removal of orthopedic devices. Full head scans were obtained using iCAT Classic software (Image patients, Hatfield, Pa), with a voxel size of 0.3 mm. The construction and analysis of the 3D images followed protocols described in previous studies^{24,26,27}. All the tomograms (48 CBCTs) of this study, in DICOM multi-file format, were imported into the ITK-SNAP software (<http://www.itksnap.org/pmwiki/pmwiki.php>), where the partial 3D models of the CO were segmented and the GF separating them from the complete 3D models^{11,22,29} constituted by the respective CBCTs T0 and T1. Thus, 192 partial 3D models were built (Figure 1). Moreover, they were exported and saved in stereolithographic (STL) format.

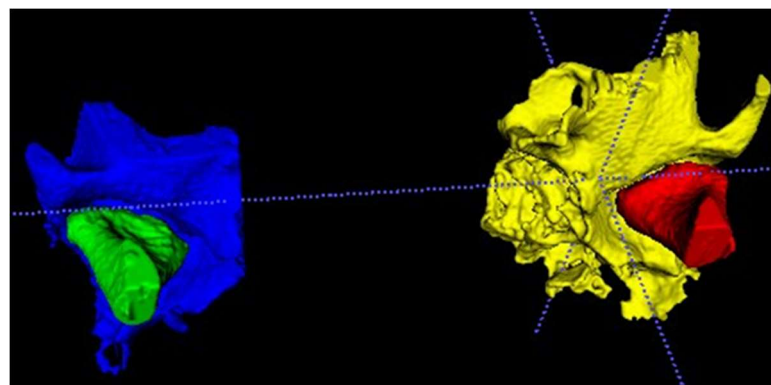


Figure1. Segmentation of the 3D models of CO and GF

In the Dolphin Imaging software, the CBCT voxels were downsized to 0.4 mm due to the limitation of the software in superimposing images with a greater resolution. Then, the posttreatment scan (T1) was superimposed onto the pretreatment CBCT (T0) (voxel-based), with records in the anterior **fossa** of the skull^{11,24} and in the mandibular symphysis^{27,30}

(Figures 2 and 3). Before the superimposition, the complete 3D model of each patient was oriented using the orbital plane, the Frankfurt horizontal plane (parallel to the floor); and the midsagittal plane determined using the Basion point, crista galli, and the glabella. To perform the superimposition on the chin, the mandibular plane remained horizontal; and the teeth, alveolar bone, and mandibular ramus were not considered^{11,27}. Following the previously described steps, the complete 3D models of T0 and T1 (oriented and registered) were exported in STL format.

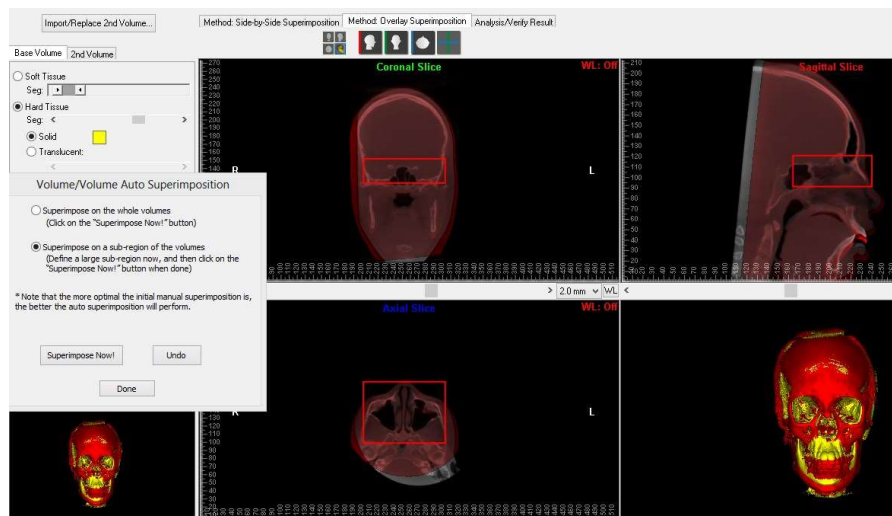


Figure 2. Superimposition of T1 on T0 in full 3D models with registration at the base of the skull

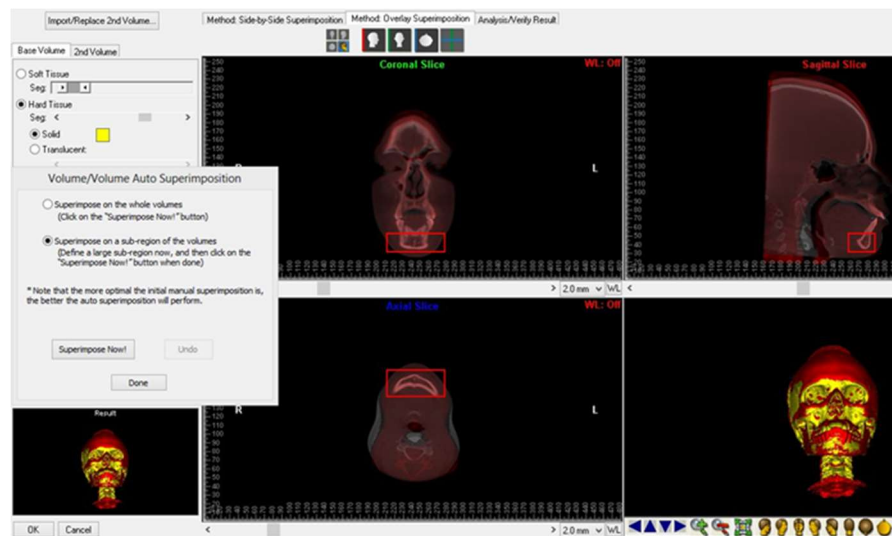


Figure 3. Superimposition of T1 on T0 in full 3D models with registration in the mandibular symphysis

After completing the orientation and superposition of the complete 3D models of T1 on T0 in the Geomagic Qualify 2013 software (3D Systems, Rock Hill, SC), a cartesian coordinate system was created for each complete model T0. Thus, all the complete 3D models shared the same coordinate system (T0 with its respective T1) with the X (axial plane), Y (coronal plane), and Z (sagittal plane) axes²⁶ (Figure 4).

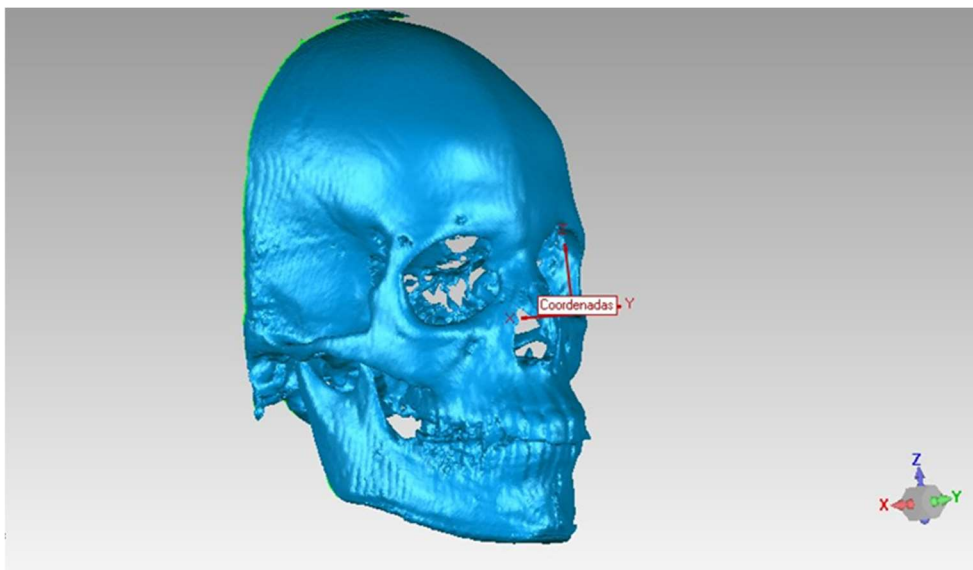


Figure 4. Complete 3D model of T0 with the coordinate system set in the Geomagic Qualify Software

In Geomagic Qualify software, full 3D models of oriented T0 and T1 superimposed and exported from Dolphin Imaging software were used to guide the alignment of the partial 3D models (CO and CG) initially segmented in ITK-SNAP software. Previously, the respective partial 3D models of T0 and T1 were duplicated and superimposed (best fit) to be trimmed, maintaining the same limits. These cutout models (CO and GF) were aligned to the respective full 3D models of T0 and T1. Individually, each partial anatomical structure was aligned to the total one, obtaining the same spatial orientation as the complete 3D models and sharing the same coordinate system²⁶ (Figure 5).

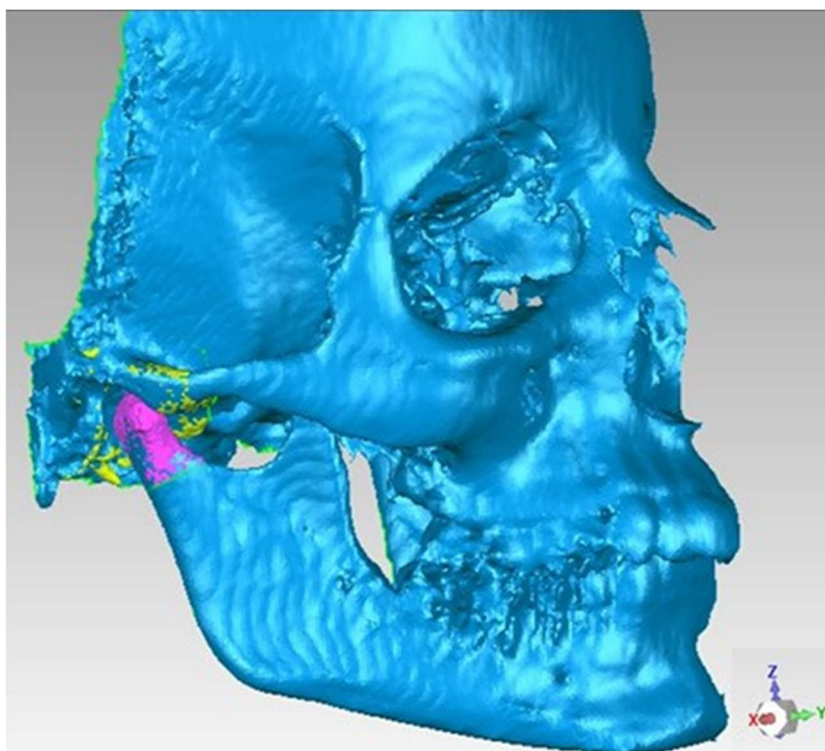


Figure 5. Partial 3D model of the CO (color pink) and GF (yellow color) aligned in the full 3D model (blue color). They all share the same coordinate system.

Since the superimposition and clipping of the partial 3D models had the same limits^{11,29}, it was possible to automatically determine the centroid point of each CO and GF in the Geomagic Qualify software. The centroid point of an anatomical structure is its geometric center, a point that has an average spatial position of all the centroids of the triangles making up the 3D structure. It represents the 3D spatial position of an anatomical region of interest (CO and GF) in relation to the three planes of space²⁶ (Figure 6).

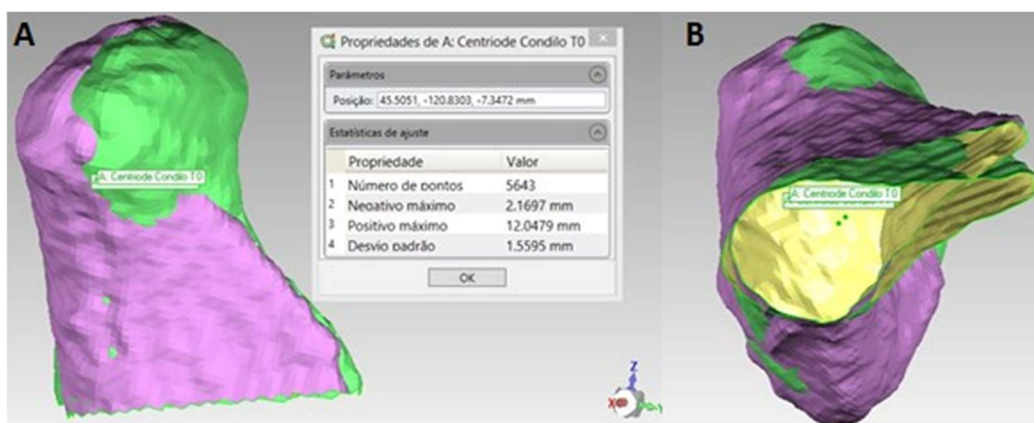


Figure 6. (A) Centriod of CO at T0 (green) and its coordinates; (B) Spatial

view of the centroids (green points) at T0 (green) and T1 (purple).

All CO and GF centroids were initially determined from the complete 3D models (T0 and T1) recorded and aligned in the anterior fossa of the skull, with which GF growth could be evaluated²⁴. To improve the assessment of condylar growth, the initial superimposition between the complete 3D models made in the symphysis was complemented with a regional recording at the level of the symphysis and body of the mandible as described in previous studies²⁷, preserving the respective systems of coordinates (T0 and T1) (Figure 7).

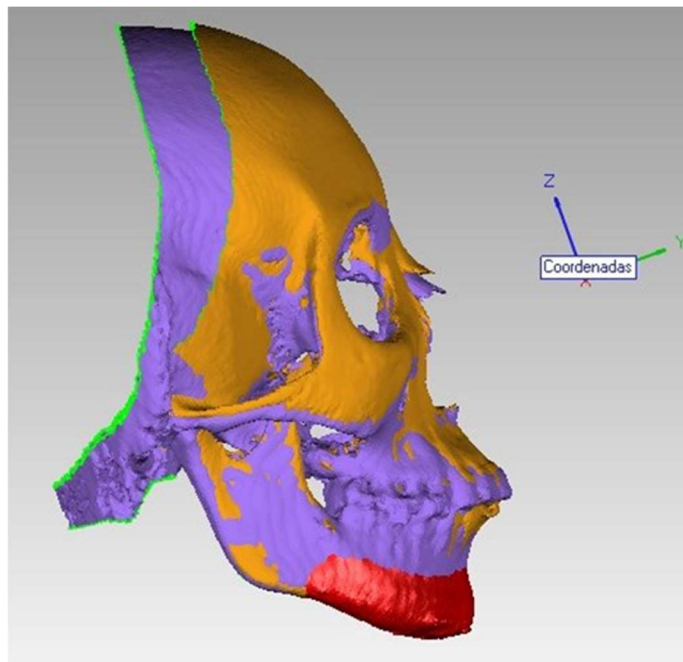


Figure 7. Mandibular regional registration of the complete 3D model of T1 in T0 encompassing the symphysis and mandibular body

Finally, the displacements and growth of the anatomical structures were determined by the difference in spatial position between the centroids of T0 and T1 of each region (CO and GF). Each centroid point had a 3D orientation with coordinates in the X (transverse), Y (anteroposterior) and Z (vertical) axes, established for each patient in the full 3D T0 image. On the X axis, the positive and negative values represented displacements to the right and left, respectively. On the Y axis, the positive and negative values represented displacements in the anterior and posterior direction, respectively. On the Z axis, the positive and negative

values represented displacements in the upper and lower directions, respectively.

To verify the reproducibility of the procedures performed in the study, a calibration was performed in ten randomly selected patients and all the 3D^{24,26,27} methodological steps were applied to the T0 and T1 tomograms. After 15 days the process was repeated. Intra and inter examiner correlations were conducted for the measurements, achieving an intraclass correlations coefficient >0.93 in all the cases.

Statistical analysis

Statistical analysis was performed with Stata 15.1 software (Stata Corp, USA). All analyses were performed with 95% confidence and $p \leq 0.05$. The normality of the sample was verified through the Shapiro Wilk test; however, considering the small sample ($n < 30$), non-parametric tests were used. To evaluate the differences between the results obtained between T0 and T1 for each treatment group (intra-group analysis), the Wilcoxon test was used. For the intergroup analysis (TB and HB), the Mann-Whitney test was used, comparing the position differences of the centroids between T0 and T1. Finally, Spearman's test was used to identify the correlation between the displacements of the CO and GF centroids in the different groups.

Results

The sample consisted of 24 growing patients with skeletal Class II, of which 12 used TB and 12 used HB for a period of 12 months. The morphological changes of the CO and GF were evaluated through the differences in positioning of the centroids of all the anatomical structures (CO and GF) between T0 and T1, in the transverse (X), anteroposterior (Y), and vertical directions (Z) for each group. A total of 96 3D images of CO (48 in T0 and 48 in T1) and 96 3D images of GF (48 in T0 and 48 in T1) were segmented.

In the TB group, a significant growth was found in the posterior direction (anteroposterior plane) of the right and left CO by 1.33 mm and 1.54 mm, respectively. Furthermore, we found a significant growth in the upper direction (vertical plane) of the right and left CO of 3.61 mm and 3.73 mm, respectively (Table 1 and Figure 8).

Table 1. Differences for changing CO between T0 and T1 in the TB group

	Axis	Time	Mean	Median	SD	Minimum	Maximum	Z	P-value*
Right condyle	X	T0	45.54	45.70	2.31	41.61	48.90	-2.667	0.00760*
		T1	46.44	46.42	2.73	41.82	50.25		
		T1-T0	0.90	1.03	0.91	-0.79	2.89		
	Y	T0	-114.40	-113.12	13.10	-136.60	-97.72	2.35	0.0186*
		T1	-115.73	-115.34	12.42	-136.41	-100.16		
		T1-T0	-1.33	-1.60	1.64	-4.05	1.73		
	Z	T0	-9.16	-8.51	2.70	-12.98	-5.06	-2.59	0.0096*
		T1	-5.56	-4.69	4.78	-13.59	0		
		T1-T0	3.61	4.32	3.28	-2.98	8.33		
Left condyle	X	T0	-44.83	-44.77	2.40	-49.66	-41.42	0.47	0.6379
		T1	-44.81	-44.76	2.05	-48.88	-42.01		
		T1-T0	0.02	-0.08	0.85	-0.96	2.10		
	Y	T0	-115.30	-113.41	13.26	-138.29	-97.84	2.28	0.023*
		T1	-116.84	-114.74	12.40	-138.01	-100.02		
		T1-T0	-1.54	-1.36	2.01	-5.38	1.45		
	Z	T0	-9.71	-9.17	2.38	-12.98	-4.85	-2.75	0.0060*
		T1	-5.97	-4.96	4.86	-15.46	1.71		
		T1-T0	3.73	3.81	3.29	-3.36	9.90		

*Wilcoxon test (signed rank test). Statistically significant.

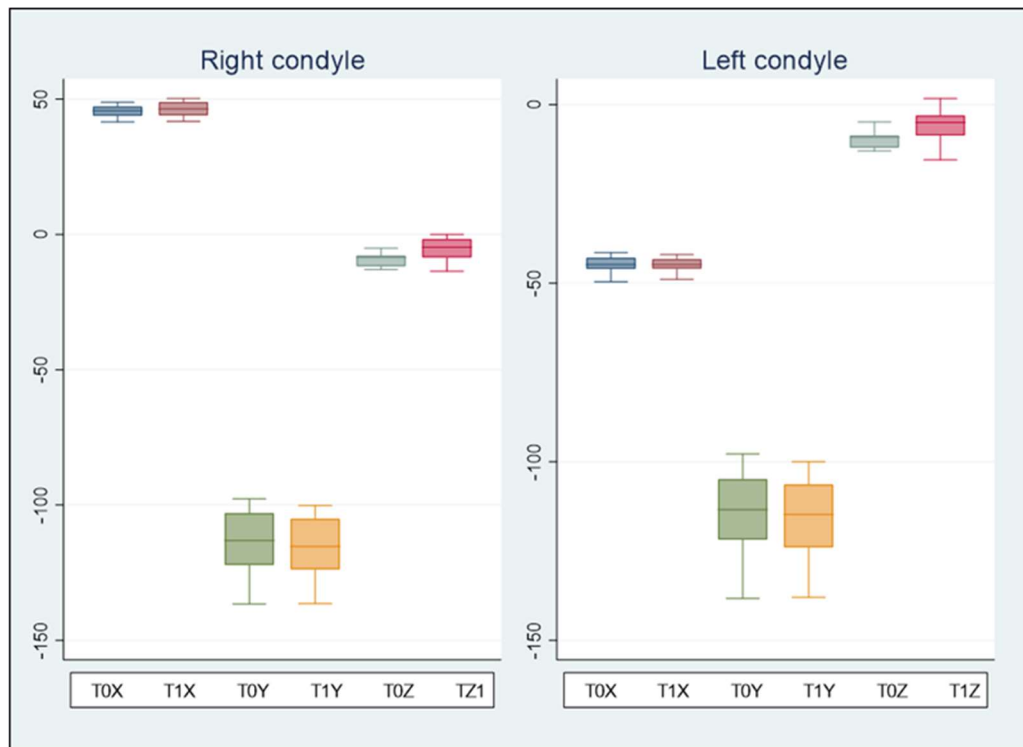


Figure 8. Box plot showing condyle values in Group TB.

Regarding the GF in the TB group, we noted a significant growth of the posterior direction of the right and left GF by 0.80 mm and 0.48 mm, respectively. GF growth in the inferior direction was also observed though insignificant (Table 2 and Figure 9).

Table 2. Different positions for GF between T0 and T1 in the TB group

	Axis	Time	Mean	Median	SD	Minimum	Maximum	Z	P-value*
GF right	X	T0	41,45	41,11	2,07	38,86	44,55	0,510	0,6098
		T1	41,56	41,51	2,39	37,29	46,20		
		T1-T0	0,12	0,19	0,93	-1,80	1,65		
	Y	T0	-116,74	-114,77	13,30	-141,82	-100,05	-2,04	0,0413*
		T1	-117,54	-116,56	12,94	-141,46	-101,87		
		T1-T0	-0,80	-0,70	1,09	-2,63	0,78		
	Z	T0	-2,38	-1,81	2,68	-6,89	0,70	-0,392	0,6949
		T1	-2,64	-2,20	2,76	-7,09	1,23		
		T1-T0	-0,26	-0,06	0,93	-2,60	0,71		
GF left	X	T0	-41,64	-41,36	2,45	-45,98	-38,74	-0,392	0,6949
		T1	-41,81	-41,59	2,77	-46,83	-37,73		
		T1-T0	-0,17	-0,40	0,99	-1,84	1,28		
	Y	T0	-117,15	-115,39	13,51	-142,06	-100,13	-2,040	0,0414*
		T1	-117,64	-116,22	13,21	-140,83	-100,45		
		T1-T0	-0,48	-0,67	0,71	-1,55	1,23		
	Z	T0	-2,33	-1,82	1,57	-5,17	-0,43	-1,569	0,1167
		T1	-3,07	-3,07	1,62	-5,58	0,57		
		T1-T0	-0,74	-0,68	1,29	-2,89	1,12		

*Wilcoxon test (signed rank test). Statistically significant.

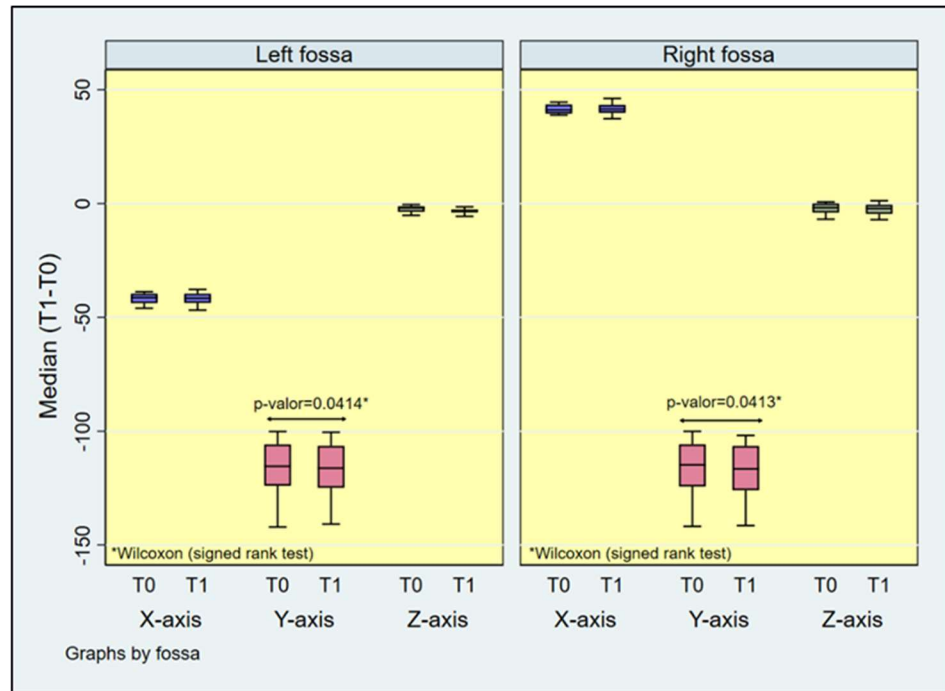


Figure 9. Box plot showing glenoid fossa values in Group TB

In the HB group, we noted a significant growth of the right and left CO in the posterior direction (anteroposterior plane) by 1.43 mm and 1.77mm respectively. We observed a significant growth in the upper direction (vertical plane) of the right and left CO by 4.56 mm and 4.53 mm, respectively. In the transverse plane, we noted a significant growth of the right and left CO by 0.70 mm and 0.63mm, respectively. Both condyles grew in a right and left direction respectively (Table 3 and Figure 10).

Table 3. Difference between the CO between T0 and T1 in group HB

	Axis	Time	Mean	Median	SD	Minimum	Maximum	Z	P-value*
Right condyle	X	T0	47,52	2,04	47,78	43,68	50,13	-2,82	0,0047*
		T1	48,22	2,17	48,08	44,33	51,24		
		T1-T0	0,70	0,58	0,74	-0,38	1,60		
	Y	T0	-112,64	12,57	-116,03	-126,71	-89,02	2.746	0,0060*
		T1	-114,07	13,13	-118,26	-128,62	-88,49		
		T1-T0	-1,43	1,21	-1,37	-3,17	0,53		
	Z	T0	-8,99	2,49	-8,78	-14,99	-4,86	-3.059	0,0022*
		T1	-4,43	3,60	-3,89	-9,99	2,15		
		T1-T0	4,56	2,06	4,52	0,77	8,26		
Left condyle	X	T0	-46,93	2,82	-46,38	-53,86	-43,12	2,080	0,0376*
		T1	-47,56	2,56	-46,86	-53,80	-44,70		
		T1-T0	-0.63	0.89	-0.74	-1.78	1.14		

Y	T0	-112,78	13,24	-118,19	-128,80	-85,87	3,059	0,0022*
	T1	-114,55	13,78	-119,75	-131,54	-86,26		
	T1-T0	-1,77	1,07	-1,82	-3,51	-0,24		
Z	T0	-9,25	2,54	-8,83	-15,63	-5,51	-2,981	0,0029*
	T1	-4,52	3,62	-4,30	-10,34	2,32		
	T1-T0	4,73	2,27	4,30	-0,16	7,83		

* Wilcoxon test (signed rank test) Statistically significant

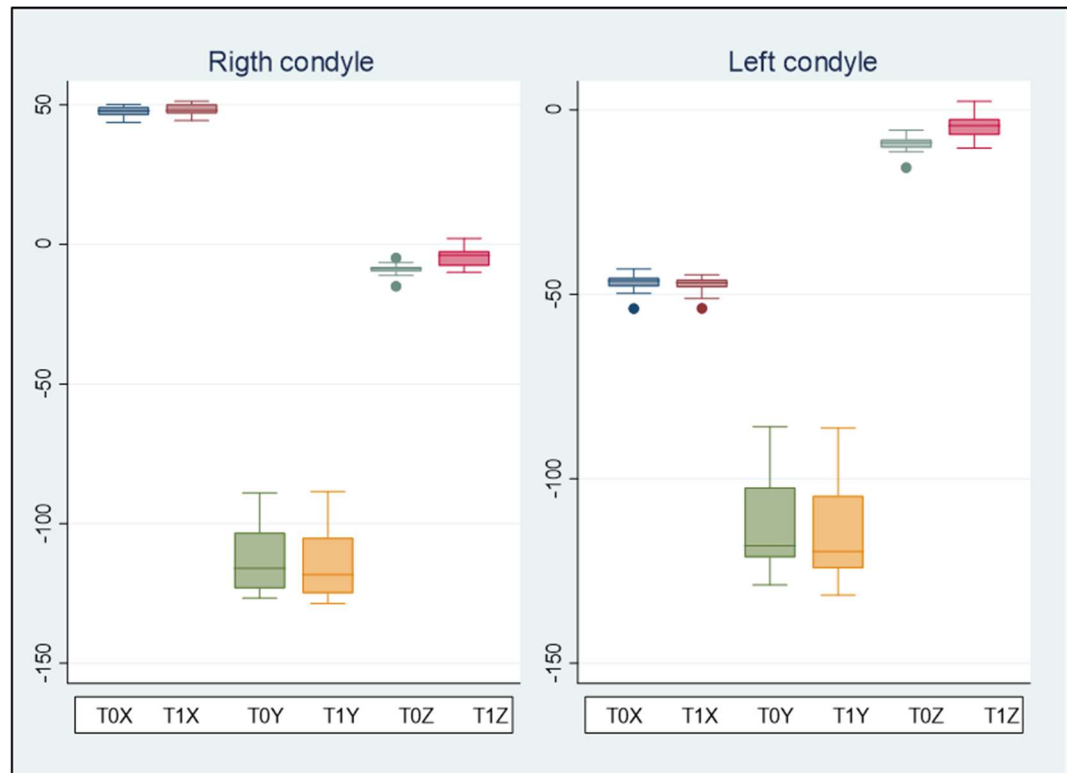


Figure 10. Box plot showing condyle values in Group HB.

Regarding the GF in the group that used the HB, only a significant growth of 0.73 mm was found in the inferior direction of the left CG. A significant growth of the right and left GF by 0.83 mm and 0.58 mm, respectively, was also observed. Both grew in the transverse plane in the right and left directions, respectively (Table 4 and Figure 11).

Table 4. Difference in positioning of the GF between T0 and T1 in the HB group

	Axis	Time	Mean	Median	SD	Minimum	Maximum	Z	P-value*
Right	X	T0	41,99	41,33	2,90	38,23	46,27	-2,824	0,0047*
		T1	42,81	42,14	2,59	39,38	46,57		
		T1-T0	0,83	0,57	0,99	-0,13	3,37		

GF Left	Y	T0	-115,45	-118,08	12,42	-133,03	-94,15	0,353	0,7240
		T1	-115,57	-118,92	11,95	-132,50	-94,27		
		T1-T0	-0,12	-0,20	1,08	-1,78	1,78		
	Z	T0	-2,06	-2,51	1,70	-4,82	0,85	0,784	0,4328
		T1	-2,31	-1,80	2,10	-6,77	1,06		
		T1-T0	-0,25	-0,53	1,00	-1,95	1,65		
	X	T0	-42,46	-41,86	4,24	-49,67	-35,31	2,197	0,0281*
		T1	-43,04	-42,79	3,92	-50,52	-36,87		
		T1-T0	-0,58	-0,70	0,85	-1,86	1,25		
GF Right	Y	T0	-115,54	-119,58	13,37	-132,72	-89,38	0,667	0,5047
		T1	-115,71	-119,68	13,34	-133,16	-88,81		
		T1-T0	-0,17	-0,19	0,75	-1,23	1,02		
	Z	T0	-1,48	-1,06	1,34	-3,74	0,27	3,059	0,0022*
		T1	-2,22	-1,88	1,78	-6,23	-0,15		
		T1-T0	-0,73	-0,39	0,77	-2,49	-0,07		

* Wilcoxon test (signed rank test) Statistically significant

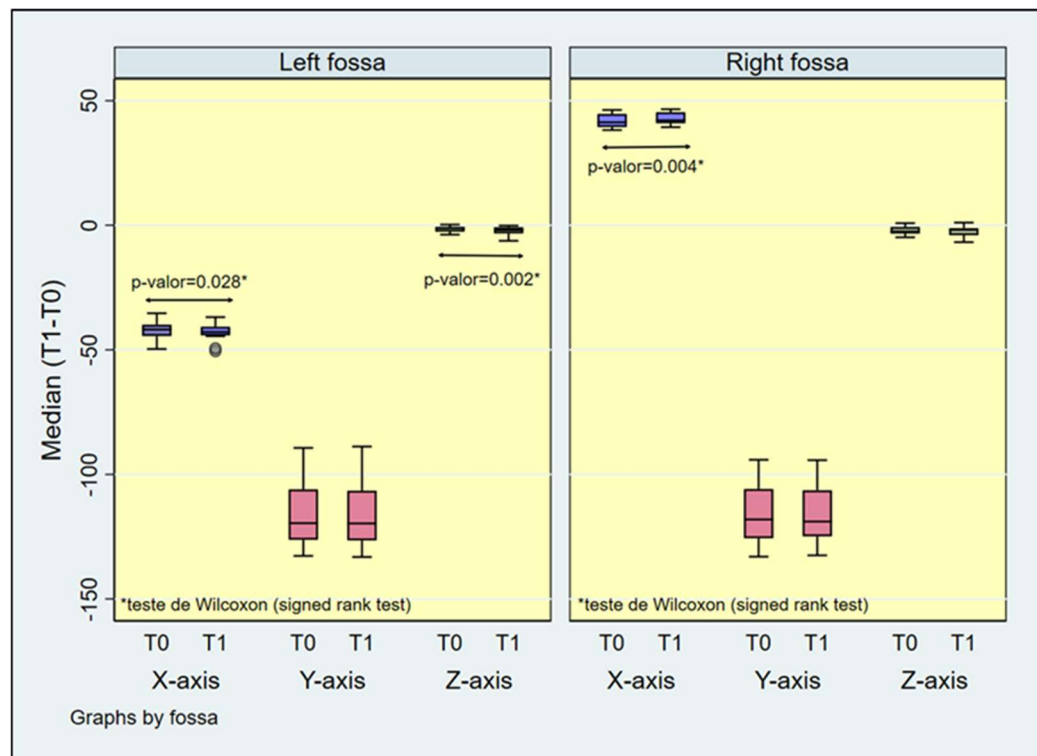


Figure 11. Box plot showing two values of the fossa in the HB group

When the differences in the displacements between the CO and GF centroids were compared between the groups that used TB and HB, no significant difference was found in relation to the displacement and growth of CO and GF in the three axes of space, X, Y and Z (Table 5 and Figure 12; Table 6 and Figure 13).

Table 5. Position differences of the CO between TB and HB.

	Axis	Time	Mean	Median	SD	Minimum	Maximum	p-value*
Right condyle	X	T1-T0_TB	0.90	0.91	-0.79	2.89	-0.462	0.644
		T1-T0_HB	0.70	0.58	-0.38	1.6		
	Y	T1-T0_TB	-1.33	1.64	-4.05	1.73	-0.058	0.954
		T1-T0_HB	-1.43	1.21	-3.17	0.53		
	Z	T1-T0_TB	3.61	3.28	-2.98	8.33	0.404	0.686
		T1-T0_HB	4.56	2.06	0.77	8.26		
Left condyle	X	T1-T0_TB	0.22	0.84	-0.96	2.09	-1.819	0.069
		T1-T0_HB	-0.58	0.85	-1.86	1.25		
	Y	T1-T0_TB	-1.54	2.01	-5.38	1.45	-0.866	0.387
		T1-T0_HB	-1.77	1.07	-3.51	-0.24		
	Z	T1-T0_TB	3.73	3.29	-3.36	9.9	0.924	0.356
		T1-T0_HB	4.73	2.27	-0.16	7.83		

*Mann-Whitney test. p>0.05 Non statistically significant

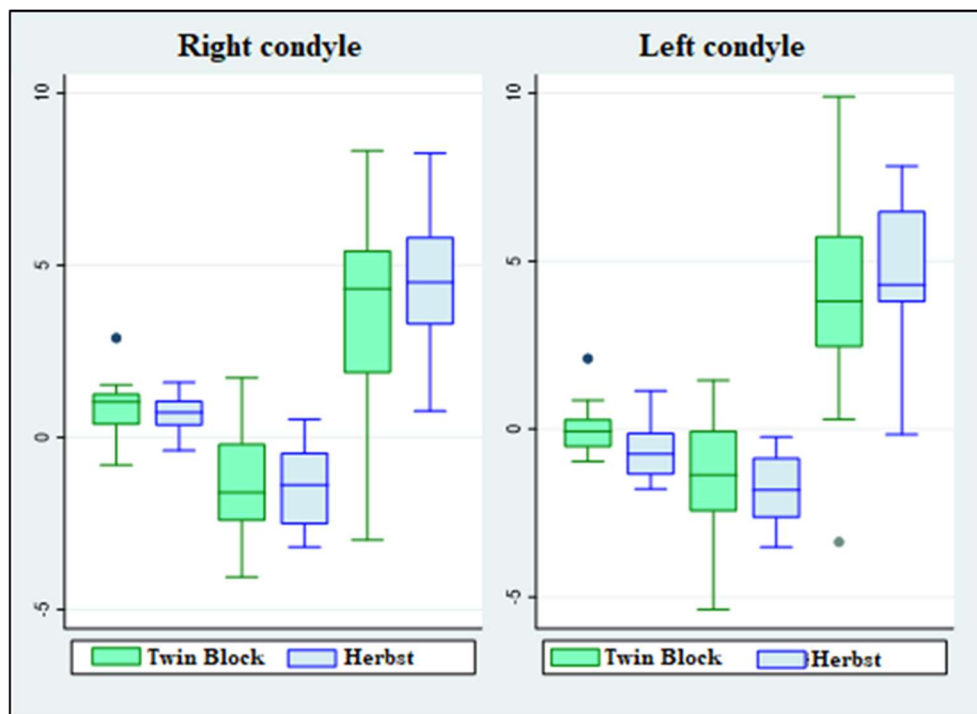


Figure 12. Box plot comparing the CO between groups using TB and HB

Table 6. Position differences of the GF between TB and HB

	Axis	Device	Media	SD	Min	Max	Z	p-value*
GF	X	T1-T0_TB	0,12	0,93	-1,8	1,65	1,560	0,119

Right		T1-T0_HB	0,83	0,99	-0,13	3,37		
	Y	T1-T0_TB	-0,8	1,09	-2,63	0,78		
		T1-T0_HB	-0,12	1,08	-1,78	1,78	1,328	0,184
	Z	T1-T0_TB	-0,26	0,93	-2,6	0,71		
		T1-T0_HB	-0,25	1,00	-1,95	1,65	-0,231	0,817
	X	T1-T0_TB	-0,17	0,99	-1,84	1,28		
GF	Y	T1-T0_TB	-0,48	0,71	-1,55	1,23	0,981	0,326
		T1-T0_HB	-0,17	0,75	-1,23	1,02		
	Z	T1-T0_TB	-0,74	1,29	-2,89	1,12	0,289	0,773
		T1-T0_HB	-0,73	0,77	-2,49	-0,07		
	X	T1-T0_TB	-0,17	0,99	-1,84	1,28		
		T1-T0_HB	-0,58	0,85	-1,86	1,25	-0,838	0,402

*Mann-Whitney test. $p > 0.05$ Non statistically significant

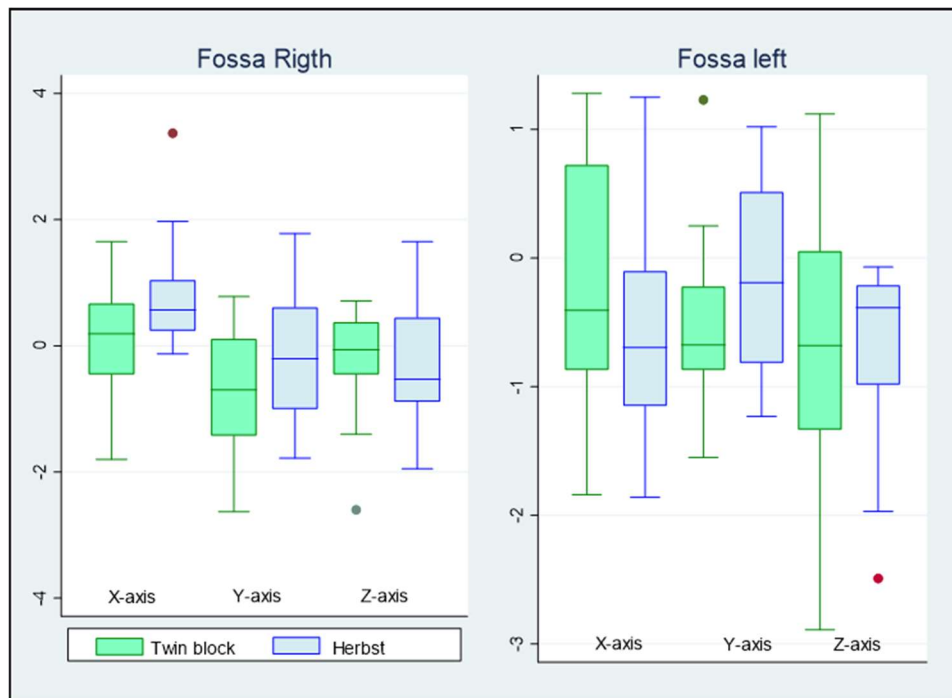


Figure 13. Box plot comparing the fossa between groups using TB and HB

When determining the correlation between the displacements of the CO and GF centroids, only in the group that used the TB, a strong positive correlation was found in the growth in the posterior direction (anteroposterior plane) of the CO and the right CG. However, on the left side the correlation was low and positive (Table 7).

Table 7 . Correlation of CO and GF positioning in the TB group

Axis	Herbst correlation	Spearman's Rho	p
------	--------------------	----------------	---

Right	X	CO – CG	0.24	0.44
	Y	CO – CG	0.75	0.004*
	Z	CO – GF	-0.53	0.07
Left	X	CO – CG	0.34	0.27
	Y	CO – CG	0.25	0.42
	Z	CO – GF	-0.09	0.76

* Spearman correlation, $p < 0.05$ Statistically significant

Discussion

Various studies have evaluated the craniofacial effects of fixed and removable functional appliances in the treatment of Class II malocclusion due to mandibular retrusion; revealing that such effects are mainly dental and minimally skeletal^{31,32}. However, primary growth centers of the mandible, and the real effect of functional appliances on the skeletal components of the temporomandibular joint are still unclear³³⁻³⁷.

Previously, morphological evaluations of the CO and GF were performed by two-dimensional methods⁵; however, with the inception CBCT, few studies have been carried out to assess the functions of CO and GF^{11,22}. . Therefore, in this study, we analyzed the skeletal effects of TB and HB appliances considering the efficiency demonstrated in previous studies^{13,14,31}.

In the present investigation, we performed 3D superimpositions of the CBCTs of 24 patients from T1 to T0, initially taking the anterior fossa of the skull base as the reference²⁴, thereby evaluating the growth of the GF. To assess the growth of CO, we performed a superimposition in the region of the symphysis of the mandible following methods described in previous studies^{27,30}. All overlays followed the voxel-based method performed in the Dolphin Imaging software. Since findings from the voxel-based and surface-based methods were similar³⁸, we performed a surface-based superposition using the Geomagic Qualify software, considering the symphysis and part of the mandibular body as reference to evaluate the condylar growth as proposed by Ruellas *et al.*²⁷.

Since CO and GF are not solid bodies with closed surfaces, the use of the centroid was proposed to identify their morphological changes during treatment. The centroid represents the geometric center of an anatomical structure. After superimposing and performing the cut delimiting the CO and the GF^{11,29}, and after creating the centroid, this point was broken down

into three axes (X, Y, Z) following the coordinate system previously assigned to the respective model (Full 3D T0). Previous studies suggested that these axes provide a more accurate 3D assessment of changes in the anatomical structure^{26,39}.

The results mainly described the displacements of the centroids related to the growth of CO and GF instead of the displacements of CO related to the effect of the devices used as described by Elfeky *et al.*¹⁷. In the TB group, a significant growth of 3.61 mm, and 3.73 mm was found in the right and left CO, respectively, in the superior direction (Z axis). This is consistent with findings by Yildirim *et al.*¹⁵, Bowen *et al.*¹⁶ (6.20 mm), Elfeky *et al.*¹⁷ (1.59 mm right and 1.10 mm left), Jiang *et al.*¹¹ and Shetty *et al.*¹². We also observed a significant growth of the right and left CO by 1.33 mm and 1.54 mm, respectively, in the posterior direction (Y axis) (Table 1). These findings are consistent with those from Yildirim *et al.*¹⁵, Bowen *et al.*¹⁶ (7.22 mm), Jiang *et al.*¹¹ and Shetty *et al.*¹². Regarding the GF, we noted a significant growth (remodeling) in the posterior direction (Y axis) by 0.80 mm and 0.48 mm on the right and left sides, respectively (Table 2). These findings are consistent with those from Jiang *et al.*¹¹, thereby suggesting that the GF remodels in an anteroposterior direction, adapting to the new position of the condyle. In addition, we observed a slight growth of the GF in the inferior direction (Z axis) by 0.26 mm and 0.74 mm on the right and left sides, respectively. This finding is inconsistent with that from Jiang *et al.*¹¹, who found areas of bone resorption in the superior wall of the GF.

In the HB group, we noted a significant growth of 4.56 mm and 4.73 mm in the right and left CO, respectively, in the superior direction (Z axis). These findings are consistent with those from Souki *et al.*¹⁹ (3.5 mm), Batista *et al.*²⁰ (8.4 mm), Fan *et al.*¹⁰ (1.5–2 mm), and Nindra *et al.*⁹ (1.35 mm). We also observed a significant growth in the right and left CO by 1.43 mm and 1.77 mm, respectively, in the posterior direction (Y axis) (Table 3). These findings are consistent with those from Croft *et al.*⁷ (2.1 mm), Souki *et al.*¹⁹ (3.5 mm) and Vilefort *et al.*²². In addition, we observed a significant growth of the GF by 0.83 mm and 0.58 mm on the right and left sides, respectively, in the lateral direction (X axis). These findings are consistent in the cross-sectional plane as described in previous studies. Again, we noted a significant growth of the GF by 0.25 mm and 0.73 mm on the right and left sides, respectively, in the inferior direction (Z axis). These results agree with those from Croft *et al.*⁷ (0.7 mm). Finally, we noticed a slight growth of the GF by 0.12 mm and 0.17 mm on the right and left sides, respectively, in the posterior direction (Y axis) (Table 4). These results agree with those from Atresh *et al.*²¹ and Croft *et al.*⁷ (0.7 mm). However, they are inconsistent with those from LeCornu *et al.*¹⁸ (1.69 mm right and 1.43 mm left) and Nindra *et al.*⁹, who observed

growth in the anterior direction. From our findings, we can deduce that the GF accompanies the CO in its growth in the posterior direction (Y axis) in both groups (TB and HB); however, in the vertical plane (Z axis), the GF tries to reach the CO and vice versa. This could be the suggested bone adaptation pattern during the use of TB and HB.

The effects of TB and HB on CO and GF were similar (Tables 5 and 6). There are no studies that compare the effect of these two devices with using CBCT on the GF. Results of previous studies such as O'Brien *et al.*⁴⁰, Shaefer *et al.*⁴¹ and Baysal *et al.*⁴² that were carried out using a two-dimensional cephalometric methodology are consistent with those found in this study, a greater mandibular growth with TB was found in the former studies, though insignificant. Nevertheless, the results of studies carried out with two-dimensional cephalometric methodology are more susceptible to error than using CBCT.

Published studies refer to various methods to assess CBCTs and their respective superimpositions. First, we established 2 tomographic times (T1 and T0) and performed the voxel based^{24,38} superposition, obtaining complete 3D models and establishing a coordinate system at T0. Second, we performed an automatic segmentation of the structures of interest (CO and GF) obtaining partial 3D models⁴³. Third, we aligned the partial 3D models on the complete 3D models already superimposed²⁶. Fourth, we established a centroid for each partial 3D model and its respective coordinates (X, Y and Z) in T1 and T0 to easily determine the displacements^{26,39}.

The sample size of the study was 12 patients per group, which is small to be considered as a stratified sample. During the evaluation of CO growth, it would be interesting to divide a larger sample according to the type of facial growth: dolichofacial, mesofacial, and brachifacial and compare the behaviors of CO and GF in the different groups.

To identify the real effect of a device, it is important to rule out the effect of growth, for which an adequate control group without any treatment is necessary. Within the named studies using TB and HB, some had a control group while others did not. Those with a control group used a standard treatment such as Class II elastics^{9,18,21} and very few a group without treatment^{7,11}. Since for ethical reasons it is increasingly difficult to find a sample of untreated patients with growing Class II malocclusion, and knowing that there are stable anatomical regions^{24,27}, an adequate validated overlapping protocol using CBCT could bring us closer to the real effect of a certain functional orthopedic device such as those applied in the present study.

When determining the correlation between the displacements of the CO and GF centroids, only in the group that used the TB, a positive correlation was found in the growth in

the posterior direction. The GF adapts to the growth of the CO, which does not seem to occur vertically, where GF and CO grow in the opposite direction but without a significant correlation. In the group that used HB, the non-significant correlation between CO and GF could be due to the sample size.

There is little evidence of 3D comparative studies evaluating the skeletal effects of TB and HB appliances in the treatment of skeletal Class II malocclusions⁴⁴. Therefore, the results of the present study seek to contribute to a better understanding of the effects of the appliances. functions most frequently used in orthodontic clinical practice.

Conclusions

1. Both groups experienced significant CO growth in the posterior and superior directions.
2. In both groups, the GF grew in the posterior and inferior direction, with significant growth in the posterior direction in the TB group.
3. The effects on CO and GF were similar on using TB and HB.
4. In the TB group, a positive correlation was found in growth in the posterior direction between CO and GF.

Funding

This article was supported in part by the Coordenação de Aperfeiçoamento de Pessoal de Nível Superior – Brazil (CAPES) – [Finance Code 001] and by the Fundação de Amparo à Pesquisa do Estado do Rio de Janeiro (FAPERJ).

References

1. McNamara J. Components of Class II Malocclusion in Children 8-10 Years of Age. *Angle Orthod* 1981; 51:177–202.
2. Hagg U, Pancherz H, Hägg U, Pancherz H. Dentofacial orthopaedics in relation to chronological age, growth period and skeletal development. An analysis of 72 male patients with class II division 1 malocclusion treated with the herbst appliance. *Eur J Orthod* 1988; 10(1):169–76.

3. Ruf S, Pancherz H. Herbst/multibracket appliance treatment of Class II division 1 malocclusions in early and late adulthood. a prospective cephalometric study of consecutively treated subjects. *Eur J Orthod* 2006; 28(4):352–60.
4. McNamaraJA, Bryan FA, Allen Bryan F. Long-term mandibular adaptations to protrusive function: an experimental study in *Macaca mulatta*. *Am J Orthod Dentofac Orthop* 1987; 92(2): 98–108.
5. Pancherz H. Vertical dentofacial changes during Herbst appliance treatment. A cephalometric investigation. *Swed Dent J Suppl* 1982;15:189–96.
6. Aida LA de A, Abrahão M, Yamashita HK, Dominguez GC. Morphological changes of condyles and Helkimo clinical dysfunction index in patients treated with herbst - Orthodontic appliance. *Braz Dent J* 2013; 24(4):313–21.
7. Croft RS, Buschang PH, English JD, Meyer R. A cephalometric and tomographic evaluation of Herbst treatment in the mixed dentition. *Am J Orthod Dentofacial Orthop* 1999;116(4):435–43.
8. Arici S. Akan H, Yakubov K, Arici N. Effects of fixed functional appliance treatment on the temporomandibular joint. *Am J Orthod Dentofac Orthop* 2008;133(6):809–14.
9. Nindra J, Sidhu MS, Kochhar AS, Dabas A, Valletta R, Rongo R, *et al.* Three-dimensional evaluation of condyle-glenoid fossa complex following treatment with herbst appliance. *J Clin Med* 2021;10(20):4730.
10. Fan Y, Schneider P, Matthews H, Roberts WE, Xu T, Wei R, *et al.* 3D assessment of mandibular skeletal effects produced by the Herbst appliance. *BMC Oral Health* 2020; 20(1):1–9.
11. Jiang Y. Lian Sun, Wang H, Zhao C, Zhang W-B, Zhang Professor W-B. Three-dimensional cone beam computed tomography analysis of temporomandibular joint response to the Twin-block functional appliance. *Korean J Orthod* 2020; 50(2): 86–97
12. Shetty VG, Shetty KN. Evaluation of skeletal changes in mandibular ramus height, corpus length, and mandibular angle changes following twin block appliance therapy using cone-beam computed tomography: A clinical prospective study. *Int J Orthod* 2021 ;12(3):115.
13. Cozza P, Baccetti T, Franchi L, De Toffol L, McNamaraJA. Mandibular changes produced by functional appliances in Class II malocclusion: A systematic review. *Am J Orthod Dentofac Orthop* 2006;129(5):599.e1-599.e12.
14. Santamaría-Villegas A, Manrique-Hernandez R, Alvarez-Varela E, Restrepo-Serna C. Effect of removable functional appliances on mandibular length in patients with class II

- with retrognathism: Systematic review and meta-analysis. *BMC Oral Health*. 2017;17(1):1–9.
15. Yildirim E, Karacay S, Erkan M. Condylar response to functional therapy with Twin-Block as shown by cone-beam computed tomography. *Angle Orthod*. 2014; 84(6):1018–25.
 16. Bowen L, Yanmin W, Fang S, Min L, Ying D, Li Z. Analysis of temporomandibular joint changes before and after Twin-block correction by cone-beam CT analysis of Class II division 1 malocclusion. *West China of Stomatology* 2013;31(6):610–4.
 17. Elfeky HY, Fayed MS, Alhammadi MS, Soliman SAZ, El Boghdadi DM. Three-dimensional skeletal, dentoalveolar and temporomandibular joint changes produced by Twin Block functional appliance. *J Orofac Orthop* 2018;79(4):245–58.
 18. Lecornu M., Cevidanes LHSS, Zhu H, Wu C-D Da, Larson B, Nguyen T, *et al*. Three-dimensional treatment outcomes in Class II patients treated with the Hrbst appliance: A pilot study. *Am J Orthod Dentofac Orthop* 2013;144(6):818–30.
 19. Souki BQ, Vilefort PLC, Oliveira DD, Andrade I, Ruellas AC, Yatabe MS, *et al*. Three-dimensional skeletal mandibular changes associated with Herbst appliance treatment. *Orthod Craniofac Res*. 2017;20(2):111–8.
 20. Batista KB dos SL, Lima T, Palomares N, Carvalho F de A, Quintão C, Miguel JAM, *et al*. Herbst appliance with skeletal anchorage versus dental anchorage in adolescents with Class II malocclusion: Study protocol for a randomised controlled trial. *Trials*. 2017;18(1):1–11.
 21. Atresh A, Cevidanes LHS, Yatabe M, Muniz L, Nguyen T, Larson B, *et al*. Three-dimensional treatment outcomes in Class II patients with different vertical facial patterns treated with the Herbst appliance. *Am J Orthod Dentofac Orthop* 2018;154(2):238-248.
 22. Cheib Vilefort PL, Farah LO, Gontijo HP, Moro A, Ruellas AC de O, Cevidanes LHS, *et al*. Condyle-glenoid fossa relationship after Herbst appliance treatment during two stages of craniofacial skeletal maturation: A retrospective study. *Orthod Craniofac Res* 2019; 22(4):345–53.
 23. Dot G, Rafflenbeul F, Salmon B. Voxel-based superimposition of Cone Beam CT scans for orthodontic and craniofacial follow-up: Overview and clinical implementation. *Int Orthod* 2020; 18(4):739–48.
 24. Cevidanes LHC, Heymann G, Cornelis MA, DeClerck HJ, Tulloch JFC. Superimposition of 3-dimensional cone-beam computed tomography models of

- growing patients. *Am J Orthod Dentofac Orthop* 2009;136(1):94–9.
25. Cevidanes LHS, Styner MA, Proffit WR. Image analysis and superimposition of 3-dimensional cone-beam computed tomography models. *Am J Orthod Dentofac Orthop* 2006;129(5):611–8.
 26. Otranto de Britto Teixeira A, Almeida MA de O, Almeida RC da C, Maués CP, Pimentel T, Ribeiro DPB, *et al.* Three-dimensional accuracy of virtual planning in orthognathic surgery. *Am J Orthod Dentofac Orthop* 2020;158(5):674–83.
 27. De Oliveira Ruellas AC, Yatabe MS, Souki BQ, Benavides E, Nguyen T, Luiz RR, *et al.* 3D mandibular superimposition: Comparison of regions of reference for voxel-based registration. *PLoS One* 2016;11(6):1–13.
 28. Baccetti T, Franchi L, McNamaraJA. The Cervical Vertebral Maturation (CVM) Method for the Assessment of Optimal Treatment Timing in Dentofacial Orthopedics. *Semin Orthod* 2005;11(3):119–29.
 29. Yatabe M, Garib D, Faco R, De Clerck H, Souki B, Janson G, *et al.* Mandibular and glenoid fossa changes after bone-anchored maxillary protraction therapy in patients with UCLP: A 3-D preliminary assessment. *Angle Orthod* 2017;87(3):423–31.
 30. Koerich L, Burns D, Weissheimer A, Claus JDP. Three-dimensional maxillary and mandibular regional superimposition using cone beam computed tomography: a validation study. *Int J Oral Maxillofac Surg* 2016;45(5):662–9.
 31. Koretsi V, Zymperdikas VF, Papageorgiou SN, Papadopoulos MA, Koretsi V, Papageorgiou SN, *et al.* Treatment effects of removable functional appliances in patients with Class II malocclusion: a systematic review and meta-analysis. *Eur J Orthod* 2015 ;37(4):418–34.
 32. Zymperdikas VF, Koretsi V, Papageorgiou SN, Papadopoulos MA. Treatment effects of fixed functional appliances in patients with Class II malocclusion: A systematic review and meta-analysis. *Eur J Orthod* 2016;38(2):113–26.
 33. Kyburz KS, Eliades T, Papageorgiou SN. What effect does functional appliance treatment have on the temporomandibular joint? A systematic review with meta-analysis. *Prog Orthod* 2019;20(1).
 34. Kinzinger GSM, Lisson JA, Booth D, Hourfar J. Are morphologic and topographic alterations of the mandibular fossa after fixed functional treatment detectable on tomograms? Visual classification and morphometric analysis. *J Orofac Orthop.* 2018; 79(6):427-439.
 35. Kinzinger GSM, Hourfar J, Kober C, Lisson JA. Mandibular fossa morphology during

- therapy with a fixed functional orthodontic appliance : A magnetic resonance imaging study. *J Orofac Orthop* 2018;79(2):116–32.
36. Ding L, Chen R, Liu J, Wang Y, Chang Q, Ren L. The effect of functional mandibular advancement for adolescent patients with skeletal class II malocclusion on the TMJ: a systematic review and meta-analysis. *BMC Oral Health* 2022;22(1):1–18.
 37. Rzuchowski G, Mikulewicz M. Bone Changes in the Condylar Process of the Mandible in Computed Tomography Images and Cephalogram in a Female Patient during a Growth Spurt Treated with a Removable Functional Appliance. *J Healthc Eng* 2020;2020: 8887182.
 38. Almukhtar A, Ju X, Khambay B, McDonald J, Ayoub A. Comparison of the accuracy of voxel based registration and surface based registration for 3D assessment of surgical change following orthognathic surgery. *PLoS One* 2014;9(4):1–6.
 39. Hsu SSP, Gateno J, Bell RB, Hirsch DL, Markiewicz MR, Teichgraeber JF, *et al.* Accuracy of a computer-aided surgical simulation protocol for orthognathic surgery: A prospective multicenter study. *J Oral Maxillofac Surg* 2013;71(1):128–42.
 40. O'Brien K, Wright J, Conboy F, Sanjie YW, Mandall N, Chadwick S, *et al.* Effectiveness of treatment for class II malocclusion with the Herbst or Twin-block appliances: A randomized, controlled trial. *Am J Orthod Dentofac Orthop* 2003;124(2):128–37.
 41. Schaefer AT, McNamaraJA, Franchi L, Baccetti T. A cephalometric comparison of treatment with the Twin-block and stainless steel crown Herbst appliances followed by fixed appliance therapy. *Am J Orthod Dentofac Orthop* 2004;126(1):7–15.
 42. Baysal A, Uysal T. Dentoskeletal effects of Twin Block and Herbst appliances in patients with Class II division 1 mandibular retrognathia. *Eur J Orthod* 2014;36(2):164–72.
 43. De Assis Ribeiro Carvalho F, Cevidan LHS, da Motta ATS, de Oliveira Almeida MA, Phillips C. Three-dimensional assessment of mandibular advancement 1 year after surgery. *Am J Orthod Dentofac Orthop*. 2010;137(4 SUPPL.):53–5.
 44. Pacha MM, Fleming PS, Johal A. A comparison of the efficacy of fixed versus removable functional appliances in children with class ii malocclusion: A systematic review. *Eur J Orthod* 2016;38(6):621–30.

2.2 An analysis of condyle and glenoid fossa alterations after utilization of the Twin Block appliance in patients Class II malocclusion: A longitudinal retrospective 3D study (Artigo científico)

Artigo submetido no periódico Journal of Orthodontics classificado no Qualis da CAPES (Coordenação de Aperfeiçoamento de Pessoal de Nível Superior), na Área de Avaliação de Odontologia, como A4.

Chávez-Sevillano Manuel Gustavo¹, Felipe de Assis Ribeiro Carvalho², Tatiana Araújo de Lima³, Daniel José Blanco-Victorio⁴, Luciana Quintanilha Pires Fernandes⁵, Cátia Cardoso Abdo Quintão⁶

¹PhD student, Department of Orthodontics, Rio de Janeiro State University, Rio de Janeiro, RJ, Brazil. Address: Boulevard 28 de Setembro, 157; Vila Isabel – Rio de Janeiro, RJ, Brazil. E-mail: mchavezs@unmsm.edu.pe.

²Professor, Department of Orthodontics, Rio de Janeiro State University, Rio de Janeiro, RJ, Brazil. Address: Boulevard 28 de Setembro, 157; Vila Isabel – Rio de Janeiro, RJ, Brazil. E-mail: carvalhofar@gmail.com.

³Professor, Department of Orthodontics, Veiga de Almeida University, Rio de Janeiro, RJ, Brazil. Address: R. Ibituruna, 108; Maracanã – Rio de Janeiro, RJ, Brazil. E-mail: tatiorto@gmail.com

⁴ Professor, Department of Medicine, Faculty of Health Sciences, University of Señor de Sipán, Lambayeque, Perú. E-mail: danielblanco92@outlook.com

⁵ PhD student, Department of Orthodontics, Rio de Janeiro State University, Rio de Janeiro, RJ, Brazil. Address: Boulevard 28 de Setembro, 157; Vila Isabel – Rio de Janeiro, RJ, Brazil. E-mail: lqpfernandes@hotmail.com.

⁶Professor, Department of Orthodontics, Rio de Janeiro State University, Rio de Janeiro, RJ,

Brazil. Address: Boulevard 28 de Setembro, 157; Vila Isabel – Rio de Janeiro, RJ, Brazil. E-mail: catiacaq@gmail.com

Abstract

Objective: This study aimed to evaluate alterations in the condyle (CO) and glenoid fossa (GF) resulting from the use of the Twin-block (TB) functional appliance in the treatment of Class II malocclusions, one year after removal of the TB.

Desing: This was a retrospective longitudinal study.

Setting: The study was conducted in Department of Orthodontics, Rio de Janeiro State University, Rio de Janeiro, Brazil.

Participants: Twelve patients (11.92 ± 1.08 years) were evaluated in the study.

Methods: The patients were evaluated using cone beam computed tomography (CBCT) recorded before (T0), during (T1: 12 months treatment), and after (T2: 12 months). Full three-dimensional (3D) models of T0, T1, and T2 were superimposed on Dolphing Imaging. Partial 3D models of the CO and GF were segmented in ITK-SNAP (version 3.6; Cognitica, Philadelphia, Pa). A coordinate system (X, Y, and Z axes) was created in each full 3D T0 and T1 model using Geomagic Qualify (3D Systems, Rock Hill, SC), followed by alignment of the partial CO and GF models. In each CO and GF, a 3D centroid point was generated, which was evaluated at T0–T1, T0–T2, and T1–T2. Wilcoxon and Friedman's multivariate tests were used at 95% confidence level.

Results: In the T0–T1 and T0–T2 periods, significant growth of the CO and the right and left GF was observed in the posterior direction. Moreover, the CO grew significantly in the upper direction, and the GF in the lower direction, but without statistical significance.

Conclusions: The patients who used TB experienced CO growth in the posterior and superior directions and GF growth in the posterior and inferior directions. The CO growth was greater than that of the GF.

Keywords: Cone Beam Computed Tomography, Class II Malocclusion, Functional Appliance.

Introduction

Class II skeletal malocclusion is one of the alterations with a high prevalence globally, accounting for approximately one third of orthodontic problems (Proffit *et al.*, 1998). The most common etiology of class II skeletal malocclusion is mandibular retrusion. When it occurs in young patients who are still growing, the main therapy consists of relocating and moving the mandible forward, while waiting for a growth stimulus at the condylar level (McNamara *et al.*, 1987). The ideal time to modify bone growth is during the pubertal growth peak (Ruf and Pancherz, 2006). Mandibular growth stimulation can be achieved using functional appliances, among which the Twin Block (TB) is one of the most used and reported in the literature (Cozza *et al.*, 2006; Bowen *et al.*, 2013; Yildirim *et al.*, 2014; Lima, 2016; Santamaria-Villegas *et al.*, 2017; Elfeky *et al.*, 2018; Mohamed *et al.*, 2020; Jiang *et al.*, 2020; Shetty *et al.*, 2021;). The aim of the procedure is to reposition and advance the mandible to stimulate growth at the level of the condyle (CO) and glenoid fossa (GF) (McNamara *et al.*, 1987).

To evaluate the skeletal and dental effects of functional orthopedic appliances, several studies have used different tools, such as cephalometric radiographs (Pancherz, 1982), magnetic resonance imaging (Aidar *et al.*, 2013), computed tomography (CT) (Croft *et al.*, 1999; Arici *et al.*, 2008), and cone beam computed tomography (CBCT) (Fan *et al.*, 2020; Jiang *et al.*, 2020; Nindra *et al.*, 2021; Shetty *et al.*, 2021). CBCT is currently considered the “gold standard” tool for evaluating bone structures in three-dimensional (3D) diagnostics in dentistry.

Yildirim *et al.* (2014) conducted a retrospective study evaluating 30 patients who used TB for 7.4 months. In this study, CO growth in the superior and posterior directions was observed. Bowen *et al.* (2013) evaluated 20 patients who used TB for 12 months, and an increase in CO height of 6.2 ± 0.61 mm and an anteroposterior increase of 7.22 ± 0.84 mm was observed. Elfeky *et al.* (2018) evaluated the condylar growth of 22 patients who used TB for 9.4 months, finding an anteroposterior dimensional increase in CO of 0.88 mm and 0.53 mm to the right and left, respectively. They also found an increase in CO height of 1.59 mm and 1.10 mm to the right and left, respectively. Finally, they described an anterior displacement of the CO of 1.5 mm and 1.3 mm to the right and left, respectively. Jiang *et al.* (2020) evaluated the CO and GF in 17 patients who used TB for 8 months. CO growth was observed in the superior and posterior directions. They also reported a displacement of CO in the anterior direction. In addition, they found that the GF was remodeled to adapt to the CO

with areas of resorption in the superior direction. Shetty *et al.* (2021) analyzed the CO of 15 patients who used TB for a 12-month period and observed CO growth in the superior and posterior directions.

The evaluation of 3D images in orthodontics has allowed the development of new tomographic superimposition methods to evaluate craniofacial bone changes. Three techniques are described in the literature: superimpositions based on landmarks, surfaces, and voxels (Dot *et al.*, 2020). Cevitanes *et al.* (2006, 2009) validated a method of superimposing 3D images in growing patients using anatomical structures such as the maxilla and mandible. Teixeira *et al.* (2020) used the geometric center of each bone structure to be superimposed, which they called centroid. The identification of the positional changes of the centroid made it possible to assess the bone modifications presented in the anatomical structure in the X, Y, and Z axes. Ruellas *et al.* (2016) identified a superposition method to evaluate CO growth based on stable structures of the jaw.

CT and CBCT allow us to quantitatively and qualitatively ascertain the bone effects resulting from the use of functional orthopedic appliances. However, the short-term and long-term effects are still not well clarified. Contradictory findings suggest that none of the existing 3D evaluation methods provide reliable measures for the GF after using functional appliances. Thus, this study aimed to evaluate the changes in CO and GF resulting from the use of TB in the treatment of class II malocclusions up to one year after appliance removal.

Material and methodology

This retrospective pilot study was reviewed and approved by the ethics committee of the Pedro Ernesto University Hospital of the State University of Rio de Janeiro (Protocol number: CEP/HUPE: 2918). A convenience sample was selected, consisting of 7 men (11.86 ± 1.07 years) and 5 women (12 ± 1.22 years). All patients underwent initial evaluation through CBCT imaging (T0) immediately after TB removal, followed by a 12-month treatment period (T1), and finally, a follow-up assessment at 12 months (T2). All the patients had an ANB angle in the range of 4.50 to 11.50 and a FMA angle of 16.70 to 36.20. The sample had the following inclusion criteria: class II skeletal relationship, class II division 1 malocclusion, ANB angle > 40 , minimum overjet of 6 mm, and vertebral stages CS3-CS4 (24). Exclusion criteria included: previous orthodontic treatment, presence of cleft lip and palate, presence of dental agenesis, or supernumerary teeth, and finally signs of temporomandibular dysfunction.

Methodology

Full head scans were obtained using iCAT classic software (Image patients, Hatfield, Pa), with a voxel size of 0.3 mm. The construction process and analysis of the 3D images followed protocols described in previous studies (Cevitanes *et al.*, 2009; Ruellas *et al.*, 2016; Teixeira *et al.*, 2020). All tomographies (36 CBCTs) were imported in DICOM multi-file format into the ITK-SNAP software (<http://www.itksnap.org/pmwiki/pmwiki.php>). Within this software, the partial 3D models of the CO were segmented, and the GF separating them from the complete 3D models (Yatabe *et al.*, 2017; Vilefort *et al.*, 2019; Jiang *et al.*, 2020), constituted by the respective CBCTs at T0, T1, and T2, was established. In total, 144 partial 3D models were built (Figure 1). All the partial 3D models built were exported and saved in stereolithographic (STL) format.

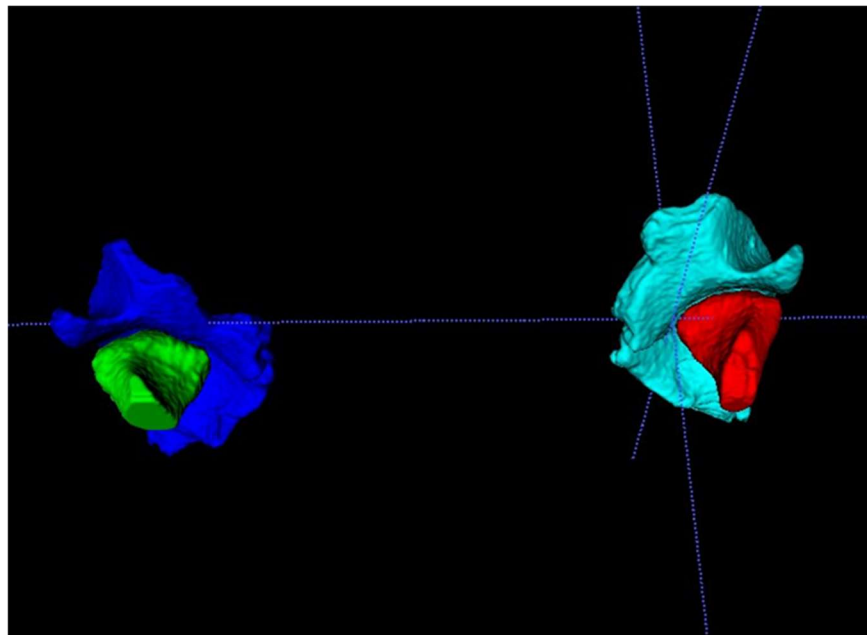


Figure 1. Segmentation of partial 3D models of CO and GF.

In the Dolphin imaging software, the CBCT voxels were downsized to 0.4 mm because of the limitation of the software in superimposing images with a greater resolution. Then, the posttreatment scan T1 and T2 were superimposed onto the pretreatment CBCT T0 (voxel-based) with records in the anterior fossa of the skull (Cevitanes *et al.*, 2009; Jiang *et al.*, 2020) and the mandibular symphysis (Koerich *et al.*, 2016; Ruellas *et al.*, 2016) (Figure 2 and 3). Before performing the superimposition of T1 and T2 at T0, the initial full 3D model (T0) of each patient was oriented using the orbital plane, the Frankfurt horizontal

plane (parallel to the floor), and the midsagittal plane, which was determined based on the basion point, crista galli, and glabella. To perform the superimposition on the chin, the mandibular plane remained horizontal, and the teeth, alveolar bone, and mandibular ramus were not considered (Ruellas *et al.*, 2016; Jiang *et al.*, 2020). After the previously described steps, the complete 3D models at T0, T1, and T2 (oriented and registered) were exported in STL format.

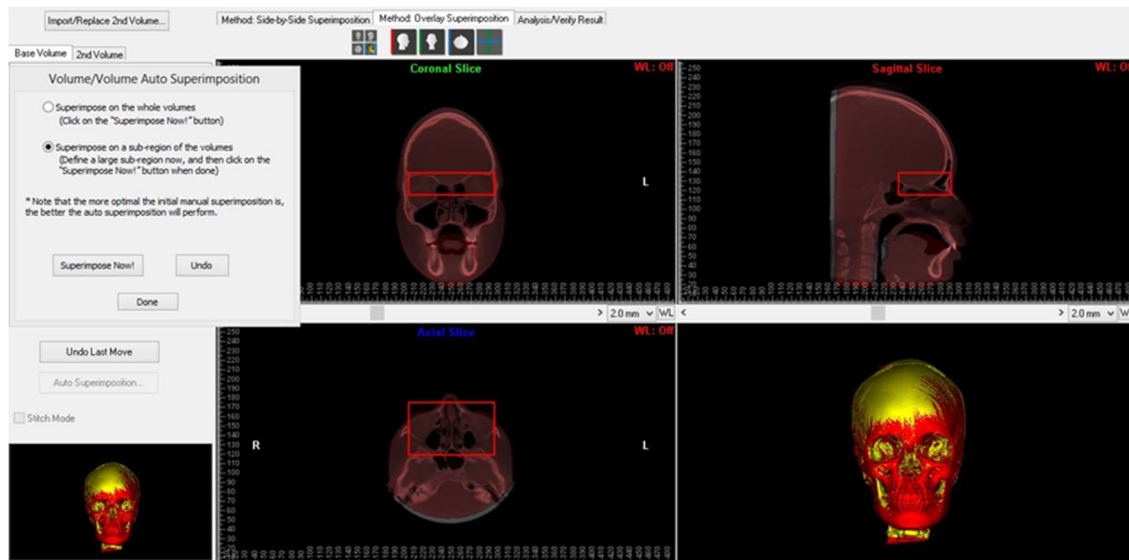


Figure 2. Superimposition of T1 on T0 in the full 3D models with registration at the base of the skull.

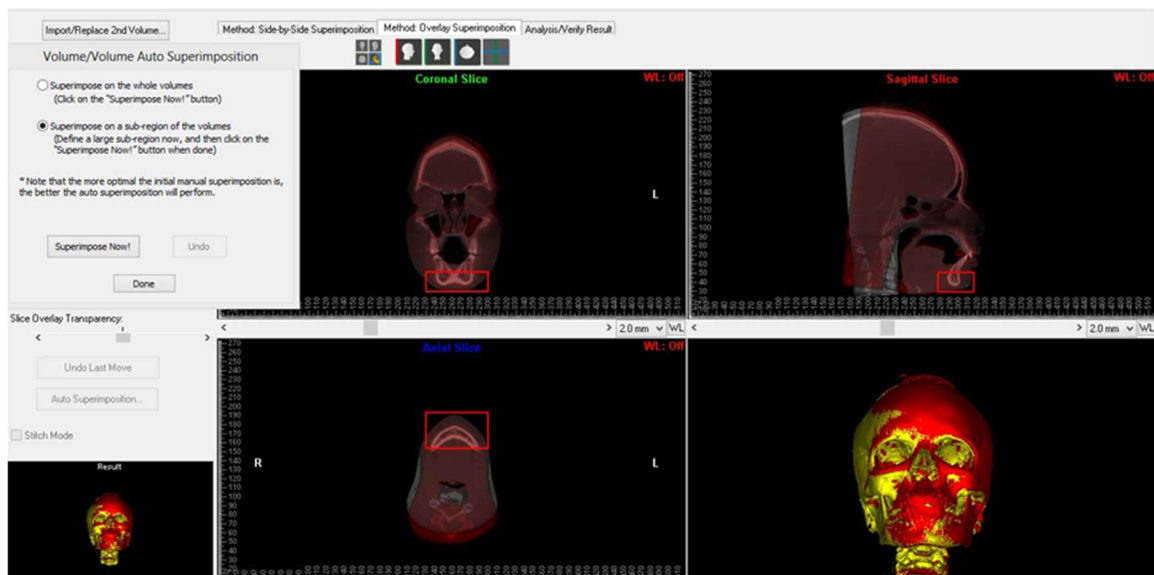


Figure 3. Superimposition of T2 on T0 in the full 3D models with registration in the mandibular symphysis.

After completing the orientation and superimposition processes of the complete 3D

models at T0, T1, and T2 in the Geomagic Qualify 2013 software (3D Systems, Rock Hill, SC), a cartesian coordinate system was created for each complete T0 model. Thus, all the complete 3D models began to share the same coordinate system (T0 with its respective T1 and T2) with the X (axial plane), Y (coronal plane), and Z (sagittal plane) axes (22) (Figure 4).

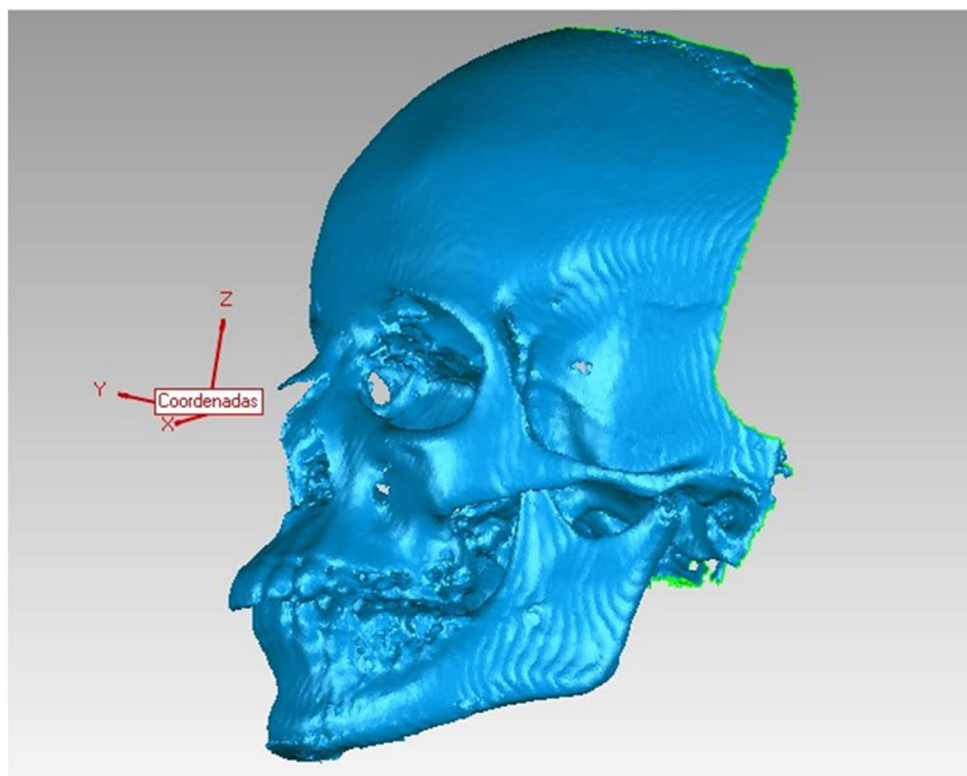


Figure 4. Complete 3D model T0 with the coordinate system established in the Geomagic Qualify software.

In the Geomagic Qualify software, the full 3D models of T0, T1, and T2 oriented, superimposed, and exported from the Dolphin imaging software were used to guide the alignment of the partial 3D models (CO and GF) initially segmented in the ITK-SNAP software. Previously, the respective partial 3D models of T0, T1, and T2 were duplicated and superimposed (best fit) (T1 and T2 on T0) for trimming, maintaining the same limits. These trimmed models (CO and GF) were aligned to the respective full 3D models of T0, T1, and T2. Individually, each partial anatomical structure was aligned to the total one to obtain the same spatial orientation as the complete 3D models and share the same coordinate system (22) (Figure 5).

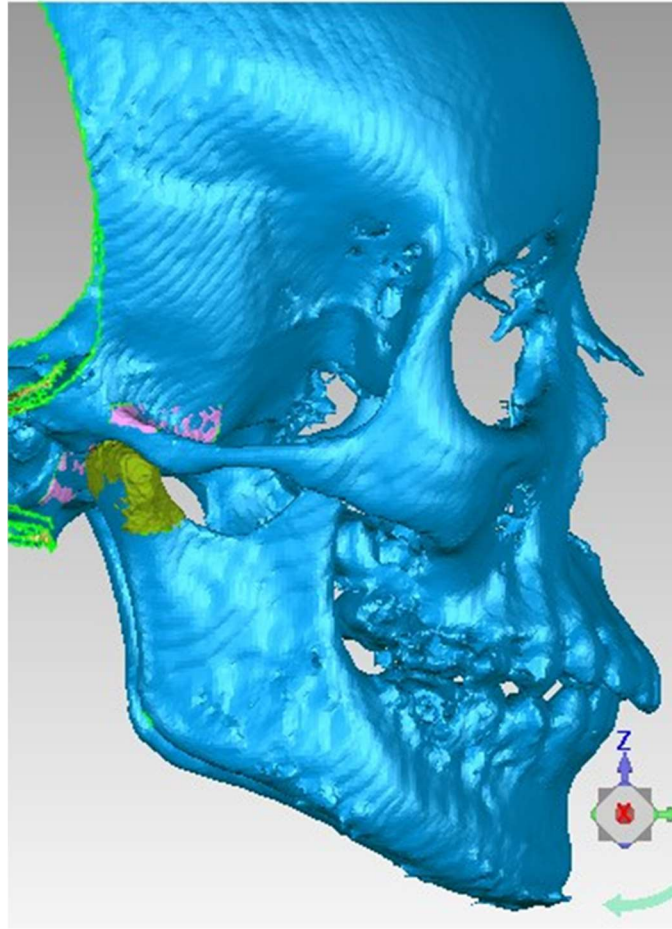


Figure 5. Partial 3D model of the CO (green color) and GF (pink color) aligned in the complete 3D model (blue color). They all share the same coordinate system.

Since the superimposition and clipping of the partial 3D models had the same limits (Yatabe *et al.*, 2017; Jiang *et al.*, 2020), it was possible to automatically determine the centroid point of each CO and GF in the Geomagic Qualify software. The centroid point of an anatomical structure is its geometric center, a point with an average spatial position of all the centroids of the triangles that make up the 3D structure. It represents the 3D spatial position of an anatomical region of interest (CO and GF) in relation to the three planes of space (Teixeira *et al.*, 2020) (Figure 6).

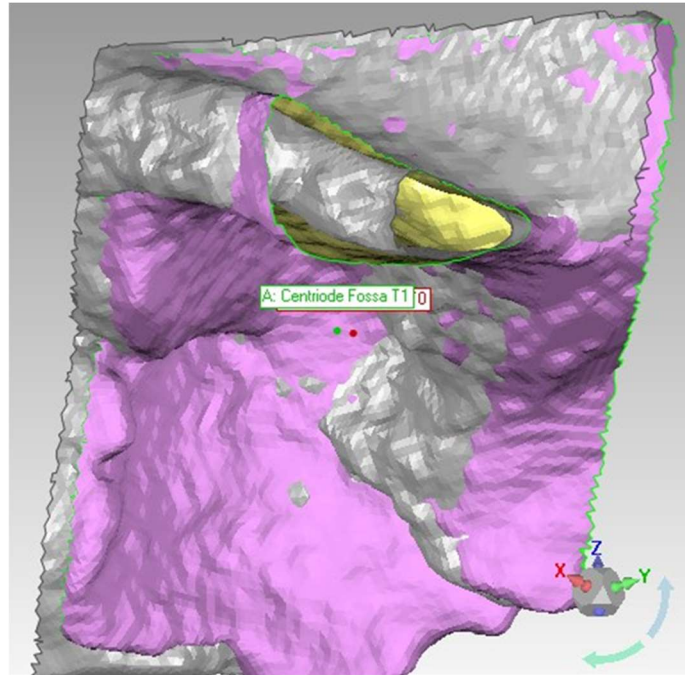


Figure 6. Centroid of the GF at T0 (red point) and T1 (green point).

All CO and GF centroids were initially calculated from the complete 3D models (T0, T1, and T2) recorded and aligned in the anterior fossa of the skull, with which GF growth could be evaluated (Cevidane *et al.*, 2009). To improve the assessment of condylar growth, the initial superimposition between the complete 3D models made in the symphysis was complemented with a regional recording at the level of the symphysis and body of the mandible, as described in previous studies (Ruellas, *et al.*, 2016) that preserved the respective coordinate systems (T0–T1 and T0–T2) (Figure 7).

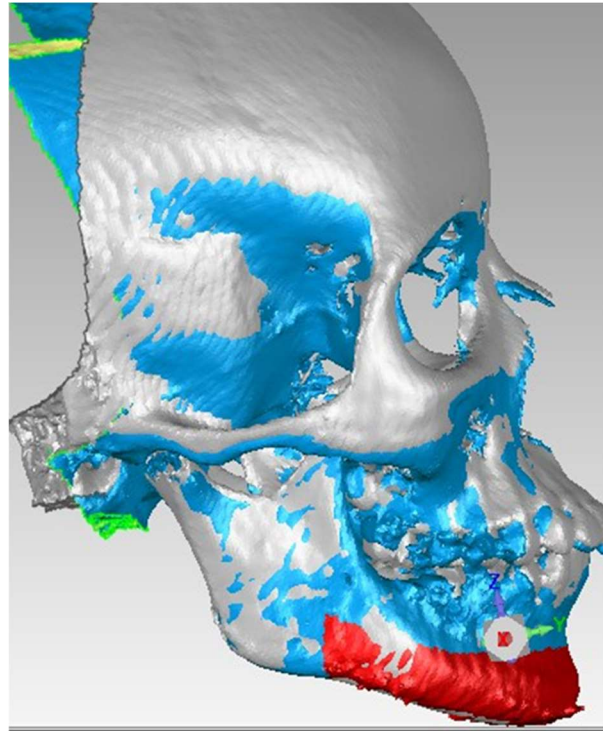


Figure 7. Regional mandibular recording of the complete 3D model T1 (gray color) in T0 (blue color) encompassing the symphysis and mandibular body.

Finally, the displacements and growth of the anatomical structures were determined by the difference in spatial position between the centroids of T0-T1, T0-T2, and T1-T2 of each region (CO and GF). Each centroid point had a 3D orientation with coordinates in the X (transverse), Y (anteroposterior), and Z (vertical) axes, established for each patient on the full 3D T0 and T1 images (for T1-T2). On the X axis, the positive and negative values represented displacements to the right and left, respectively. On the Y axis, the positive and negative values represented displacements in the anterior and posterior directions, respectively. On the Z axis, the positive and negative values represented displacements in the upper and lower directions, respectively.

To verify the reproducibility of the procedures performed in this study, calibration was performed in six randomly selected patients, and all the 3D (Cevitanes *et al.*, 2009; Ruellas *et al.*, 2016; Teixeira *et al.*, 2020) methodological steps were applied to the T0, T1, and T2 tomographies. The process was repeated after 15 days. Intra-examiner correlations were conducted for the measurements, achieving an intraclass correlations coefficient >0.93 .

Statistical analysis

Statistical analysis was performed using STATA 15.1 software (Stata Corp, USA). All analyzes were performed with 95% confidence and $p \leq 0.05$. The normality of the sample was verified through the Shapiro–Wilk test; however, considering the small sample size ($n < 30$), nonparametric tests were used. The Wilcoxon test was used to evaluate the differences in the results obtained between T0–T1, T0–T2, and T1–T2 (intra-group analysis). The Friedman multivariate test was used to compare the position differences of the centroids between T0, T1, and T2. Finally, a post-hoc test with Wilcoxon test and Bonferroni adjustment was used to identify significant differences in the displacements of the CO and GF centroids at different study times.

Results

The sample consisted of 12 growing patients with skeletal class II who used TB for a period of 12 months. The morphological changes in CO and GF were assessed through differences in the positioning of the centroids of all the anatomical structures (CO and GF) between T0, T1, and T2, in the transverse (X), anteroposterior (Y), and vertical (Z) directions for each analysis time period. A total of 72 3D images of the CO (24 in T0, 24 in T1 and 24 in T2) and 72 3D images of the GF (24 in T0, 24 in T1, and 24 in T2) were segmented. In the T0-T1 period, a statistically significant growth of 1.33 mm ($p = 0.0161$) and 1.54 mm ($p = 0.0210$) was observed in the posterior direction (anteroposterior plane) of the right and left CO, respectively. A statistically significant growth in the upper direction (vertical plane) of the right and left CO of 3.61 mm ($p = 0.0068$) and 3.73 mm ($p = 0.0034$), respectively, was also observed (Table 1 and Figure 8).

Table 1. Difference in CO positioning between T0 and T1

	Axis	Time	Mean	SD	Median	Min	Max	Z	P-value
Right CO	X	T0	45.54	2.31	45.70	41.61	48.90	-2.667	0.0049*
		T1	46.44	2.73	46.42	41.82	50.25		
		T1-T0	0.90	0.91	1.03	-0.79	2.89		
	Y	T0	-114.40	13.10	-113.12	-136.60	-97.72	2.353	0.0161*
		T1	-115.73	12.42	-115.34	-136.41	-100.16		
		T1-T0	-1.33	1.64	-1.60	-4.05	1.73		
	Z	T0	-9.16	2.70	-8.51	-12.98	-5.06	-2.590	0.0068*
		T1	-5.56	4.78	-4.69	-13.59	0.00		
		T1-T0	3.61	3.28	4.32	-2.98	8.33		

Left CO	X	T0	-44.83	2.40	-44.77	-49.66	-41.42	0.471	0.6772
		T1	-44.81	2.05	-44.76	-48.88	-42.01		
		T1-T0	0.02	0.85	-0.08	-0.96	2.10		
	Y	T0	-115.30	13.26	-113.41	-138.29	-97.84	2.275	0.0210*
		T1	-116.84	12.40	-114.74	-138.01	-100.02		
		T1-T0	-1.54	2.01	-1.36	-5.38	1.45		
	Z	T0	-9.71	2.38	-9.17	-12.98	-4.85	-2.746	0.0034*
		T1	-5.97	4.86	-4.96	-15.46	1.71		
		T1-T0	3.73	3.29	3.81	-3.36	9.90		

* Wilcoxon test (signed rank test). Statistically significant

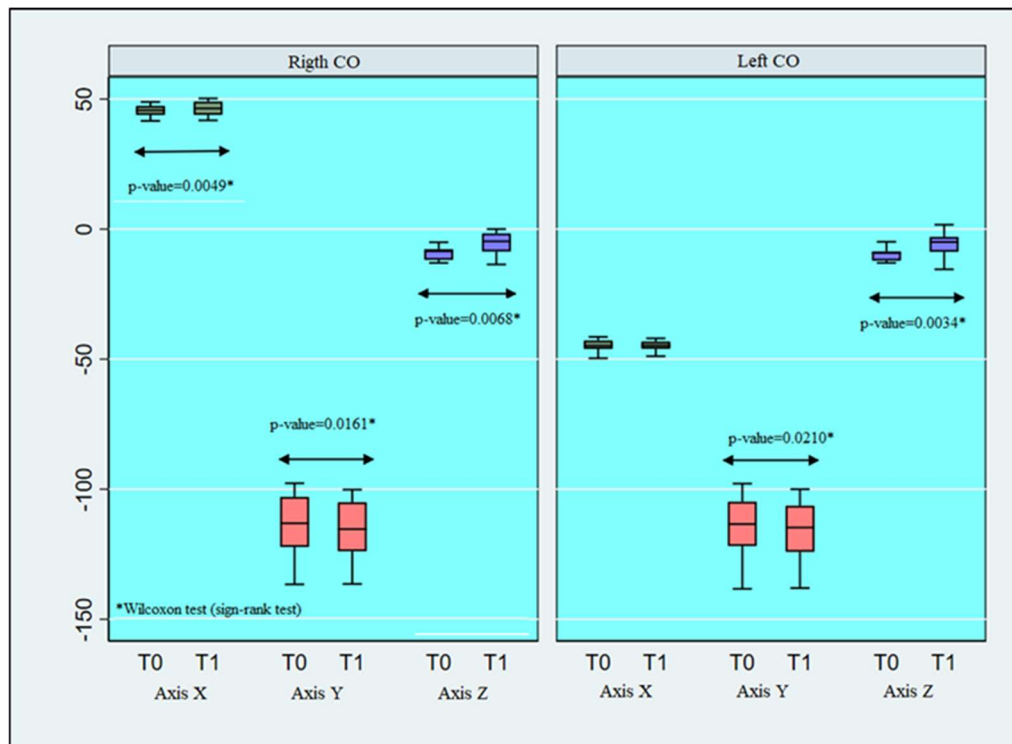


Figure 8. Box plot with representation of condyle values at time T0 and T1

Regarding the GF in the period T0-T1, a statistically significant growth in the posterior direction of the right and left GF of 0.80 mm ($p = 0.0400$) and 0.48 mm ($p = 0.0425$) was found, respectively. GF growth in the inferior direction was also observed but was not significant (Table 2 and Figure 9).

Table 2. Difference in GF positioning between T0 and T1.

	Axis	Time	Mean	SD	Median	Min	Max	Z	P-value
Right GF	X	T0	41.45	41.11	2.07	38.86	44.55	-0.510	0.6494
		T1	41.56	41.51	2.39	37.29	46.20		
		T1-T0	0.12	0.19	0.93	-1.80	1.65		

Left GF	Y	T0	-116.74	-114.77	13.30	-141.82	-100.05	2.040	0.0400*
		T1	-117.54	-116.56	12.94	-141.46	-101.87		
		T1-T0	-0.80	-0.70	1.09	-2.63	0.78		
	Z	T0	-2.38	-1.81	2.68	-6.89	0.70	0.392	0.7334
		T1	-2.64	-2.20	2.76	-7.09	1.23		
		T1-T0	-0.26	-0.06	0.93	-2.60	0.71		
	X	T0	-41.64	-41.36	2.45	-45.98	-38.74	0.392	0.7334
		T1	-41.81	-41.59	2.77	-46.83	-37.73		
		T1-T0	-0.17	-0.40	0.99	-1.84	1.28		
	Y	T0	-117.15	-115.39	13.51	-142.06	-100.13	2.040	0.0425*
		T1	-117.64	-116.22	13.21	-140.83	-100.45		
		T1-T0	-0.48	-0.67	0.71	-1.55	1.23		
	Z	T0	-2.33	-1.82	1.57	-5.17	-0.43	1.569	0.1294
		T1	-3.07	-3.07	1.62	-5.58	0.57		
		T1-T0	-0.74	-0.68	1.29	-2.89	1.12		

* Wilcoxon test (signed rank test). Statistically significant

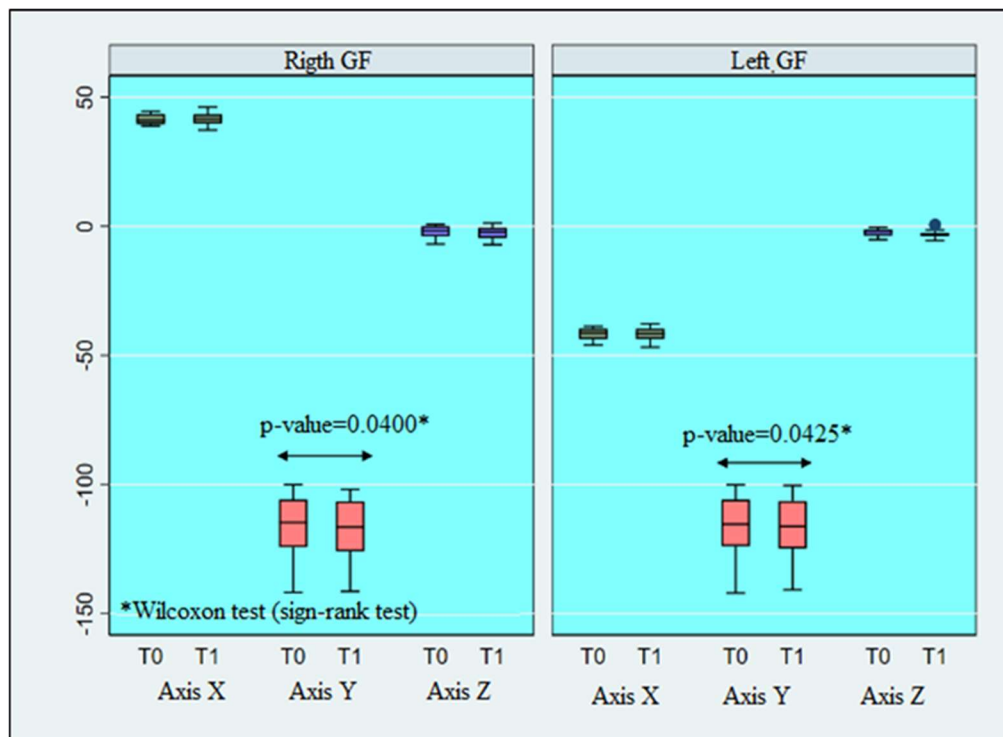


Figure 9. Position of the glenoid fossa at time T0 and T1

In the T0-T2 period, a statistically significant growth of 2.34 mm ($p = 0.0010$) and 2.16 mm ($p = 0.0005$) was observed in the posterior direction (anteroposterior plane) of the right and left CO, respectively. A statistically significant growth in the upper direction (vertical plane) of the right and left CO of 7.23 mm ($p = 0.0005$) and 7.28 mm ($p = 0.0005$), respectively, was also observed. In the transverse plane, a statistically significant growth of

the right and left CO of 1.46 mm ($p = 0.0005$) and 1.02 mm ($p = 0.0005$), respectively, was also observed. Both condyles grew in the right and left directions, respectively (Table 3 and Figure 10).

Table 3. Difference in CO positioning between T0 and T2

	Axis	Time	Mean	SD	Median	Min	Max	Z	P-value
Right CO	X	T0	45.54	2.31	45.7	41.61	48.9	-3.061	0.0005*
		T2	47.00	2.65	47.08	42.21	50.81		
		T2-T0	1.46	0.64	1.44	0.53	2.86		
	Y	T0	-114.40	13.10	-113.12	-136.60	-97.72	2.982	0.0010*
		T2	-116.74	12.93	-116.87	-138.45	-100.38		
		T2-T0	-2.34	1.40	-2.40	-3.97	0.28		
	Z	T0	-9.16	2.70	-8.51	-12.98	-5.06	-3.061	0.0005*
		T2	-1.93	4.10	-2.12	-7.92	3.69		
		T2-T0	7.23	2.90	6.95	3.40	11.49		
Left CO	X	T0	-44.83	2.40	-44.77	-49.66	-41.42	3.059	0.0005*
		T2	-45.85	2.34	-45.69	-50.19	-43.01		
		T2-T0	-1.02	0.63	-0.90	-2.72	-0.43		
	Y	T0	-115.30	13.26	-113.41	-138.29	-97.84	3.059	0.0005*
		T2	-117.46	12.88	-115.48	-139.95	-100.66		
		T2-T0	-2.16	1.47	-2.22	-4.35	-0.35		
	Z	T0	-9.71	2.38	-9.17	-12.98	-4.85	-3.059	0.0005*
		T2	-2.43	3.96	-2.63	-7.96	4.10		
		T2-T0	7.28	2.95	6.72	4.02	12.29		

* Wilcoxon test (signed rank test). Statistically significant

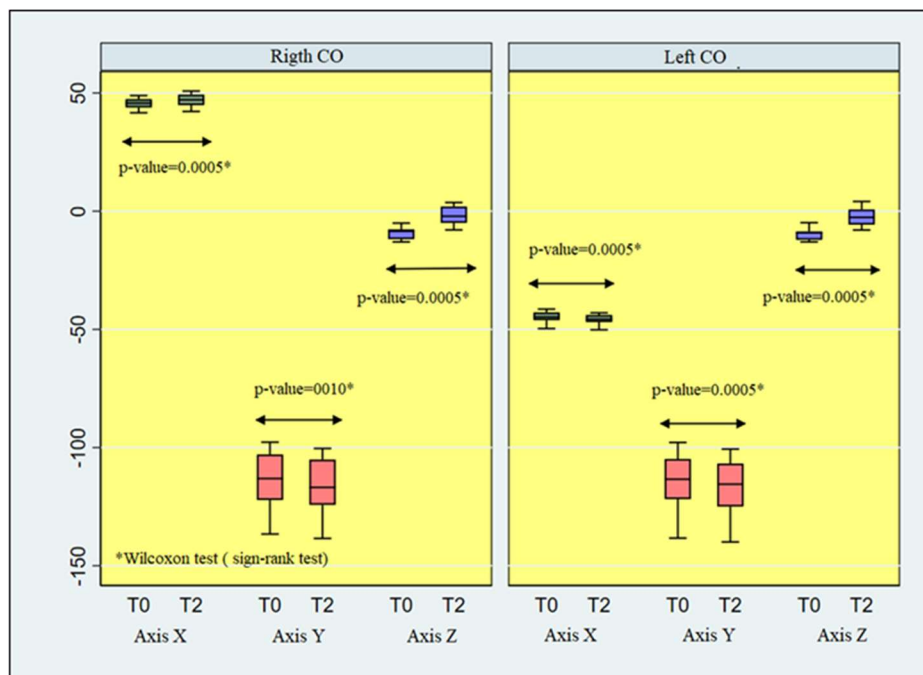


Figure 10. Box plot with representation of condyle values at time T0 and T2

Regarding the GF in the T0-T2 period, a statistically significant growth of 1.59 mm ($p = 0.0210$) and 1.77 mm ($p = 0.0005$) was observed in the posterior direction (anteroposterior plane) of the right and left GF, respectively. A statistically significant growth in the inferior direction of the left GF of 1.09 mm ($p = 0.0381$) and a non-significant growth of the right GF of 0.55 mm ($p = 0.3804$) was also observed. Finally, a non-statistically significant growth of the right and left GF of 0.73 mm ($p = 0.0923$) and 0.76 mm ($p = 0.1763$), respectively, was also observed. Growth was observed in the transverse plane in the right and left directions, respectively (Table 4 and Figure 11).

Table 4. Difference in GF positioning between T0 and T2.

	Axis	Time	Mean	SD	Median	Min	Max	Z	P-value
Right GF	X	T0	41.45	2.07	41.11	38.86	44.55	-1.726	0.0923
		T2	42.18	2.58	41.56	38.28	47.27		
		T2-T0	0.73	1.58	0.48	-2.64	2.72		
	Y	T0	-116.74	13.30	-114.77	-141.82	-100.05	2.275	0.0210*
		T2	-118.33	12.83	-116.28	-139.84	-101.42		
		T2-T0	-1.59	1.80	-1.86	-3.51	1.98		
	Z	T0	-2.38	2.68	-1.81	-6.89	0.70	0.941	0.3804
		T2	-2.93	2.51	-2.90	-6.46	0.69		
		T2-T0	-0.55	1.46	-0.34	-3.56	1.50		
Left GF	X	T0	-41.64	2.45	-41.36	-45.98	-38.74	1.412	0.1763
		T2	-42.40	2.84	-42.31	-47.89	-38.30		
		T2-T0	-0.76	1.65	-0.54	-3.72	1.63		
	Y	T0	-117.15	13.51	-115.40	-142.06	-100.13	3.059	0.0005*
		T2	-118.92	13.88	-118.28	-142.87	-100.29		
		T2-T0	-1.77	1.61	-1.51	-5.19	-0.01		
	Z	T0	-2.33	1.57	-1.82	-5.17	-0.43	2.080	0.0381*
		T2	-3.42	1.86	-3.60	-5.75	0.24		
		T2-T0	-1.09	1.48	-1.32	-3.40	1.36		

* Wilcoxon test (signed rank test). Statistically significant

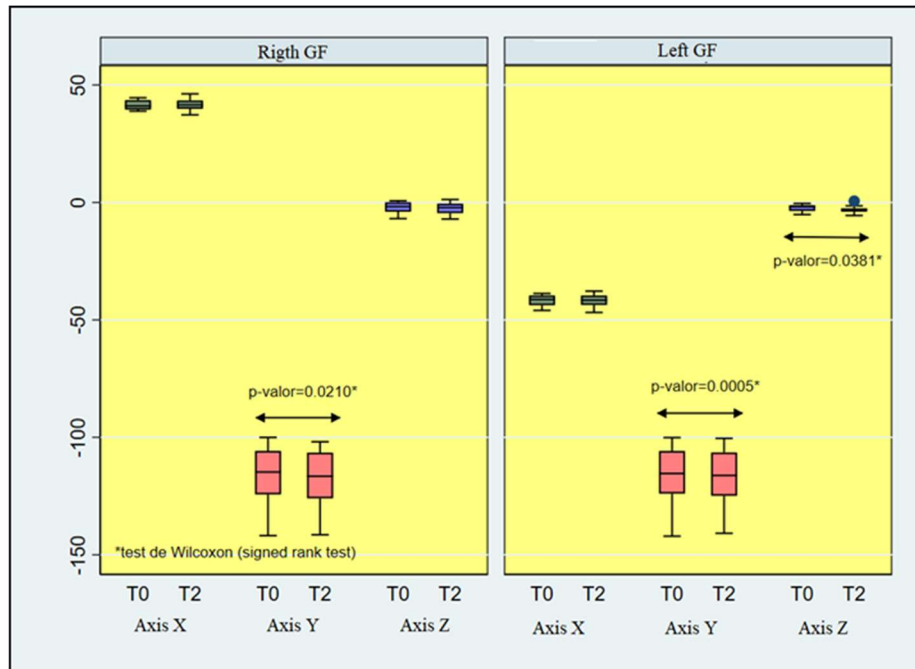


Figure 11. Position of the glenoid fossa at time T0 and T2

In the period T1-T2, a statistically significant growth in the posterior direction (anteroposterior plane) of the right CO of 1.01 mm ($p = 0.0469$) and non-significant growth of the left CO of 0.62 mm ($p = 0.3394$) was observed. A statistically significant growth in the upper direction (vertical plane) of the right and left CO of 3.62 mm ($p = 0.0010$) and 3.54 mm ($p = 0.0005$), respectively, was also observed (Table 5 and Figure 12).

Table 5. Difference in CO positioning between T1 and T2.

	Axis	Time	Mean	SD	Median	Min	Max	Z	P-value
Right CO	X	T1	46.44	2.73	46.42	41.82	50.25	-2.981	0.0010*
		T2	47.00	2.65	47.08	42.21	50.81		
		T2-T1	0.56	0.34	0.54	-0.03	1.32		
	Y	T1	-115.73	12.42	-115.34	-136.41	-100.16	2.002	0.0469*
		T2	-116.74	12.93	-116.87	-138.45	-100.38		
		T2-T1	-1.01	1.50	-0.66	-4.04	0.62		
	Z	T1	-5.56	4.78	-4.69	-13.59	0.00	-2.981	0.0010*
		T2	-1.93	4.10	-2.12	-7.92	3.69		
		T2-T1	3.62	2.62	2.75	-0.08	9.12		
Left CO	X	T1	-44.81	2.05	-44.76	-48.88	-42.01	2.981	0.0010*
		T2	-45.85	2.34	-45.69	-50.19	-43.01		
		T2-T1	-1.04	0.83	-0.91	-2.63	0.05		
	Y	T1	-116.84	12.40	-114.74	-138.01	-100.02	1.020	0.3394
		T2	-117.46	12.88	-115.48	-139.95	-100.66		
		T2-T1	-0.62	1.24	-0.74	-3.94	2.66		

	T2-T1	-0.62	1.65	-0.62	-3.54	1.59		
Z	T1	-5.97	4.86	-4.96	-15.46	1.71		
	T2	-2.43	3.96	-2.63	-7.96	4.10	-3.059	0.0005*
	T2-T1	3.54	2.79	2.55	0.56	9.46		

* Wilcoxon test (signed rank test). Statistically significant

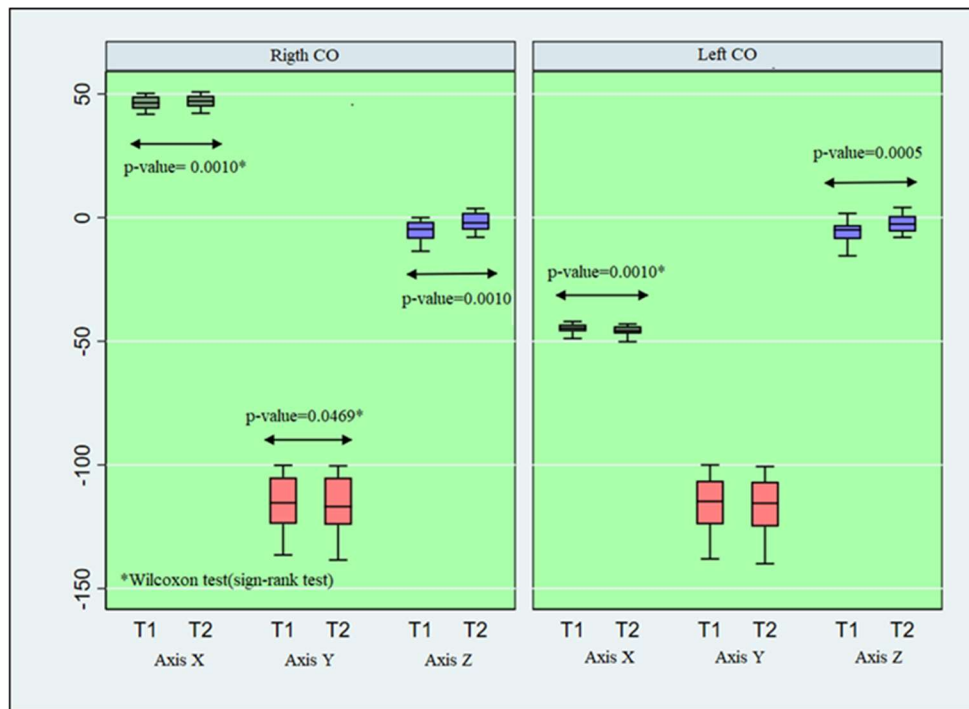


Figure 12. Box plot with representation of condyle values at time T1 and T2

Regarding the GF in the period T1–T2, a statistically significant growth of 1.29 mm ($p = 0.0269$) in the posterior direction of the left GF and non-significant growth of 0.79 mm ($p = 0.1895$) in the right GF was observed. GF growth in the inferior direction was also observed but was not significant (Table 6 and Figure 13).

Table 6. Difference in GF positioning between T1 and T2.

	Axis	Time	Mean	SD	Median	Min	Max	Z	P-value
Right GF	X	T1	41.56	2.39	41.50	37.29	46.2		
		T2	42.18	2.58	41.56	38.28	47.27	-1.647	0.1099
		T2-T1	0.61	1.71	0.88	-3.10	4.27		
	Y	T1	-117.54	12.94	-116.57	-141.46	-101.87		
		T2	-118.33	12.83	-116.28	-139.84	-101.42	1.374	0.1895
		T2-T1	-0.79	1.61	-0.61	-3.62	1.62		
	Z	T1	-2.64	2.76	-2.20	-7.09	1.23		
		T2	-2.93	2.51	-2.90	-6.46	0.69	0.784	0.4697

		T2-T1	-0.28	1.45	-0.38	-2.60	2.12		
Left GF	X	T1	-41.81	2.77	-41.59	-46.83	-37.73	0.941	0.3804
		T2	-42.40	2.84	-42.31	-47.89	-38.30		
		T2-T1	-0.59	1.67	-1.09	-3.27	2.26		
	Y	T1	-117.64	13.21	-116.23	-140.83	-100.45	2.197	0.0269*
		T2	-118.92	13.88	-118.28	-142.87	-100.29		
		T2-T1	-1.29	1.50	-1.10	-4.22	0.37		
	Z	T1	-3.07	1.62	-3.07	-5.58	0.57	0.628	0.5693
		T2	-3.42	1.86	-3.60	-5.75	0.24		
		T2-T1	-0.35	1.10	-0.14	-2.37	0.92		

* Wilcoxon test (signed rank test). Statistically significant

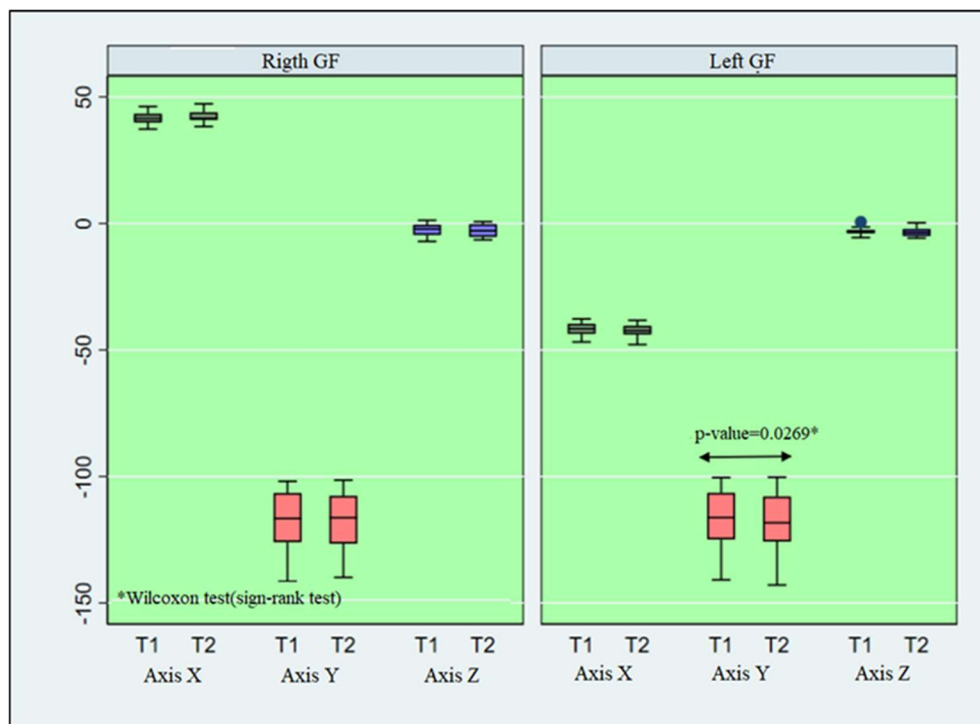


Figure 13. Position of the glenoid fossa at time T1 and T2

When the differences in the displacements of the CO centroids were compared between the T0–T1, T0–T2, and T1–T2 time periods according to the Friedman test for paired samples, statistically significant differences were found in the three space axes, X, Y, and Z. Moreover, the post-hoc test with Wilcoxon test and Bonferroni adjustment found significant differences between the subgroups (Table 7).

Table 7. Difference in positioning of the right and left CO at time T0, T1 and T2.

Right side CO					Global difference			
Group	Group	p	(1)	Significance	X ²	p	(2)	Effect size

1	2	(3)			
Axis X					
T0	T1	0.015	*		
T0	T2	0.008	**	20.2	0.000041 0.840
T1	T2	0.003	**		
Axis Y					
T0	T1	0.048	*		
T0	T2	0.01	**	10.3	0.00593 0.427
T1	T2	0.136	ns		
Axis Z					
T0	T1	0.032	*		
T0	T2	0.008	**	18.5	0.000096 0.771
T1	T2	0.003	**		
Left side CO					
Axis X					
T0	T1	1	ns		
T0	T2	0.001	**	15.2	0.000509 0.632
T1	T2	0.003	**		
Axis Y					
T0	T1	0.063	ns		
T0	T2	0.001	**	12.2	0.00228 0.507
T1	T2	1	ns		
Axis Z					
T0	T1	0.01	*		
T0	T2	0.001	**	22.2	0.000015 0.924
T1	T2	0.001	**		

(1) Wilcoxon test, p.adjust.method = "Bonferroni"

(2) Friedman test

(3) Kendall W test

* Statistically significant with $p < 0.05$; ** Statistically significant with $p < 0.01$

When the differences in the displacements of the GF centroids were compared between the time periods T0–T1, T0–T2, and T1–T2 according to the Friedman test for paired samples, no statistically significant differences were found in the three space axes X, Y, and Z. Additionally, the post-hoc test with Wilcoxon test and Bonferroni adjustment did not show significant differences between the subgroups (Table 8).

Table 8. Difference in positioning of the right and left GF at time T0, T1 and T2.

Right side GF	
Difference between groups	Global difference

Group 1	Group 2	p (1)	Significance	χ^2	p (2)	Effect size (3)
Axis X						
T0	T1	1	ns	6.43	0.0402	0.268
T0	T2	0.277	ns			
T1	T2	0.33	ns			
Axis Y						
T0	T1	0.136	ns	5.66	0.0590	0.236
T0	T2	0.063	ns			
T1	T2	0.504	ns			
Axis Z						
T0	T1	1	ns	0.167	0.920	0.00694
T0	T2	1	ns			
T1	T2	1	ns			
Left side GF						
Axis X						
T0	T1	1	ns	2.17	0.338	0.0903
T0	T2	0.528	ns			
T1	T2	1	ns			
Axis Y						
T0	T1	0.128	ns	14	0.00091	0.583
T0	T2	0.001	**			
T1	T2	0.081	ns			
Axis Z						
T0	T1	0.387	ns	3.87	0.144	0.161
T0	T2	0.11	ns			
T1	T2	1	ns			

1) Wilcoxon test, p.adjust.method = "Bonferroni"

(2) Friedman test

(3) Kendall W test

** Statistically significant with $p < 0.05$; ** Statistically significant with $p < 0.01$

Discussion

During the treatment of class II malocclusion due to mandibular retrusion, clinical studies have demonstrated the presence of supplementary mandibular growth (Santamaría-Villegas *et al.*, 2017). However, other investigations have shown that the effects of mandibular propelling functional devices are mainly dental rather than skeletal (Koretsi *et al.*, 2015; Zymperdikas *et al.*, 2016). Since the CO is considered as one of the main growth

centers of the mandible (McNamara *et al.*, 1987), initial morphological evaluations of the CO and GF were performed using two-dimensional methods (Pancherz, 1982). However, with the introduction of the CBCT, very few studies have been conducted to evaluate the real effect on CO and GF (Cheib Vilefort *et al.*, 2019; Jiang *et al.*, 2020).

Pacha *et al.* (2016) reviewed the quality of studies that compared the efficacy of fixed and removable functional appliances in the treatment of growing patients with class II malocclusion. Among the removable appliances, TB was shown to improve sagittal skeletal discrepancy, increase mandibular length, and significantly reduce overjet. Limitations of the studies analyzed were a lack of long-term treatment results and a lack of control of cephalometric magnifications. Thus, the aim of the present study was to evaluate CO and GF alterations resulting from the use of TB in the treatment of class II malocclusions up to one year after removal of the functional apparatus.

In the present investigation, 3D superimpositions of the CBCTs of 12 patients from the T1–T0, T2–T0, and T2–T1 periods were performed, initially taking the anterior fossa of the skull base as a reference (Cevitanes *et al.*, 2009), which allowed to evaluate mainly the growth and remodeling of the GF. To evaluate the remodeling and growth of the CO, an overlay in the region of the symphysis of the mandible was performed with the methodology proposed in previous studies (Ruellas *et al.*, 2016; Koerich *et al.*, 2016). All superimpositions followed the voxel-based method performed in the Dolphin imaging software. Considering that there is no statistically significant difference between the results of superimpositions following the voxel-based and surface-based method (Koretsi *et al.*, 2015), a regional surface-based superimposition was additionally performed in the Geomagic Qualify software considering the symphysis region and part of the mandibular body to obtain a better evaluation of the condylar growth, as proposed by Ruellas *et al.* (2016).

Knowing that CO and GF are not solid bodies with closed surfaces, the use of the centroid was proposed to identify morphological changes during treatment. The centroid represents the geometric center of the anatomical structure. After superimposing and performing the cut delimiting the CO and GF (Yatabe *et al.*, 2017; Jiang *et al.*, 2020) and creating the centroid, this point was broken down into three axes (X, Y, Z) following the coordinate system previously assigned to the respective model (Full 3D T0 and T1). Previous studies (Hsu *et al.*, 2013; Teixeira *et al.*, 2020) suggested that these axes provide a more accurate 3D assessment of changes in the anatomical structure.

In the study, the displacements of the centroids were mainly described, suggesting that the remodeling and growth of the CO and GF instead of the displacements of the CO were

related to the effect of the devices used, as described by Elfeky *et al.* (2018). During the T0-T1 period, a statistically significant growth of 3.61 mm ($p = 0.0068$) and 3.73 mm ($p = 0.0034$) was found in the right and left CO, respectively, in the superior direction (Z axis). These results are consistent with those found by Yildirim *et al.* (2014), Bowen *et al.* (2013) (6.20 mm), Elfeky *et al.* (2018) (1.59 mm right and 1.10 mm left), Jiang *et al.* (2020), and Shetty *et al.* (2021). A statistically significant growth of the right and left CO of 1.33 mm ($p = 0.0161$) and 1.54 mm ($p = 0.0210$), respectively, in the posterior direction (Y axis) was also found (Table 1). These results are in agreement with those found by Yildirim *et al.* (2014), Bowen *et al.* (2013) (7.22 mm), Jiang *et al.* (2020), and Shetty *et al.* (2021). Regarding the GF, a statistically significant growth (remodeling) of 0.80 mm ($p = 0.0400$) and 0.48 mm ($p = 0.0425$) was found in the posterior direction (Y axis) on the right and left sides, respectively (Table 2). These results are consistent with the findings of Jiang *et al.* (2020), suggesting that the GF is remodeled in an anterior-posterior direction, adapting to the new position of the condyle. A slight growth of the GF in the inferior direction (Z axis) of 0.26 mm ($p = 0.7334$) and 0.74 mm ($p = 0.1294$) was also observed on the right and left sides, respectively. However, it was not significant. This growth in the inferior direction is not consistent with the results of Jiang *et al.* (2020), who found areas of bone resorption in the upper wall of the CO and GF.

During the T0-T2 period, a statistically significant growth of 7.23 mm ($p = 0.0005$) and 7.28 mm ($p = 0.0005$) was found in the right and left CO, respectively, in the superior direction (Z axis). A statistically significant growth of 2.34 mm ($p = 0.0010$) and 2.16 mm ($p = 0.005$) was observed in the right and left CO, respectively, in the posterior direction (Y axis) (Table 3). In relation to the GF, a statistically significant growth of 1.59 mm ($p = 0.0210$) and 1.77 mm ($p = 0.0005$) was found in the posterior direction (Y axis) on the right and left sides, respectively. A slight growth of the GF of 0.55 mm ($p = 0.3804$) and 1.09 mm ($p = 0.0381$) was also observed in the inferior direction (Z axis) on the right and left sides, respectively (Table 4). It is suggested that the direction of growth of CO and GF followed the same pattern after removing the apparatus, which can be corroborated in tables 5 and 6 (T1-T2), respectively. This could be related to the fact that the patients were still growing even without the use of TB.

When the effects of TB on CO were compared during the T0-T1, T0-T2, and T1-T2 periods, statistically significant differences were found (Table 7). A growth of the right and left CO in a superior and posterior direction was suggested, which is consistent with previous studies (Bowen *et al.*, 2013; Yildirim *et al.*, 2014; Elfeky *et al.*, 2018; Jiang *et al.*, 2020;

Shetty *et al.*, 2021). When the effects of TB on GF were compared during the T0–T1, T0–T2, and T1–T2 periods, no statistically significant differences were found (Table 8). However, according to the values found, a remodeling and growth of the GF in the posterior and inferior directions was suggested.

Few studies have used CBCT to quantitatively and qualitatively identify the effect of TB on GF (Jiang *et al.*, 2020). According to the results found, it is suggested that GF accompanies the CO in its growth in a posterior direction (Y axis). However, in the vertical plane (Z axis), GF attempts to reach the CO and vice versa. This could be part of the bone adaptation pattern suggested during treatment with TBs. Moreover, comparing the results shown in Tables 1–6, it can be suggested that the degree of CO movement in the three periods evaluated (T0–T1, T0–T2, and T1–T2) was greater than the degree of GF movement.

As CBCTs involve exposing the patient to a low dose of radiation similar to the set of radiographs indicated for orthodontic patients (panoramic, lateral cephalometric, and carpal), this procedure was ethically acceptable. In addition, as it is a very specific sample, it was difficult to find records of patients with class II division 1 with an overjet of at least 6 mm and in the peak phase of pubertal growth, who had received treatment with TB and had been examined with CBCT. The CBCTs were indicated to determine the most reliable alterations of the bone structures with the use of the TB functional apparatus and to quantify the stability of the treatment. Post-treatment CBCT was only indicated for patients who needed a 3D reassessment to achieve adequate completion.

Based on the available evidence, we can summarize the main steps followed in this work. First, three tomographic time points (T0, T1 and T2) were established, and the voxel-based (Cevitanes *et al.*, 2009; Almukhtar *et al.*, 2014) superposition (T0–T1, T0–T2 and T1–T2) was performed to obtain complete 3D models and establish a coordinate system at T0 and T1. Second, automatic segmentation of the structures of interest (CO and GF) was performed to acquire partial 3D models (De Assis Ribeiro Carvalho *et al.*, 2010). Third, the partial 3D models were aligned on the complete 3D models already superimposed (Teixeira *et al.*, 2020). Fourth, the centroid of each partial 3D model and its respective coordinates (X, Y, and Z) were established to evaluate the displacement that occurred (Hsu *et al.*, 2013; Teixeira *et al.*, 2020).

A limitation of this study is not being able to compare in 3D the growth of CO and GF of a group treated with TB to the normal growth of an untreated control group. However, it is suggested that the results obtained may help to understand the skeletal effects produced by TB during treatment. During the evaluation of CO growth, it would be interesting to divide a

larger sample according to the type of facial growth: dolichofacial, mesofacial, and brachyfacial, and to compare the behavior of CO and GF in the different groups.

The methodology used in this study was tested, validated, and previously used in the study by Texeira *et al.* (2020), which verified its accuracy in evaluating bone displacements involved in virtual surgical planning, the same accuracy analysis of skeletal displacement required by our study. Yildirim *et al.* (2014) and Elfeky *et al.* (2018) who also used a 3D methodology in TB patients did not guide the head scans or use a cartesian coordinate system. The retrospective and longitudinal design of this study allowed to meet the demand for systematic reviews on the effects of mandibular thrusters (Santamaría-Villegas *et al.*, 2017).

The calibration was performed by a single examiner with the tomographies of six patients. All steps of the 3D methodology were repeated within an interval of 15 days, comparing the reproducibility of the amount of displacement of the CO and GF centroids in the Geomagic Qualify software. Calibration was performed following the recommendation of the systematic review by Gaber *et al.* (2017). Non-parametric tests were used, as the normality test is not reliable with the small sample size.

The decomposition of the centroid point in the Cartesian coordinates X, Y, and Z was previously performed only in studies evaluating the accuracy of virtual surgical planning carried out by Hsu *et al.* (2013) and Texeira *et al.* (2020). According to Gaber's systematic review (2017), this 3D assessment method is more accurate than other methods.

Conclusion

The conclusions of the present study are: (1) the patients who used TB had a statistically significant growth of CO towards the posterior and superior directions; (2) the patients who used TB had growth of the GF towards the posterior and inferior directions, being significant in the posterior direction; (3) the amount of movement of the CO in the two periods evaluated was greater than the amount of movement of the GF and (4) the GF accompanies the CO in its growth towards a posterior direction. However, in the vertical plane, the GF attempts to catch up with the CO and vice versa.

Declaring of conflicting interest

The author(s) declared no potential conflicts of interest with respect to the research, authorship, and/or publication of this article

Funding

This article was supported by the Fundação de Amparo à Pesquisa do Estado do Rio de Janeiro (FAPERJ).

ORCID iD

Manuel Gustavo Chávez-Sevillano <https://orcid.org/0000-0002-7042-4250>

References

- Aidar LA de A, Abrahão M, Yamashita HK, Dominguez GC (2013) Morphological changes of condyles and Helkimo clinical dysfunction index in patients treated with herbst - Orthodontic appliance. *Braz Dent J* 24:313–21.
- Almukhtar A, Ju X, Khambay B, McDonald J, Ayoub A (2014) Comparison of the accuracy of voxel based registration and surface based registration for 3D assessment of surgical change following orthognathic surgery. *PLoS One* 9:1–6.
- Arici S, Akan H, Yakubov K, Arici N (2008) Effects of fixed functional appliance treatment on the temporomandibular joint. *Am J Orthod Dentofac Orthop* 133:809–14
- Baccetti T, Franchi L, McNamara JA (2005) The Cervical Vertebral Maturation (CVM) Method for the Assessment of Optimal Treatment Timing in Dentofacial Orthopedics. *Semin Orthod* 11:119–29.
- Bowen L, Yanmin W, Fang S, Min L, Ying D, Li Z (2013) Analysis of temporomandibular joint changes before and after Twin-block correction by cone-beam CT analysis of Class II division 1 malocclusion. *West China of Stomatology* 31:610–4.
- Cevidanes LHC, Heymann G, Cornelis MA, DeClerck HJ, Tulloch JFC (2009). Superimposition of 3-dimensional cone-beam computed tomography models of growing patients. *Am J Orthod Dentofac Orthop* 136:94–9.
- Cevidanes LHS, Styner MA, Proffit WR (2006) Image analysis and superimposition of 3-dimensional cone-beam computed tomography models. *Am J Orthod Dentofac Orthop* 129:611–8.
- Cheib Vilefort PL, Farah LO, Gontijo HP, Moro A, Ruellas AC de O, Cevidanes LHS, et al. (2019) Condyle-glenoid fossa relationship after Herbst appliance treatment during two stages of craniofacial skeletal maturation: A retrospective study. *Orthod Craniofac Res* 22:345–53.

- Cozza P, Baccetti T, Franchi L, De Toffol L, McNamara JA (2006) Mandibular changes produced by functional appliances in Class II malocclusion: A systematic review. *Am J Orthod Dentofac Orthop* 129:599.e1-599.e12.
- Croft RS, Buschang PH, English JD, Meyer R. A cephalometric and tomographic evaluation of Herbst treatment in the mixed dentition (1999) *Am J Orthod Dentofacial Orthop* 116:435–43.
- De Assis Ribeiro Carvalho F, Cevidanes LHS, da Motta ATS, de Oliveira Almeida MA, Phillips C (2010) Three-dimensional assessment of mandibular advancement 1 year after surgery. *Am J Orthod Dentofac Orthop* 137:53–5.
- De Oliveira Ruellas AC, Yatabe MS, Souki BQ, Benavides E, Nguyen T, Luiz RR, et al. (2016) 3D mandibular superimposition: Comparison of regions of reference for voxel-based registration. *PLoS One* 11:1–13.
- Dot G, Rafflenbeul F, Salmon B (2020) Voxel-based superimposition of Cone Beam CT scans for orthodontic and craniofacial follow-up: Overview and clinical implementation. *Int Orthod* 18:739–48.
- Elfeky HY, Fayed MS, Alhammadi MS, Soliman SAZ, El Boghdadi DM (2018) Three-dimensional skeletal, dentoalveolar and temporomandibular joint changes produced by Twin Block functional appliance. *J Orofac Orthop* 79:245–58.
- Fan Y, Schneider P, Matthews H, Roberts WE, Xu T, Wei R, et al. (2020) 3D assessment of mandibular skeletal effects produced by the Herbst appliance. *BMC Oral Health* 20:1–9.
- Gaber RM, Shaheen E, Falter B, Araya S, Politis C, Swennen GRJ, et al. (2017) A Systematic Review to Uncover a Universal Protocol for Accuracy Assessment of 3-Dimensional Virtually Planned Orthognathic Surgery. *J Oral Maxillofac Surg* 75:2430–40.
- Hsu SSP, Gateno J, Bell RB, Hirsch DL, Markiewicz MR, Teichgraeber JF, et al. (2013) Accuracy of a computer-aided surgical simulation protocol for orthognathic surgery: A prospective multicenter study. *J Oral Maxillofac Surg* 71:128–42.
- Jiang Y, Lian Sun , Wang H, Zhao C, Zhang W-B (2020). Three-dimensional cone beam computed tomography analysis of temporomandibular joint response to the Twin-block functional appliance. *Korean J Orthod* 2234–7518.
- Koerich L, Burns D, Weissheimer A, Claus JDP (2016). Three-dimensional maxillary and mandibular regional superimposition using cone beam computed tomography: a validation study. *Int J Oral Maxillofac Surg* 45:662–9.
- Koretsi V, Zymperdikas VF, Papageorgiou SN, Papadopoulos MA, Koretsi V, Papageorgiou SN, et al. (2015) Treatment effects of removable functional appliances in patients with Class II malocclusion: a systematic review and meta-analysis. *Eur J Orthod* 37:418–34.

- Lima T. (2016) Three-dimensional assesment of dentoskeletal mandibular changes resulting from treatment with Herbts and Twin Block appliances. State University of Rio de Janeiro.
- McNamara JA, Bryan FA, Allen Bryan F (1987) Long-term mandibular adaptations to protrusive function: an experimental study in *Macaca mulatta*. *Am J Orthod Dentofac Orthop* 92:98–108.
- Mohamed MAH, Abdallah KF, Hussein FA, Abdel Hameed Mohamed M, Farouk Abdallah K, Ahmed Hussein F (2020). Three-dimensional assessment of mandibular condylar volume and position subsequent to twin block functional therapy of skeletal class II malocclusion accompanied by low-level laser therapy. *Dent J* 8:115.
- Nindra J, Sidhu MS, Kochhar AS, Dabas A, Valletta R, Rongo R, et al. (2021) Three-dimensional evaluation of condyle-glenoid fossa complex following treatment with herbst appliance. *J Clin Med* 10:4730.
- Otranto de Britto Teixeira A, Almeida MA de O, Almeida RC da C, Maués CP, Pimentel T, Ribeiro DPB, et al. (2020) Three-dimensional accuracy of virtual planning in orthognathic surgery. *Am J Orthod Dentofac Orthop* 158:674–83.
- Pacha MM, Fleming PS, Johal A (2016) A comparison of the efficacy of fixed versus removable functional appliances in children with class ii malocclusion: A systematic review. *Eur J Orthod* 38:621–30.
- Pancherz H. (1982) Vertical dentofacial changes during Herbst appliance treatment. A cephalometric investigation. *Swed Dent J* 15:189–96.
- Proffit WR, Field, Moray LJ (1998). Prevalence of malocclusion and orthodontic treatment need in the United States: estimates from the N-HANES III survey. *Int J Adult Orthod Otho Surg* 13:97–106.
- Ruf S, Pancherz H (2006) Herbst/multibracket appliance treatment of Class II division 1 malocclusions in early and late adulthood. a prospective cephalometric study of consecutively treated subjects. *Eur J Orthod* 28:352–60.
- Santamaría-Villegas A, Manrique-Hernandez R, Alvarez-Varela E, Restrepo-Serna C (2017) Effect of removable functional appliances on mandibular length in patients with class II with retrognathism: Systematic review and meta-analysis. *BMC Oral Health* 17:1–9.
- Shetty VG, Shetty KN (2021). Evaluation of skeletal changes in mandibular ramus height, corpus length, and mandibular angle changes following twin block appliance therapy using cone-beam computed tomography: A clinical prospective study. *Int J Orthod Rehabil* 12:115.

Yatabe M, Garib D, Faco R, De Clerck H, Souki B, Janson G, et al. (2017) Mandibular and glenoid fossa changes after bone-anchored maxillary protraction therapy in patients with UCLP: A 3-D preliminary assessment. *Angle Orthod* 87:423–31.

Yildirim E, Karacay S, Erkan M (2014) Condylar response to functional therapy with Twin-Block as shown by cone-beam computed tomography. *Angle Orthod* 84:1018–25.

Zymperdikas VF, Koretsi V, Papageorgiou SN, Papadopoulos MA (2016) Treatment effects of fixed functional appliances in patients with Class II malocclusion: A systematic review and meta-analysis. *Eur J Orthod* 38:113–26.

CONCLUSÃO

Considerando os resultados dos dois estudos apresentados, conclui-se que com ambos os aparelhos TB e HB se conseguiu crescimento do CO y da CG em direção posterior, sendo significativo o crescimento da CG com o aparelho TB. Além disso, com ambos os aparelhos houve crescimento do CO em direção superior e da CG em direção inferior. Não houve diferença significativa nos efeitos sobre CO e CG quando TB e HB foram usados, e finalmente com ambos os aparelhos a quantidade de crescimento de CO foi sempre maior do que a quantidade de crescimento da CG.

REFERÊNCIAS

- AIDAR L.A. de A. *et al.* Morphological changes of condyles and Helkimo clinical dysfunction index in patients treated with herbst - Orthodontic appliance. **Brazilian Dental Journal**, v. 24, n.4, p. 313–21, 2013.
- AL-SALEH M.A.Q. *et al.* Changes in temporomandibular joint morphology in class II patients treated with fixed mandibular repositioning and evaluated through 3D imaging: A systematic review. **Orthodontics and Craniofacial Research**, v, 18, n. 4, p. 185–201, 2015.
- ARICI S. *et al.* Effects of fixed functional appliance treatment on the temporomandibular joint. **American Journal of Orthodontics and Dentofacial Orthopedics**, v. 133, n. 6, p. 809–14, 2008.
- ATRESH A. *et al.* Three-dimensional treatment outcomes in Class II patients with different vertical facial patterns treated with the Herbst appliance. **American Journal of Orthodontics and Dentofacial Orthopedics**, v. 154, n. 2, p. 238-248, 2018.
- BACCETTI T. *et al.* The Cervical Vertebral Maturation (CVM) Method for the Assessment of Optimal Treatment Timing in Dentofacial Orthopedics. **Seminars in Orthodontics**, v. 11, n. 3, p. 119–29, 2005.
- BATISTA K. B. dos S. L. Herbst appliance with skeletal anchorage versus dental anchorage in adolescents with Class II malocclusion: Study protocol for a randomised controlled trial. **Trials**, v. 18, n. 1, p. 1–11, 2017.
- BOWEN L. *et al.* Analysis of temporomandibular joint changes before and after Twin-block correction by cone-beam CT analysis of Class II division 1 malocclusion . **West China of Stomatology**, v. 31, n. 6, p. 610–4, 2013.
- CEVIDANES L. H. C. *et al.* Superimposition of 3-dimensional cone-beam computed tomography models of growing patients. **American Journal of Orthodontics and Dentofacial Orthopedics**, v. 136, n. 1, p. 94–9, 2009.
- CEVIDANES L. H. S. *et al.* Image analysis and superimposition of 3-dimensional cone-beam computed tomography models. **American Journal of Orthodontics and Dentofacial Orthopedics**, v. 129, n. 5, p. 611–8, 2006.
- CHEIB VILEFORT P.L. *et al.* Condyle-glenoid fossa relationship after Herbst appliance treatment during two stages of craniofacial skeletal maturation: A retrospective study. **Orthodontics and Craniofacial Research**, v. 22, n. 4, p. 345–53, Nov. 2019.
- COZZA P. *et al.* Mandibular changes produced by functional appliances in Class II malocclusion: A systematic review. **American Journal of Orthodontics and Dentofacial Orthopedics**, v. 129, n. 5, p. 599.e1-599.e12, 2006.
- CROFT R. S. *et al.* A cephalometric and tomographic evaluation of Herbst treatment in the mixed dentition. **American Journal of Orthodontics and Dentofacial Orthopedics**, v. 116,

n. 4, p. 435–43, 1999.

DE OLIVEIRA RUELLAS A.C. *et al.* 3D mandibular superimposition: Comparison of regions of reference for voxel-based registration. **PLoS ONE**, v. 11, n. 6, p. 1–13, 2016.

DING L. *et al.* The effect of functional mandibular advancement for adolescent patients with skeletal class II malocclusion on the TMJ: a systematic review and meta-analysis. **BMC Oral Health**, v. 22, n. 1, p. 1–18, 2022.

DOT G., RAFFLENBEUL F., SALMON, B. Voxel-based superimposition of Cone Beam CT scans for orthodontic and craniofacial follow-up: Overview and clinical implementation. **International Orthodontics**, v. 18, n. 4, p. 739–48, 2020.

ELFEKY H. Y. *et al.* Three-dimensional skeletal, dentoalveolar and temporomandibular joint changes produced by Twin Block functional appliance. **Journal of Orofacial Orthopedics**, v. 79, n. 4, p. 245–58, 2018.

FAN, Y. *et al.* 3D assessment of mandibular skeletal effects produced by the Herbst appliance. **BMC Oral Health**, v. 20, n. 1, p. 1–9, 2020.

HAGG, U., PANCHERZ, H. Dentofacial orthopaedics in relation to chronological age, growth period and skeletal development. An analysis of 72 male patients with class II division 1 malocclusion treated with the herbst appliance. **European Journal of Orthodontics**, v. 10, n. 1, p. 169–76, 1988.

JIANG Y *et al.* Three-dimensional cone beam computed tomography analysis of temporomandibular joint response to the Twin-block functional appliance. **Korean Journal of Orthodontics**, v. 50, n. 2, p. 86–97, 2020.

KINZINGER *et al.* Are morphologic and topographic alterations of the mandibular fossa after fixed functional treatment detectable on tomograms? Visual classification and morphometric analysis. **Journal of Orofacial Orthopedics**, v. 79, n. 6, p. 427-439, 2018.

KINZINGER *et al.* Mandibular fossa morphology during therapy with a fixed functional orthodontic appliance : A magnetic resonance imaging study. **Journal of Orofacial Orthopedics**, v. 79, n. 2, p. 116–32 , 2018.

KORETSI, V. *et al.* Treatment effects of removable functional appliances in patients with Class II malocclusion: a systematic review and meta-analysis. **European Journal of Orthodontics** , v. 37, n. 4, p. 418–34, 2015.

KYBURZ, K. S.; ELIADES, T.; PAPAGEORGIOU, S. N. What effect does functional appliance treatment have on the temporomandibular joint? A systematic review with meta-analysis. **Progress in Orthodontics**, v. 20, n. 1, p. 1-13, 2019.

LIMA, T. **Three-dimensional assesment of dentoskeletal mandibular changes resulting from treatment with Herbts and Twin Block appliances.** [s.l.] State University of Rio de Janeiro., 2016.

LECORNU, M. *et al.* Three-dimensional treatment outcomes in Class II patients treated with

the Herbst appliance: A pilot study. **American Journal of Orthodontics and Dentofacial Orthopedics**, v. 144, n. 6, p. 818–30, 2013.

MCNAMARA, J. Components of Class II Malocclusion in Children 8-10 Years of Age. **The Angle Orthodontist**, v. 51, n. 3, p. 177–202, 1981.

MCNAMARA, J. *et al.* Long-term mandibular adaptations to protrusive function: an experimental study in Macaca mulatta. **American Journal of Orthodontics and Dentofacial Orthopedics**, v. 92, n. 2, p. 98–108, 1987.

MOHAMED, M. A. H. *et al.* Three-dimensional assessment of mandibular condylar volume and position subsequent to twin block functional therapy of skeletal class II malocclusion accompanied by low-level laser therapy. **Dentistry Journal**, v. 8, n.4, p. 115, 2020.

NINDRA, J. *et al.* Three-dimensional evaluation of condyle-glenoid fossa complex following treatment with herbst appliance. **Journal of Clinical Medicine**, v. 10; n. 20, p. 4730, 2021.

OTRANTO, T. *et al.* Three-dimensional accuracy of virtual planning in orthognathic surgery. **American Journal of Orthodontics and Dentofacial Orthopedics**, v. 158, n. 5, p. 674–83, 2020.

PANCHERZ, H. Vertical dentofacial changes during Herbst appliance treatment. A cephalometric investigation. **Swedish dental journal. Supplement**, v. 15, p. 189–96, 1982.

RUF, S.; PANCHERZ., H. Herbst/multibracket appliance treatment of Class II division 1 malocclusions in early and late adulthood. a prospective cephalometric study of consecutively treated subjects. **European journal of orthodontics**, v. 28, n. 4, p. 352–60, 2006.

RZUCHOWSKI, G.; MIKULEWICZ, M. Bone Changes in the Condylar Process of the Mandible in Computed Tomography Images and Cephalogram in a Female Patient during a Growth Spurt Treated with a Removable Functional Appliance. **Journal of Healthcare Engineering**, v. 2020, 2020.

RUELLAS, A. *et al.* Common 3-dimensional coordinate system for assessment of directional changes. **American Journal of Orthodontics and Dentofacial Orthopedics**, v. 149, n. 5, p. 645–56, 2016.

SANTAMARIA-VILLEGAS, A. *et al.* Effect of removable functional appliances on mandibular length in patients with class II with retrognathism: Systematic review and meta-analysis. **BMC Oral Health**, v. 17, n. 1, p. 1–9, 2017.

SANTANA, L. G. *et al.* Incremental or maximal mandibular advancement in the treatment of class II malocclusion through functional appliances: A systematic review with meta-analysis. **Orthodontics and Craniofacial Research**, v. 23, n. 4, p. 371–84. 9, 2020.

SHETTY, V.; SHETTY, K. Evaluation of skeletal changes in mandibular ramus height, corpus length, and mandibular angle changes following twin block appliance therapy using cone-beam computed tomography: A clinical prospective study. **International Journal of Orthodontic Rehabilitation**, v. 12, n. 3, p. 115, 2021

SOUKI, B. *et al.* Three-dimensional skeletal mandibular changes associated with Herbst appliance treatment. **Orthodontics and Craniofacial Research**, v. 20, n. 2, p. 111–8, 2017.

TAYLOR, K. L. *et al.* Three-dimensional comparison of the skeletal and dentoalveolar effects of the Herbst and Pendulum appliances followed by fixed appliances: A CBCT study. **Orthodontics and Craniofacial Research**, v. 23, n. 1, p. 72–81, 2020.

YATABE, M. *et al.* Mandibular and glenoid fossa changes after bone-anchored maxillary protraction therapy in patients with UCLP: A 3-D preliminary assessment. **Angle Orthodontist**, v. 87, n. 3, p. 423–31, 2017.

YILDIRIM, E.; KARACAY, S.; ERKAN, M. Condylar response to functional therapy with Twin-Block as shown by cone-beam computed tomography. **The Angle Orthodontist**, v. 84, n. 6, p. 1018–25, 2014

ZYMPERDIKAS, V. F. *et al.* Treatment effects of fixed functional appliances in patients with Class II malocclusion: A systematic review and meta-analysis. **European Journal of Orthodontics**, v. 38, n. 2, p. 113–26, 2016.

ANEXO A - Metodologia do Estudo

Análise 3D das imagens tomográficas

O processo da construção e das análises das imagens 3D seguiram protocolos que foram publicados previamente (Teixeira et al, 2020).

Construção dos modelos de superfície 3D no programa ITK-SNAP

Todas as tomografias deste estudo, em formato DICOM multi-file, foram importadas para o programa ITK-SNAP. As ferramentas de segmentação 3D do ITK-SNAP foram utilizadas para construir modelos virtuais 3D (côndilo e cavidade glenóide) separados de todas as estruturas anatômicas de interesse (Yatabe *et al.*, 2017; Cheib *et al.*, 2019; Jiang *et al.*, 2020;), nas tomografias T0 e T1, de todos os pacientes que concluíram os 12 meses de tratamento com os propulsores mandibulares. Em total foram construídos 192 modelos virtuais 3D (Figura 1).

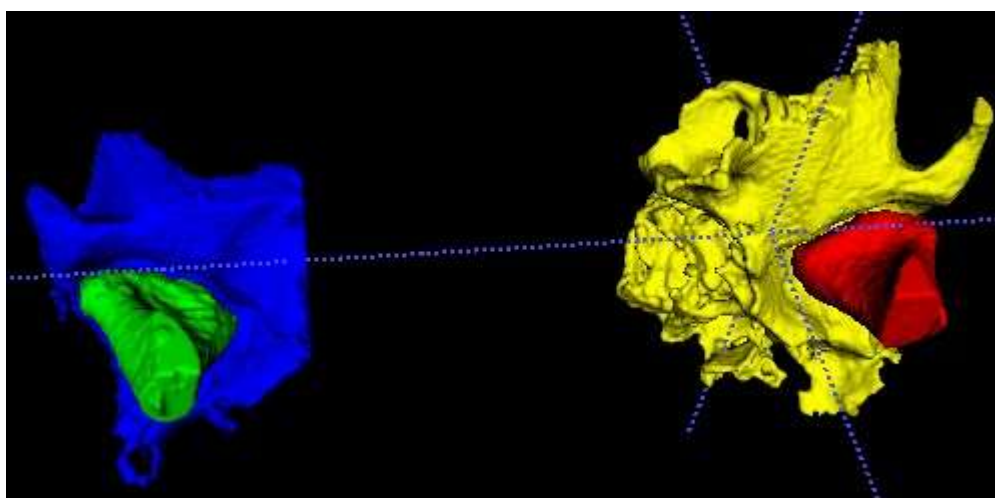


Figura 1. Segmentação do côndilo e da cavidade glenóide

Finalizada a construção dos modelos 3D, todos os modelos foram exportados para o formato estéreo litográfico (STL).

Construção dos modelos totais de superfície 3D no programa Dolphin Imagin

O programa Dolphin Imagin foi utilizado para compactar as tomografias, orientar a

cabeça dos pacientes em T1 na tomografia T0, efetuar a superposição das TCFCs com registro na base anterior do crânio (Cevidanes *et al.*, 2009) e com registro no mento (Ruellas *et al.*, 2016).

Para fazer a superposição de T1 em T0, inicialmente como referências foram utilizadas o plano orbital, o plano horizontal de Frankfurt e o plano médio-sagital. Para fazer a superposição no mento, o plano mandibular ficou horizontal. Foi utilizado um método totalmente automático de registro, baseado em voxel, que dispensa a necessidade de localizar pontos. A última etapa no programa consistiu em exportar os arquivos de malha de superfície STL dos modelos 3D, dos tecidos duros totais de T0 e T1 (orientados y registrados) da base de dados interna do Dolphin Imagin, para uma pasta comum (Figura 2, 3 e 4).

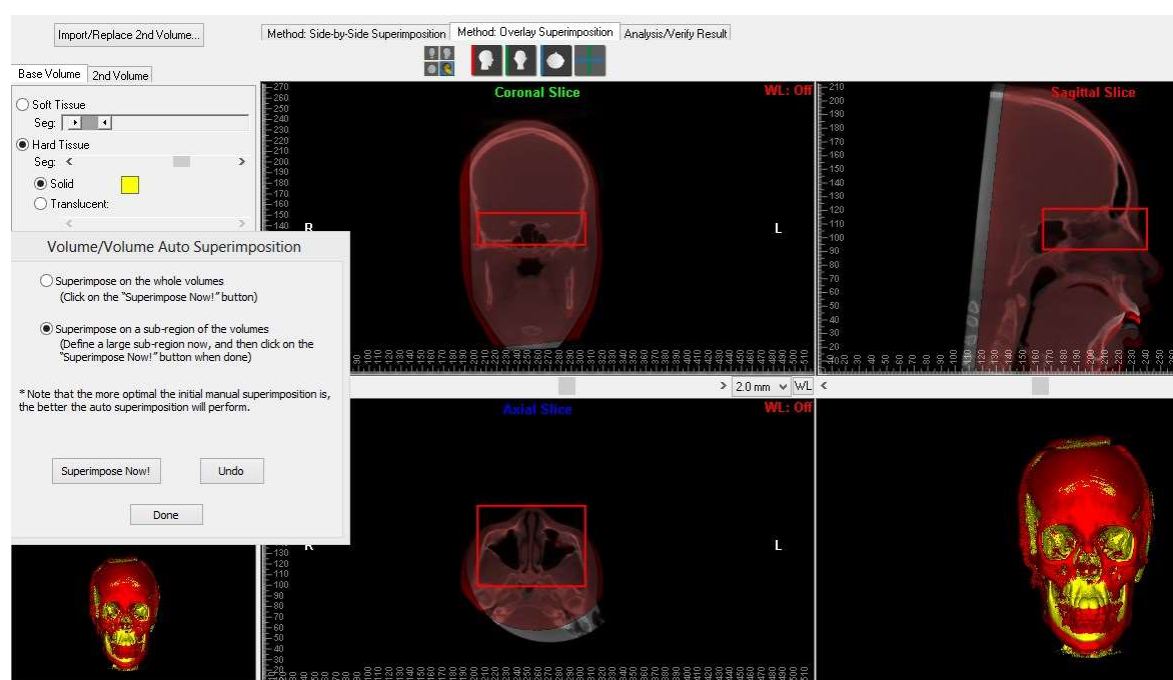


Figura 2. Superposição de T1 em T0 na base de crânio

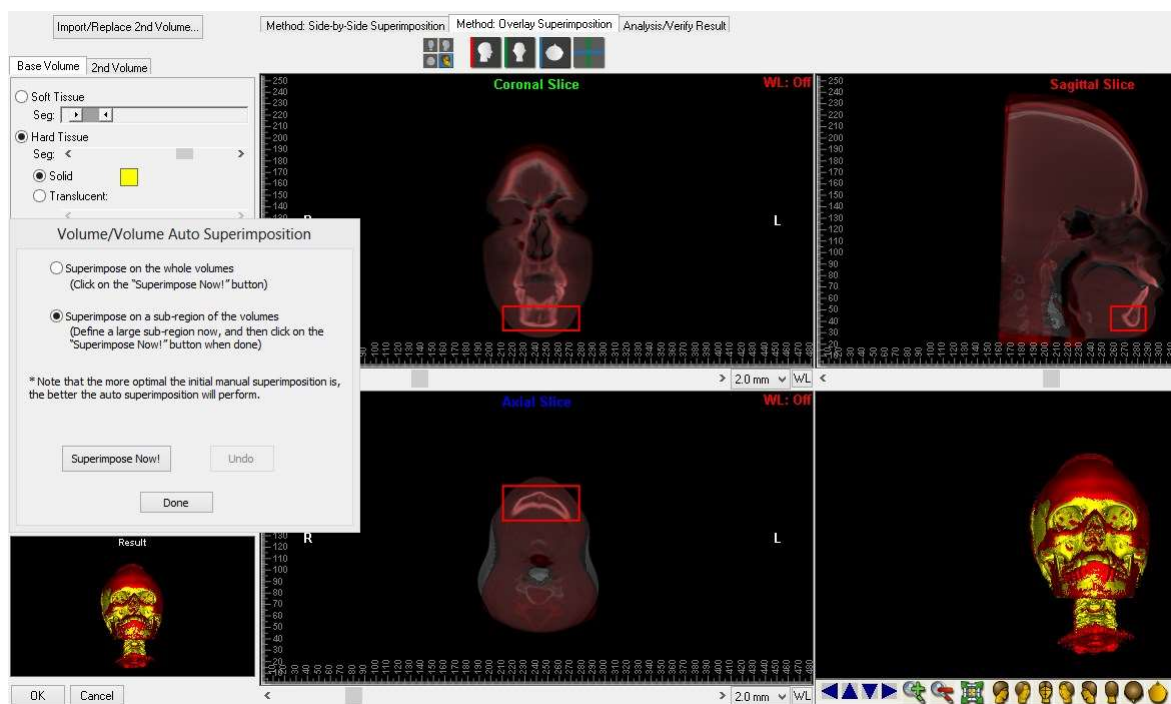


Figura 3. Superposição de T1 em T0 no mento

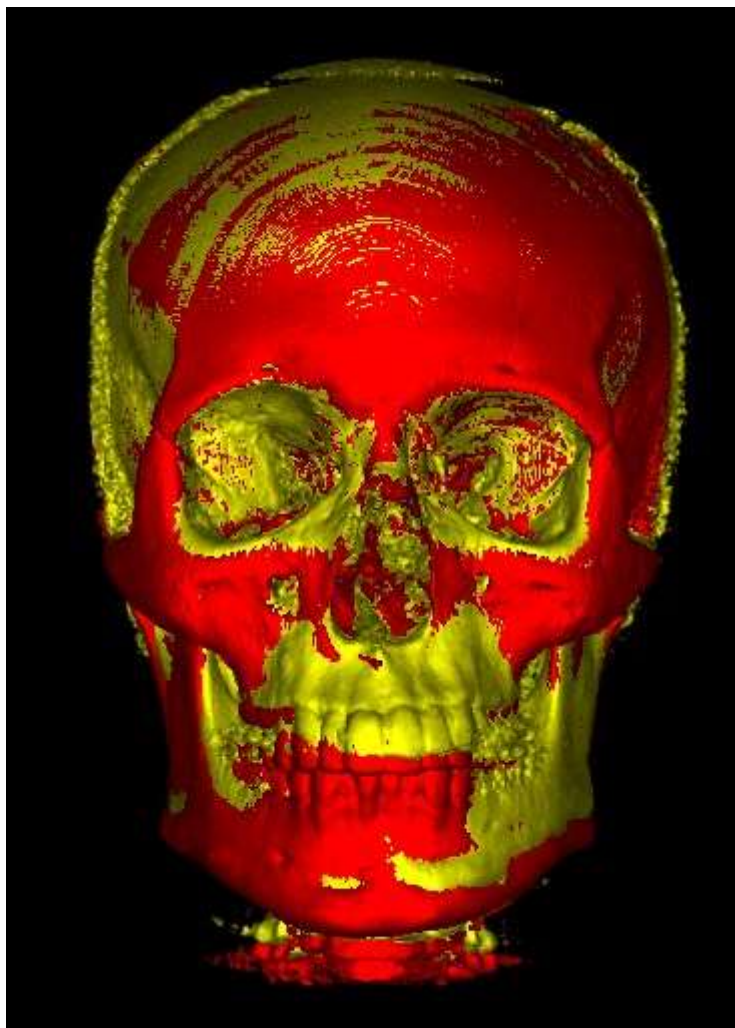


Figura 4. Modelo T1 (vermelho) registrado e orientado em T0 (amarelo) na base anterior do crânio.

Orientação dos modelos totais nos planos cartesianos no programa Geomagic Qualify.

Todo estudo que utiliza tomografias seriadas com diferentes orientações de cabeça para analisar a direção das mudanças esqueléticas ocorridas no mesmo paciente, depende do estabelecimento de um sistema de coordenadas comum, para que as projeções direcionais sejam consistentes entre as imagens obtidas (Ruellas *et al.*, 2016).

Depois de concluídos os processos de orientação e superposição das tomografias T0 e T1 (no programa Dolphin Imagin), todos os modelos 3D totais gerados por segmentação automática a partir destas TCFCs passaram a compartilhar o mesmo sistema de coordenadas (T0 com seu respectivo T1) com eixos, X, Y e Z com base nos planos axial, coronal e sagital no programa Geomagic Qualify (Figura 5).

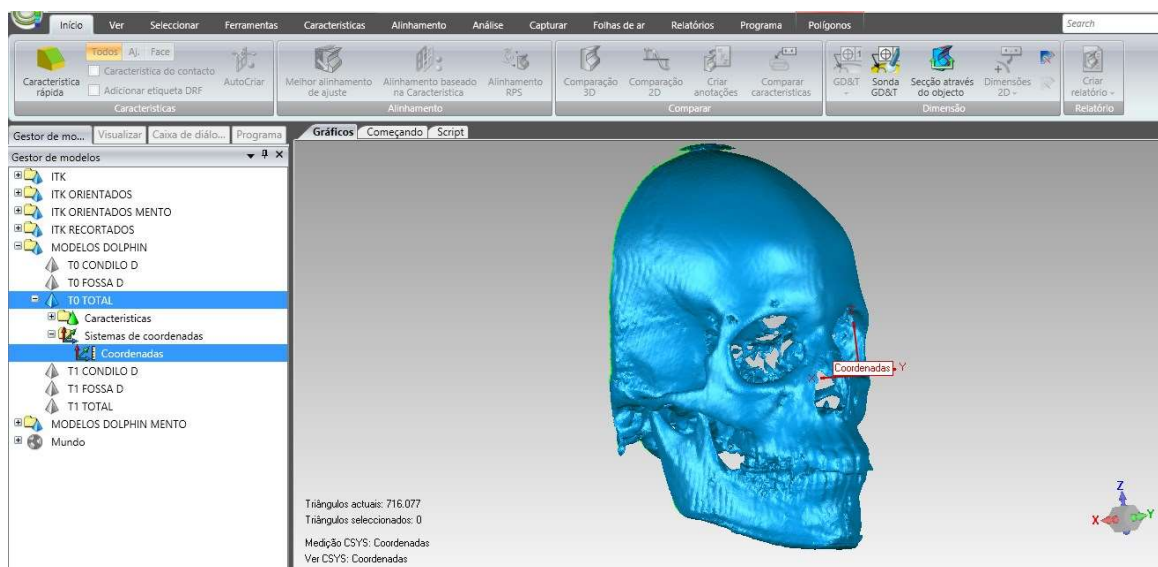


Figura 5. Sistema de coordenadas em T0 estabelecido no programa Geomagic Qualify

Orientação dos modelos 3D parciais precisos (gerados pelo ITK-SNAP) nos modelos 3D totais orientados y registrados (gerados pelo Dolphin Imaging).

Os modelos 3D de tecido duro totais de T0 e T1 orientados e registrados (exportados do Dolphin Imaging) foram utilizados para guiar o alinhamento dos modelos 3D parciais (gerados pelo ITK-SNAP) no Geomagic Qualify.

Prevista sobreposição e recorte exato com iguais dimensões (de T0 e T1 gerados pelo ITK-SNAP), todos os modelos parciais precisos (côndilo e cavidade glenóide) foram alinhados aos modelos totais e registrados de T0 e T1. Cada estrutura anatômica parcial foi alinhada à total individualmente. Ao final os modelos parciais precisos de T0 e T1 obtiveram a mesma orientação espacial dos modelos totais T0 e T1 e compartilharam o mesmo sistema de coordenadas (Figura 6).

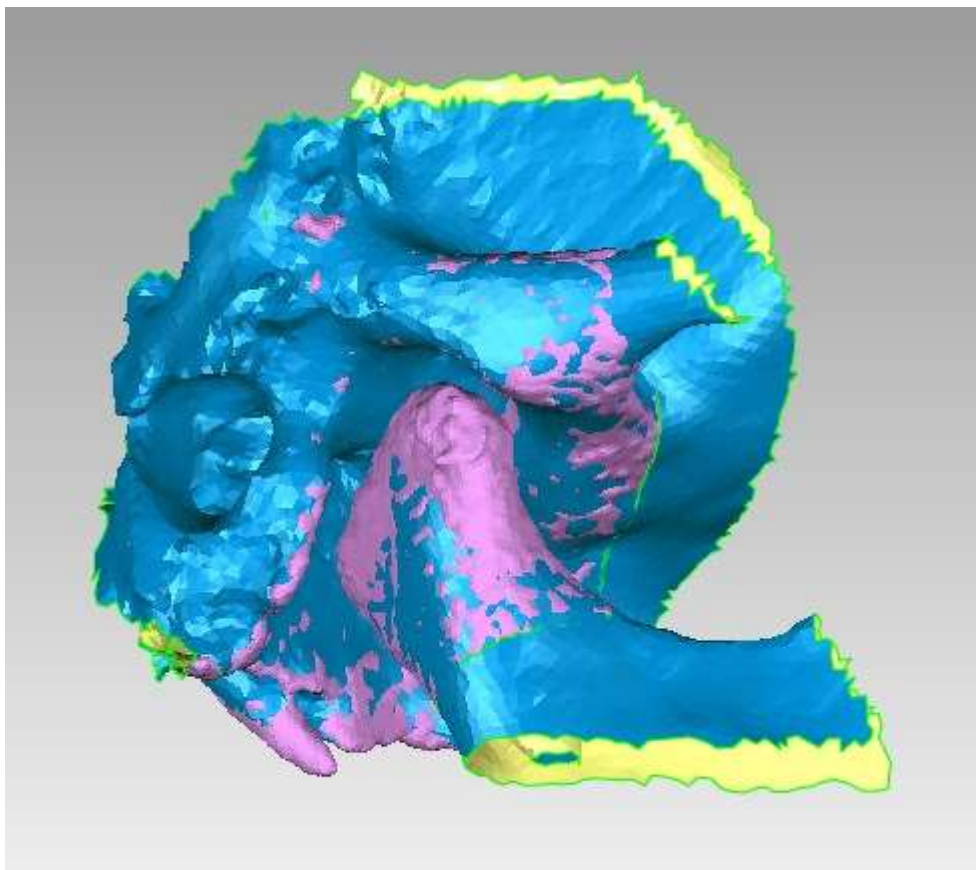


Figura 6. Alinhamento dos modelos 3D parciais (rosa) sobre os modelos 3D totais (azul claro)

Criação automática do ponto centroide dos modelos 3D parciais: Côndilo e Cavidade Glenóide

No presente estudo, foi utilizado um ponto geométrico automaticamente determinado pelo Geomagic Qualify, para representar a posição espacial de uma estrutura anatômica (côndilo e cavidade glenóide) de interesse: o centroide. O ponto centroide de uma estrutura anatômica é o seu centro geométrico; um ponto que possui uma posição espacial média de todos os centroides dos triângulos que compõem o objeto 3D (Teixeira *et al.*, 2020).

Para criar o ponto centroide das estruturas anatômicas parciais (côndilo e cavidade glenóide), foi necessário recortar as malhas das superfícies dos objetos 3D com os mesmos limites anatômicos. Logo a criação do ponto centroide foi efetuada individualmente para todas as estruturas anatômicas parciais de T0 e T1 (Figura 7 e 8).

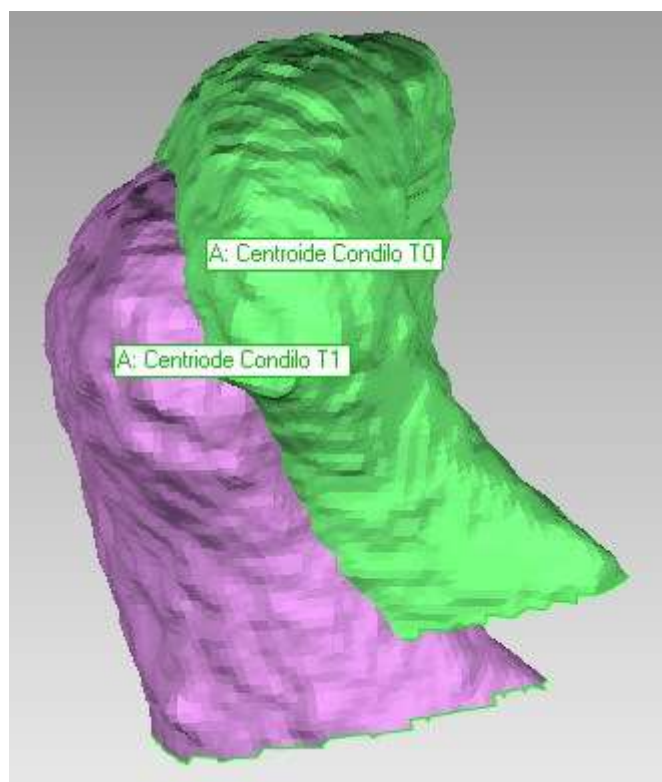


Figura 7. Registro do centroide do côndilo em T0 e T1.

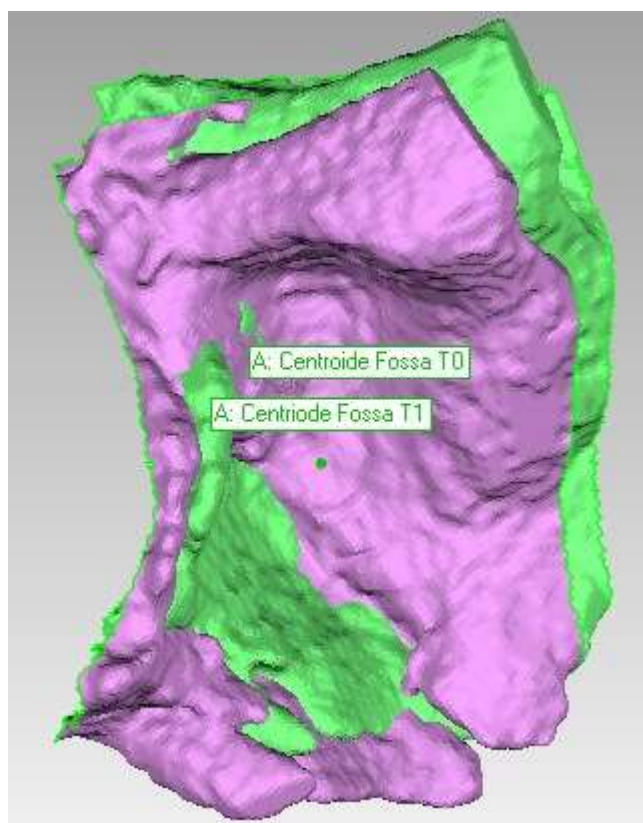


Figura 8. Registro do centroide da cavidade glenóide em T0 e T1

Registro total na base do crânio

Os centroides do côndilo e da cavidade glenóide, inicialmente, foram calculados a partir de estruturas registradas e alinhadas na base anterior do crânio. Logo, o deslocamento total observado entre os centroides de T0 e T1, foi resultante das alterações esqueléticas (crescimento), principalmente na cavidade glenóide. No côndilo, poder-se-ia considerar crescimento ou deslocamento.

Registro regional mandibular para avaliar o crescimento do côndilo no programa Geomagic Qualify.

Os centroides dos côndilos esquerdos e direito haviam sido calculados a partir do registro na base anterior do crânio. Logo, o deslocamento total observado entre os centroides de T0 e T1 dos côndilos era resultante do crescimento e deslocamento de várias estruturas esqueléticas. Para isolar o crescimento condilar, foi necessário efetuar um registro regional entre os modelos 3D das mandíbulas de T1 em T0 dos modelos totais (Figura 9). Ao final, todos os modelos 3D totais estavam registrados em sínfise e corpo da mandíbula (Ruellas *et al.*, 2016), conservando o respectivo sistema de coordenadas criado inicialmente no modelo total T0 (modelo total T1 registrado no modelo total T0).

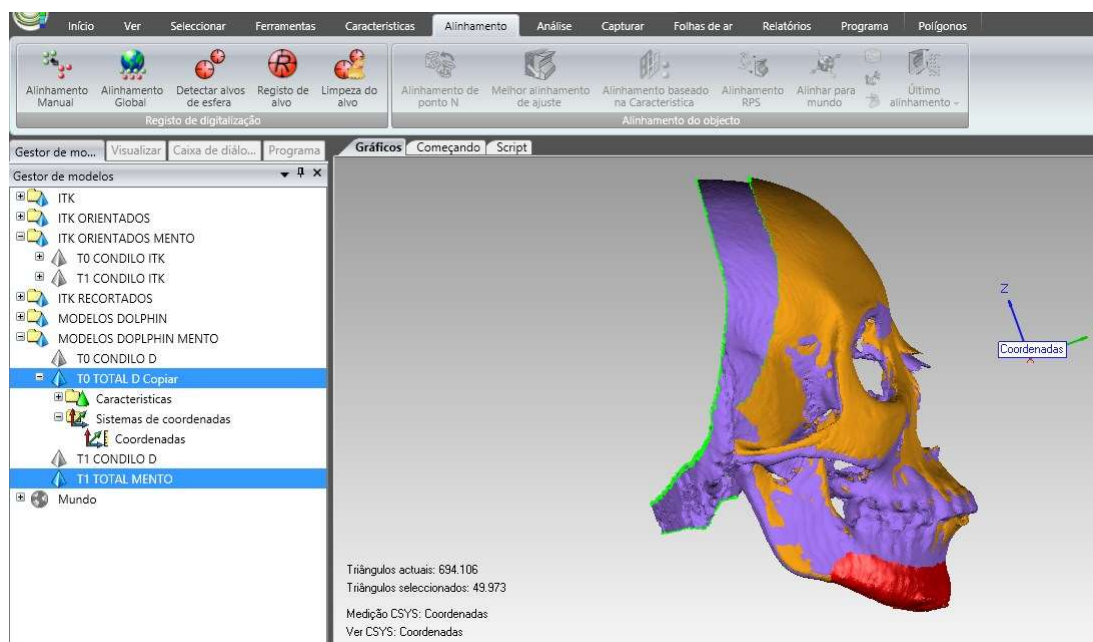


Figura 9. Registro regional mandibular de T1 em T0.

Avaliação quantitativa dos deslocamentos dos centroides dos modelos 3D das estruturas esqueléticas (côndilo e cavidade glenóide).

Os deslocamentos e crescimento das estruturas anatômicas, foram determinados pela diferença de posição espacial entre os centroides de T0 e T1 de cada região. Cada ponto centroide possuiu uma orientação espacial 3D, com coordenadas X (Transversal), Y (anteroposterior) e Z (vertical), orientadas por um Sistema de Coordenadas Individualizadas, estabelecido para cada paciente na imagem 3D total T0, na etapa prévia ao tratamento. O centroide forneceu informação sobre o deslocamento da estrutura anatômica nos três planos do espaço (no programa Geomagic Qualify). Para o eixo X, os valores positivos indicaram o deslocamento para a direita e os valores negativos indicaram o deslocamento para a esquerda. Para o eixo Y, os valores positivos indicaram o deslocamento na direção anterior e os valores negativos indicaram o deslocamento na direção posterior. Para o eixo Z, os valores positivos indicaram o deslocamento na direção superior e os valores negativos na direção inferior.

ANEXO B- Aprovação do Comitê de Ética em Pesquisa 1 e Pesquisa 2



UNIVERSIDADE DO ESTADO DO RIO DE JANEIRO
HOSPITAL UNIVERSITÁRIO PEDRO ERNESTO
COMITÊ DE ÉTICA EM PESQUISA



Rio de Janeiro, 17 de maio de 2011

Do: Comitê de Ética em Pesquisa

Prof.: Wille Cigman

Para: Aut. Tábiana Araújo de Lima – Orient. Profª. Cécia Cardoso A. Quintão

Registro CEP/HUPE: 2918 (este número deverá ser citado nas correspondências referentes ao projeto)
CAAE: 0067.0.228.000-11

O Comitê de Ética em Pesquisa do Hospital Universitário Pedro Ernesto, após avaliação, considerou o projeto, "AVALIAÇÃO TRIDIMENSIONAL DOS EFEITOS DO APARELHO FUNCIONAL TWIN BLOCK NO TRATAMENTO DE MALOCCLUSÕES DE CLASSE II EM PACIENTES EM FASE DE MÁXIMA VELOCIDADE DE CRESCIMENTO PUBERAL" aprovado, encontrando-se este dentro dos padrões éticos da pesquisa em seres humanos, conforme Resolução n.º196 sobre pesquisa envolvendo seres humanos de 10 de outubro de 1996, do Conselho Nacional de Saúde, bem como o termo de consentimento livre e esclarecido.

O pesquisador deverá informar ao Comitê de Ética qualquer acontecimento ocorrido no decorrer da pesquisa.

O Comitê de Ética solicita a V. Sª., que ao término da pesquisa encaminhe a esta comissão um sumário dos resultados do projeto.


Prof. Wille Cigman
Presidente do Comitê de Ética em Pesquisa


CEP - COMITÊ DE ÉTICA EM PESQUISA
AV. VINTE E OITO DE SETEMBRO, 77 TERREO - VILA ISABEL - CEP 20551-030
TEL: 21 2587-6353 - FAX: 21 2264-0853 - E-mail: cep-hupe@uerj.br

ANEXO C - Política de compartilhamento de artigos American Journal of Orthodontics and Dentofacial Orthopedics

Sharing options Open access options

On a preprint server **+**

On my personal blog or website

+ On my institutional

repository- You can post your

accepted author manuscript immediately to an institutional repository and make this publicly available after an embargo period has expired.

Remember that for gold open access articles, you can post your **published journal article** and immediately make it publicly available.

On a subject repository (or other non-commercial repository) **+**

On Scholarly Collaboration Network (SCN), such as Mendeley or Scholar Universe **+**

ANEXO D – Autorização dos Coautores artigo I**AUTORIZAÇÃO**

Autorizo que o trabalho intitulado Analysis of three-dimensional condyle and glenoid fossa alterations following treatment with Twin Block and Herbst functional appliances for the treatment of Class II malocclusions, no qual sou coautor, seja usado na tese de doutorado do aluno Manuel Gustavo Chávez Sevillano.



Cátia Abdo Quintão



Documento assinado digitalmente
TATIANA ARAUJO DE LIMA
Data: 26/04/2024 20:32:58-0300
Verifique em <https://validar.iti.gov.br>

Tatiana Araújo de Lima




Jose Augusto Mendes Miguel



Documento assinado digitalmente
KLAUS BARRETTO DOS SANTOS LOPES BATISTA
Data: 26/04/2024 21:11:11-0300
Verifique em <https://validar.iti.gov.br>

Klaus Barreto dos Santos Lopes Batista

Luciana Quintanilha 

Daniel Blanco-Vitorio

Felipe de Asis Ribeiro Carvalho 

ANEXO E – Autorização dos Coautores artigo 2**AUTORIZAÇÃO**

Autorizo que o trabalho intitulado *An analysis of condyle and glenoid fossa alterations after utilization of the Twin Block appliance in patients Class II malocclusion: A longitudinal retrospective 3D study*, no qual sou coautor, seja usado na tese de doutorado do aluno Manuel Gustavo Chávez Sevillano.

Felipe de Assis Ribeiro Carvalho



Tatiana Araújo de Lima

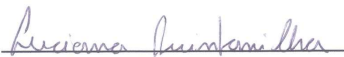


Documento assinado digitalmente
TATIANA ARAUJO DE LIMA
Data: 26/04/2024 20:32:58-0300
Verifique em <https://validar.iti.gov.br>

Daniel Blanco-Vitório



Luciana Quintanilha



Catia Abdo Quintão



ANEXO F - Constancia de Submissão para a Revista American Journal of Orthodontic and Dentofacial Orthopedic do artigo 1

Dear Manuel Gustavo Chávez-Sevillano,

Dr Luciana Quintanilha Pires Fernandes submitted this manuscript via Elsevier's online submission system, Editorial Manager, and you have been listed as a Co-Author of this submission. Elsevier asks Co-Authors to confirm their consent to be listed as Co-Author and track the papers status. In order to confirm your connection to this submission, please click here to confirm your co-authorship:

<https://www.editorialmanager.com/ajodo/i.asp?i=284587&i=LN8LHKPW>

If you have not yet registered for the journal on Editorial Manager, you will need to create an account to complete this confirmation. Once your account is set up and you have confirmed your status as Co-Author of the submission, you will be able to view and track the status of the submission as it goes through the editorial process by logging in at <https://www.editorialmanager.com/ajodo/>. If you did not co-author this submission, please contact the Corresponding Author directly at lgofernandes@hotmail.com.

Thank you,

American Journal of Orthodontics & Dentofacial Orthopedics

More information and support

FAQ: What is Editorial Manager Co-Author registration?

https://service.elsevier.com/app/answers/detail/a_id/28460/supporthub/publishing/kw/co-author+editorial+manager/

You will find information relevant for you as an author on Elsevier's Author Hub: <https://www.elsevier.com/authors>

FAQ: How can I reset a forgotten password?

https://service.elsevier.com/app/answers/detail/a_id/28452/supporthub/publishing/

For further assistance, please visit our customer service site: <https://service.elsevier.com/app/home/supporthub/publishing/>

Here you can search for solutions on a range of topics, find answers to frequently asked questions, and learn more about Editorial Manager via interactive tutorials. You can also talk 24/7 to our customer support team by phone and 24/7 by live chat and email

In compliance with data protection regulations, you may request that we remove your personal registration details at any time. (Use the following URL: <https://www.editorialmanager.com/ajodo/i.asp?i=r>). Please contact the publication office if you have any questions.

De: em.ajodo.0.86aca1fd5b017a@editorialmanager.com <em.ajodo.0.86aca1fd5b017a@editorialmanager.com> em nome de American Journal of Orthodontics <em@editorialmanager.com>

Enviado: sexta-feira, 13 de outubro de 2023 15:47

Para: Luciana Quintanilha Pires Fernandes <lgofernandes@hotmail.com>

Assunto: Submission Confirmation for the AJO-DO

Dear Dr. Fernandes,

Your submission titled "Analysis of three-dimensional condyle and glenoid fossa alterations following treatment with Twin Block and Herbst functional appliances for the treatment of Class II malocclusions" has been received by the American Journal of Orthodontics & Dentofacial Orthopedics.

You will be able to check on the progress of your paper by logging in to Editorial Managers as an author. The URL is <https://na01.safelinks.protection.outlook.com/?url=https%3A%2F%2Fwww.editorialmanager.com%2Fajodo%2F&data=05%7C01%7C%7Cbf470ebd9bb64322238c08dbcc147b91%7C84df9e7fe9f640afb435aaaaaaaaaaaa%7C1%7C0%7C638328160578639814%7CUnknown%7CTWFpbGZsb3d8eyJWljoIjV2luMzliLjBtIjE6IjEhaWwLJXVCI6Mn0%3D%7C3000%7C%7C%7C&sdata=eR0melx4GE4DBBf1oMR3CxYIYV915U7Ee9kLL%2FOn3l%3D&reserved=0>

Your manuscript will be given a reference number once an Editor has been assigned.

Thank you for submitting your work to this journal.

Kind regards,

American Journal of Orthodontics & Dentofacial Orthopedics

Manuscript submission: <https://na01.safelinks.protection.outlook.com/?url=http%3A%2F%2Fwww.editorialmanager.com%2Fajodo%2F&data=05%7C01%7C%7Cbf470ebd9bb64322238c08dbcc147b91%7C84df9e7fe9f640afb435aaaaaaaaaaaa%7C1%7C0%7C638328160578639814%7CUnknown%7CTWFpbGZsb3d8eyJWljoIjV2luMzliLjBtIjE6IjEhaWwLJXVCI6Mn0%3D%7C3000%7C%7C%7C&sdata=erR4VHZB4CvW1iq5syV81FGBfh3QAXHsAMZBHRQuCRk%3D&reserved=0>
Journal website: <https://na01.safelinks.protection.outlook.com/?url=http%3A%2F%2Fwww.ajodo.org%2F&data=05%7C01%7C%7Cbf470ebd9bb64322238c08dbcc147b91%7C84df9e7fe9f640afb435aaaaaaaaaaaa%7C1%7C0%7C638328160578639814%7CUnknown%7CTWFpbGZsb3d8eyJWljoIjV2luMzliLjBtIjE6IjEhaWwLJXVCI6Mn0%3D%7C3000%7C%7C%7C&sdata=an%2BEfRMVMyDIHmxSfGT85k2Bo7Pzd3ymCtdXc1QNE%3D&reserved=0>

ANEXO G - Constancia de Submissão para a Revista Journal of Orthodontic do artigo 2

10-Oct-2023

Dear Dr. Fernandes:

Your manuscript entitled "An analysis of condyle and glenoid fossa alterations after utilization of the Twin Block appliance in patients Class II malocclusion: A longitudinal retrospective 3D study" has been successfully submitted online and is presently being given full consideration for publication in Journal of Orthodontics.

Your manuscript ID is JOO-23-0157.

You have listed the following individuals as authors of this manuscript:

Chávez Sevillano, Manuel; Carvalho, Felipe; Lima, Tatiana; Blanco-Victorio, Daniel José; Fernandes, Luciana; Quintão, Cátia

Please mention the above manuscript ID in all future correspondence or when calling the office for questions. If there are any changes in your street address or e-mail address, please log in to ScholarOne Manuscripts at <https://mc.manuscriptcentral.com/joo> and edit your user information as appropriate.

You can also view the status of your manuscript at any time by checking your Author Center after logging in to <https://mc.manuscriptcentral.com/joo>.

As part of our commitment to ensuring an ethical, transparent and fair peer review process Sage is a supporting member of ORCID, the Open Researcher and Contributor ID (<https://orcid.org/>). We encourage all authors and co-authors to use ORCID IDs during the peer review process. If you have not already logged in to your account on this journal's ScholarOne Manuscripts submission site in order to update your account information and provide your ORCID identifier, we recommend that you do so at this time by logging in and editing your account information. In the event that your manuscript is accepted, only ORCID IDs validated within your account prior to acceptance will be considered for publication alongside your name in the published paper as we cannot add ORCID IDs during the Production steps. If you do not already have an ORCID ID you may login to your ScholarOne account to create your unique identifier and automatically add it to your profile.

Thank you for submitting your manuscript to Journal of Orthodontics.

Sincerely,

Christo Hall

Journal of Orthodontics

jorthodontics@gmail.com